

กราฟีนออกไซด์-ไทโอเลตควอเทอร์ในซีไอโทซานเพื่อเป็นตัวพาสำหรับนำส่งยาต้านมะเร็ง

นางสาวพรรณทิพา โกระวิโยธิน

จุฬาลงกรณ์มหาวิทยาลัย
CHULALONGKORN UNIVERSITY

บทคัดย่อและแฟ้มข้อมูลฉบับเต็มของวิทยานิพนธ์ตั้งแต่ปีการศึกษา 2554 ที่ให้บริการในคลังปัญญาจุฬาฯ (CUIR)
เป็นแฟ้มข้อมูลของนิสิตเจ้าของวิทยานิพนธ์ ที่ส่งผ่านทางบัณฑิตวิทยาลัย

The abstract and full text of theses from the academic year 2011 in Chulalongkorn University Intellectual Repository (CUIR)
are the thesis authors' files submitted through the University Graduate School.

วิทยานิพนธ์นี้เป็นส่วนหนึ่งของการศึกษาตามหลักสูตรปริญญาวิทยาศาสตรมหาบัณฑิต
สาขาวิชาปิโตรเคมีและวิทยาศาสตร์พอลิเมอร์
คณะวิทยาศาสตร์ จุฬาลงกรณ์มหาวิทยาลัย
ปีการศึกษา 2557
ลิขสิทธิ์ของจุฬาลงกรณ์มหาวิทยาลัย

GRAPHENE OXIDE-THIOLATED QUATERNIZED CHITOSAN
AS ANTICANCER DRUG DELIVERY CARRIERS

Miss Pantipa Koraviyotin



A Thesis Submitted in Partial Fulfillment of the Requirements
for the Degree of Master of Science Program in Petrochemistry and Polymer Science
Faculty of Science
Chulalongkorn University
Academic Year 2014
Copyright of Chulalongkorn University

Thesis Title	GRAPHENE QUATERNIZED ANTICANCER CARRIERS	OXIDE-THIOLATED CHITOSAN AS DRUG DELIVERY
By	Miss Pantipa Koraviyotin	
Field of Study	Petrochemistry and Polymer Science	
Thesis Advisor	Associate Professor Nattaya Ngamrojanavanich, Ph.D.	

Accepted by the Faculty of Science, Chulalongkorn University in Partial Fulfillment of the Requirements for the Master's Degree

..... Dean of the Faculty of Science
(Professor Supot Hannongbua, Dr.rer.nat.)

THESIS COMMITTEE

..... Chairman
(Assistant Professor Warinthorn Chavasiri, Ph.D.)

..... Thesis Advisor
(Associate Professor Nattaya Ngamrojanavanich, Ph.D.)

..... Examiner
(Assistant Professor Varawut Tangpasuthadol, Ph.D.)

..... External Examiner
(Assistant Professor Nitinat Suppakarn, Ph.D.)

พรรณทิพา โกรระวิโยธิน : กราฟีนออกไซด์-ไทโอเลตควอเทอร์ไนซ์ไคโทซานเพื่อเป็นตัวพาสำหรับนำส่งยาต้านมะเร็ง (GRAPHENE OXIDE-THIOLATED QUATERNIZED CHITOSAN AS ANTICANCER DRUG DELIVERY CARRIERS) อ.ที่ปรึกษาวิทยานิพนธ์หลัก: รศ. ดร.นาคยา งามโรจนวณิชย์, 117 หน้า.

จุดประสงค์ของงานวิจัยนี้คือ การปรับปรุงคุณสมบัติการยึดติดเยื่อเมือกของคอมโพลีเมอร์กราฟีนออกไซด์ เป็นตัวพาสำหรับนำส่งยาต้านมะเร็งเพื่อยืดระยะเวลาการยึดติดที่เป็นข้อจำกัดในระบบทางเดินอาหาร โดยทำการสังเคราะห์ กราฟีนออกไซด์-ไทโอเลตควอเทอร์ไนซ์ไคโทซาน (G-TQCS) เพื่อเป็นตัวพาสำหรับนำส่งยาต้านมะเร็ง ผ่านกระบวนการเอมิเคชัน โดยการยึดติดไทโอเลต-ควอเทอร์ไนซ์ไคโทซาน (TQCS) กับกราฟีนออกไซด์ (GO) ด้วยพันธะโควาเลนต์ และพิสูจน์เอกลักษณ์ด้วยเทคนิค FTIR, TGA, SEM และ AFM ศึกษาการยึดติดเยื่อเมือกโดยวิธี Periodic Acid Schiff ที่สภาวะจำลองทางเดินอาหาร (pH 1.2, 4.0 และ 6.4) พบว่าที่ pH 1.2 G-TQCS มีความสามารถยึดติดเยื่อเมือกมากกว่าไคโทซาน 10.67 เท่า และมากกว่าไทโอเลตควอเทอร์ไนซ์ไคโทซาน 1.45 เท่า จึงนำ G-TQCS มาใช้เป็นตัวพาสำหรับนำส่งและควบคุมการปลดปล่อยเคอร์คิวมิน (Cur) ซึ่งเป็นตัวยาต้านมะเร็งจากธรรมชาติ โดยเตรียมเป็นลักษณะฟิล์มคอมโพลีเมอร์ ทำการศึกษาลักษณะทางกายภาพด้วยเทคนิค FTIR และ AFM รวมทั้งประสิทธิภาพในการกักเก็บและอัตราการปลดปล่อยยา นอกจากนี้ยังศึกษาฤทธิ์ในการยับยั้งเซลล์มะเร็ง CHAGO และ SW620 จากการศึกษาพบว่า G-TQCS-Cur มีประสิทธิภาพในการควบคุมการกักเก็บยาประมาณ 90 เปอร์เซ็นต์ และสามารถปลดปล่อยเคอร์คิวมินได้ในระดับคงที่นานถึง 12 ชั่วโมง ยิ่งกว่านั้น ฟิล์มคอมโพลีเมอร์ดังกล่าวยังมีฤทธิ์ในการยับยั้งเซลล์มะเร็ง SW620 ดีกว่าตัวยาเคอร์คิวมินบริสุทธิ์เมื่อระยะเวลาในการบ่มนานขึ้น โดยค่า IC_{50} ของปริมาณเคอร์คิวมินที่ใช้ จากในเคอร์คิวมินบริสุทธิ์ $1.07 \pm 0.03 \mu\text{g/mL}$ ลดลงเป็น $0.80 \pm 0.02 \mu\text{g/mL}$ ใน G-TQCS-Cur ที่ 72 ชั่วโมง ดังนั้น G-TQCS จึงเป็นคอมโพลีเมอร์ชนิดใหม่ที่น่าสนใจสำหรับใช้เป็นตัวพาสำหรับนำส่งยาต้านมะเร็งในทางชีวการแพทย์โดยเฉพาะในสภาวะแวดล้อมที่มีความเป็นกรด

5472045923 : MAJOR PETROCHEMISTRY AND POLYMER SCIENCE

KEYWORDS: GRAPHENE OXIDE / MUCOADHESIVE / THIOLATED POLYMER

PANTIPA KORAVIYOTIN: GRAPHENE OXIDE-THIOLATED QUATERNIZED CHITOSAN AS ANTICANCER DRUG DELIVERY CARRIERS. ADVISOR: ASSOC. PROF. NATTAYA NGAMROJANAVANICH, Ph.D., 117 pp.

The objective of this research is to improve mucoadhesive properties of graphene oxide composites for anticancer drug delivery in order to extend its period time in gastrointestinal tract. The graphene oxide-thiolated quaternized chitosan (G-TQCS) as anticancer drug delivery carrier was synthesized by covalent attachment of graphene oxide (GO) with thiolated quaternized chitosan (TQCS) via amidation process and characterized by FTIR, TGA, SEM and AFM. The mucoadhesion of G-TQCS was measured by the Periodic Acid Schiff (PAS) and studied in simulated gastric tract (pH 1.2, 4.0 and 6.4). The results showed mucoadhesive property of GO and TQCS significantly higher than pure chitosan (CS) at all three pH environment. At pH 1.2, G-TQCS displayed a 10.67 and 1.45-fold stronger mucoadhesion than CS and TQCS, respectively. On the other hand, at pH 4.0 and 6.4 the mucoadhesion of G-TQCS were decreased due to the intra-attractive force between thiol and epoxy group immobilized on GO sheet, hindering the adsorption on mucin. Additionally, curcumin (Cur) using as a model natural anticancer drug for anticancer drug carrier of G-TQCS were investigated. The drug-loaded composite film (G-TQCS-Cur) was characterized by FTIR, AFM. Entrapment efficiency, in vitro drug release behavior and cytotoxicity (CHAGO and SW620 cell lines) were also studied. The obtained composite film of Cur loaded in G-TQCS not only exhibited over 90% drug entrapment efficiency but also prolonged release of Cur for up to 12 h. Moreover, G-TQCS-Cur showed higher cytotoxicity than pure Cur against cancer cell lines, especially SW620 cells when increase incubation time. After 72 h incubation decreased IC_{50} value decreased from $1.07 \pm 0.03 \mu\text{g/mL}$ of pure Cur to $0.80 \pm 0.02 \mu\text{g/mL}$ of G-TQCS-Cur. Therefore, G-TQCS is an attractive novel composite as an anticancer drug delivery carrier for biomedical application, especially at acidic environment.

Field of Study: Petrochemistry and Polymer Science Student's Signature

Science Advisor's Signature

Academic Year: 2014

ACKNOWLEDGEMENTS

I would like to express my deepest appreciation and gratitude to my advisor, Associate Professor Dr. Nattaya Ngamrojanavanich, for her excellent suggestion, guidance, encouragement and supportiveness throughout the entire period of conducting this thesis. I would like to thank Associate Professor Dr. Nongnuj Muangsin for their suggestion, helping and teaching me the experimental techniques throughout this work.

Furthermore, the author also thanks the Institutional Biotechnology and Genetic Engineering, Chulalongkorn University, Bangkok 10330, Thailand for providing the equipment, chemicals, cell culture and facilities.

I would also like to thank Assistant Professor Dr. Warinthorn Chavasiri, Assistant Professor Dr. Varawut Tangpasuthadol and Assistant Professor Dr. Nitinat Suppakarn attending as the chairman and members of my thesis committee, respectively, for their kind guidance and valuable suggestions and comments.

Additionally, I wish to express my grateful thank to The 90th Anniversary of Chulalongkorn University Fund (Ratchadaphiseksomphot Endowment Fund) for supporting my thesis.

Finally, I would like to express thanks to my family for their care and supports to make my study successful. Thanks are also due to everyone who has contributed suggestions and supports throughout my research.

CONTENTS

	Page
THAI ABSTRACT	iv
ENGLISH ABSTRACT.....	v
ACKNOWLEDGEMENTS	vi
CONTENTS.....	vii
LIST OF TABLES	x
LIST OF FIGURES	xi
LIST OF ABBREVIATIONS.....	xiv
CHAPTER I INTRODUCTION.....	1
1.1 Introduction.....	1
1.2 The objectives of this research	12
1.3 The scope of research	12
CHAPTER II THEORY AND LITERATURE REVIEWS	14
2.1 Cancer	14
2.3 Mucoadhesive property	18
2.4 Graphene oxide	24
2.5 Thiolated polymer.....	26
2.6 Curcumin	27
2.7 MTT assay	30
CHAPTER III EXPERIMENTAL.....	32
3.1 Materials	32
3.1.1 Polymer and Material	32
3.1.2 Model drug	32
3.1.3 Cell cultures.....	32
3.1.4 Chemicals	33
3.2 Preparation of graphene oxide conjugated with chitosan and Thiolated quaternized chitosan (G-CS and G-TQCS)	34
3.2.1 Synthesis of Thiolated quaternized chitosan (TQCS)	34
3.2.2 Synthesis of graphite oxide (GO).....	35

	Page
3.2.3 Synthesis of G-CS and G-TQCS	35
3.3 Characterization	37
3.3.1. Fourier transformed infrared spectroscopy (FT-IR).....	37
3.3.2. ¹ H Nuclear Magnetic Resonance spectroscopy (NMR)	37
3.3.3 Thermogravimetric analysis (TGA)	38
3.3.4 Scanning Electron Microscope (SEM).....	38
3.3.5 Atomic Force microscopy (AFM).....	38
3.4 Determination of the thiol group and disulfide group content	38
3.5 In vitro bioadhesion of mucin to CS, TQCS, GO, G-CS and G-TQCS	40
3.6 Pharmaceutical applications	41
3.6.1 Preparation of curcumin loaded composite films.....	41
3.6.2 Characterization of the Cur-loaded composite films.....	42
3.6.3 Study of the drug behavior of the Cur-loaded composite films	43
3.7 Cytotoxicity assay.....	45
CHAPTER IV RESULT AND DISCUSSION.....	47
4.1 Synthesis of GO, TQCS and G-TQCS	47
4.2 Characterization and thermal properties of CS, CS derivatives and GO conjugated with CS or TQCS	49
4.2.1 Fourier Transform Infrared Spectroscopy (FTIR).....	49
4.2.2 Nuclear Magnetic Resonance Spectroscopy (¹ H-NMR)	52
4.2.3 Thermogravimetric analysis (TGA)	54
4.2.4. Scanning Electron Microscope (SEM).....	57
4.2.5. Atomic Force Microscope (AFM).....	58
4.3 Degree of substitution of thiol and disulfide contents in TQCS and G-TQCS	60
4.4 Mucoadhesive properties	61
4.4.1 Mucus glycoprotein assay	61
4.4.2 Adsorption of mucin on polymer or composites	62
4.5 Characterization of CS, TQCS, GO, G-CS and G-TQCS loaded curcumin.....	68
4.5.1 Fourier Transform Infrared Spectroscopy (FTIR).....	68

	Page
4.5.2. Atomic Force Microscope (AFM).....	72
4.7 <i>In vitro</i> curcumin release profiles	75
4.8 In Vitro Cytotoxicity Studies of Curcumin and Curcumin-loaded composite films.....	79
CHAPTER V CONCLUSION.....	85
REFERENCES	87
APPENDIX.....	95
APPENDIX A.....	96
APPENDIX B	98
APPENDIX C.....	101
APPENDIX D.....	104
APPENDIX E.....	111
VITA.....	117



LIST OF TABLES

Table 1 Amounts of thiol groups and disulfide bonds on TQCS and G-TQCS (1:10 w/w).....	60
Table 2 The amount of adsorption of mucin on CS, TQCS, GO, GO-CS and G-TQCS (ratio of GO: CS or CS derivatives are 1:10 w/w) at pH 1.2, 4.0 and 6.4 PBS buffer.....	66
Table 3 The percentages of loading and entrapment of curcumin loaded polymer and composites.....	75



LIST OF FIGURES

Figure 1 a) Thiolated polymers (Thiomers) b) Mechanism of disulfide bond formation between thiomers and mucus glycoproteins (mucins)	2
Figure 2 Chemical structure of graphene oxide (GO).....	3
Figure 3 Chemical structure of thiolated quaternized chitosan.....	5
Figure 4 Synthesis scheme of incorporation CS and TQCS with GO a) G-CS and b) G-TQCS.....	7
Figure 5 Chemical structure of Curcumin (Cur).....	8
Figure 6 Synthesis scheme of G-CS and G-TQCS	10
Figure 7 Illustration of drug loaded mucoadhesive nanocomposite a) G-CS and b) G-TQCS.....	11
Figure 8 Cell division of normal and cancer cell [35]	14
Figure 9 Presentation of controlled release system.....	15
Figure 10 An illustration of the zero-order controlled drug release [37].....	16
Figure 11 Presentation of diffusion controlled release	16
Figure 12 Presentation of swelling controlled release	17
Figure 13 Presentation of erosion controlled release: a) Bulk erosion and b) Surface erosion.....	18
Figure 14 A proposed illustration of mucin [3]	19
Figure 15 The two steps of the mucoadhesion [3]	21
Figure 16 The structural model of graphene oxide (GO).....	25
Figure 17 The formation of covalent bond between thiolated polymer and mucin [8].....	27
Figure 18 Chemical structures of major metabolites of curcumin in rodents and humans [22]	29
Figure 19 The principle of cytotoxicity (MTT) assay [53].....	31
Figure 20 The schematically synthesized of Route A) G-CS and Route B) G-TQCS	36
Figure 21 Synthesis scheme of graphene oxide-thiolated quaternized chitosan (G-TQCS).....	48

Figure 22 FTIR spectra of a) chitosan, b) quaternized chitosan and c) thiolated quaternized chitosan d) graphene oxide, e) G-CS and f) G-TQCS.....	51
Figure 23 ¹ H NMR spectra of a) chitosan, b) quaternized chitosan and c) thiolated quaternized chitosan.....	53
Figure 24 TGA and DTG data of a) chitosan, b) quaternized chitosan and c) thiolated quaternized chitosan.....	55
Figure 25 TGA and DTG data of a) graphene oxide, b) G-CS and c) G-TQCS.....	56
Figure 26 SEM images (a) GO, (b) G-CS and (c) G-TQCS (scale bar 2.0 μm).....	57
Figure 27 AFM images (tapping mode) of (a) GO, (b) G-CS (c) G-TQCS with concentrations of 0.01 mg/ ml. Image dimensions are 2.0 μm x 2.0 μm	59
Figure 28 Adsorption of mucin on CS, TQCS, GO, G-CS and G-TQCS at pH 1.2, 4.0 and 6.4 PBS buffer	66
Figure 29 Representative the interaction between a) G-CS and b) G-TQCS with mucin at pH value rang in stomach (pH 1.2) and small intestine (pH4.0 and 6.4).....	67
Figure 30 FTIR spectra of a)curcumin, b) chitosan, c) thiolated quaternized chitosan, d) chitosan-curcumin and e) thiolated quaternized chitosan-curcumin.....	70
Figure 31 FTIR spectra of a) graphene oxide, b) G-CS, c) G-TQCS, d) GO-Cur, e) G-CS-Cur and f) G-TQCS-Cur.....	71
Figure 32 AFM images (tapping mode) of (a) GO-Cur, (b) G-CS-Cur (c) G-TQCS-Cur with concentrations of 0.01 mg/ ml. Image dimensions are 2.0 μm x 2.0 μm	73
Figure 33 Release profiles of CS-Cur, TQCS-Cur, GO-Cur, G-CS-Cur and G-TQCS-Cur at pH 1.2	78
Figure 34 Release profiles of CS-Cur, TQCS-Cur, GO-Cur, G-CS-Cur and G-TQCS-Cur at pH 6.4	78
Figure 35 Cell viability of (a) CHAGO (lung cancer cell) and (b) SW620 (colon cancer cell) treated with Curcumin (Cur) for 24, 48 and 72 h (MTT assay)	81
Figure 36 Cell viability of (a) CHAGO (lung cancer cell) and (b) SW620 (colon cancer cell) treated with 100 μg/mL of CS, TQCS, GO, G-CS and G-TQCS for 24, 48 and 72 h (MTT assay)	82
Figure 37 Cell viability of (a) CHAGO (lung cancer cell) and (b) SW620 (colon cancer cell) treated with 300 μg/mL of free (right) and Cur-loaded (left) composite films for 24, 48 and 72 h (MTT assay).....	83

Figure 38 IC₅₀ of (a) CHAGO (lung cancer cell) and (b) SW620 (colon cancer cell) treated with CS-Cur, TQCS-Cur, GO-Cur, G-CS and G-TQCS for 72 h (MTT assay).....84



LIST OF ABBREVIATIONS

%	percentage
µg	microgram
µL	microliter
µmol	micromole
cm ⁻¹	unit of wave number
conc.	concentration
HT	homocysteine-thiolactone
PAS	periodic acid schiff
Cur	curcumin
QCS	quaternized chitosan
TQCS	thiolated quaternized chitosan
FTIR	fourier transform infrared spectrophotometer
TGA	thermogravimetric analysis
SEM	scanning electron microscopy
AFM	atomic force microscopy
NMR	nuclear magnetic resonance
°C	degree Celsius (centigrade)
%DQ	degree of quaternization
EE	entrapment efficiency
g	gram
h	hour
M	concentration in molar
mg	milligram
min	minute
mL	milliliter
MW	molecular weight
nm	nanometer
µm	micrometer
pH	power of hydrogen ion or the negative

ppm	part per million
KBr	potassium bromide
rpm	round per minute
S.D.	standard deviation
t	time
v/v	volume/volume
w/w	weight/weight
w/v	weight/volume
MTT	3-(4,5-dimethylthiazol2-yl)-2,5-diphenyl tetrazolium bromide
δ	chemical shift
D ₂ O	deuterium oxide
DMSO	dimethylsulfoxide
EDC	1-Ethyl-3-(3-dimethylaminopropyl)carbodiimide
PBS	phosphate buffered saline

CHAPTER I

INTRODUCTION

1.1 Introduction

Cancer is the most common cause of death worldwide during the last decade. The World Health Organization (WHO) suggests that cancer is the leading causes of death worldwide, accounting for 8.2 million deaths in 2012, of which 70% would be contributed from developing countries [1]. One of the most abundant and traditional administrations of anticancer drug delivery is oral route main advantage being greatest safety, convenience and patient compliance. Oral administration is available to systemic circulation for execution of therapeutic response, mostly this has low aqueous solubility, poor intestinal permeability and gastrointestinal instability also restricts the progression for oral route [2]. However, recent advances in mucoadhesive polymeric nanoparticles as drug delivery carrier are potential advantages in overcoming these limitations.

The mucoadhesive polymers have gained considerable interest as a drug delivery carrier of achieving site-specific in the use of transmucosal systems provide a means of enhancing retention at defined sites that improve prolong period of attachment, lower drug concentration and reduce the dose-related side effects. Mucoadhesion is a complex process and numerous theories include mechanical-interlocking, electrostatic, diffusion–interpenetration, adsorption and fracture processes [3]. The mucus be consist of water and mucin glycoproteins which have rich of

sialic acid ($pK_a = 2.6$), sulphate, and carboxylate content result in mucin behaving as an anionic polyelectrolyte at neutral pH [4]. The polymer structural and functional group including chain flexibility, strong hydrophilic functional groups (carboxyl ($-\text{COOH}$), hydroxyl ($-\text{OH}$) and amine ($-\text{NH}_2$) groups), ionic charge and thiol group ($-\text{SH}$) can have an effect on the degree of polymer/mucus interaction [5, 6]. Mucoadhesive polymers generally contain of numerous polar functional groups. Consequently, polymers interact with the mucus not only through non-covalent bond via electrostatic interaction, hydrogen bonding or hydrophobic bonding but also through thiol groups, thus resulting in the formation of disulfide bonds [7].

The thiolated polymers (Thiomers) (Fig.1a) are polymers presence thiol groups on side chains exhibited high mucoadhesive property. The thiol groups allow the formation of covalent bonds with cysteine-rich sub domains of the mucus glycoprotein, also covalently immobilized in the mucus layer by the formation of disulphide bonds (Fig.1b) that leading to increased time of adhesion and improved bioavailability.

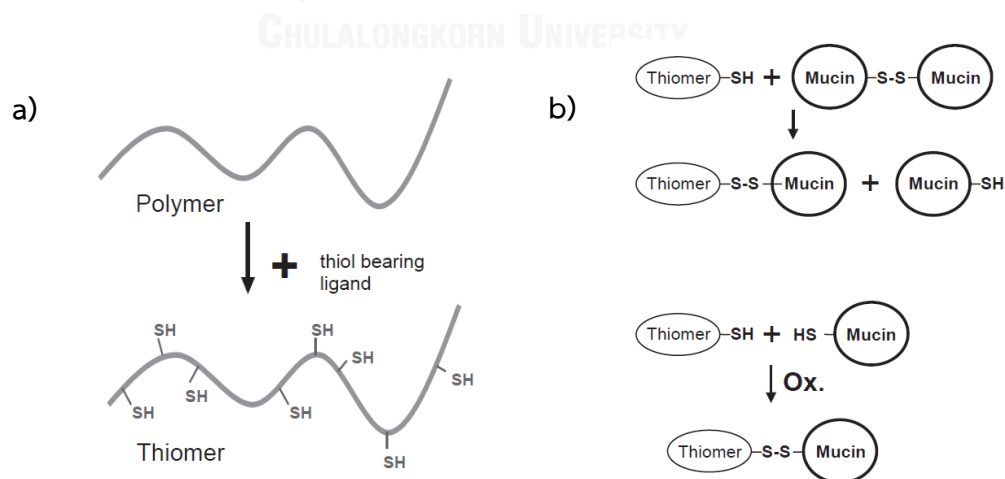


Figure 1 a) Thiolated polymers (Thiomers) b) Mechanism of disulfide bond formation between thiomers and mucus glycoproteins (mucins)

At lower pH, thiomers are less reactive because of their thiol groups become only reactive when interpenetrating the mucus layer. Therefore, thiomers of lower pH form promising more disulfide bonds with mucin [8].

Graphene oxide (GO), the individual-layer of graphene decorated with oxygen functional groups (such as hydroxyl, epoxy, and carboxyl) on both the basal planes and edges, has prepared by the chemical treatment via oxidation (Fig.2). The oxygen functional groups are potential advantages of GO to approach chemical functionalization through either covalent or non-covalent attachment such as π - π stacking and electrostatic or hydrophobic interactions. Additionally, the biocompatibility, conjugated structure, high specific surface area and especially produced from low cost precursor therefore GO is a novel material for biomedical application that can be exploited to achieve high drug loading of poorly soluble and π -conjugated structure drugs without compromising efficiency [9, 10]. Consequently, an efficient way to improve properties of graphene such as solubility, interfacial interactivity with a target matrix and bioavailability is covalently grafting polymers onto GO sheet.

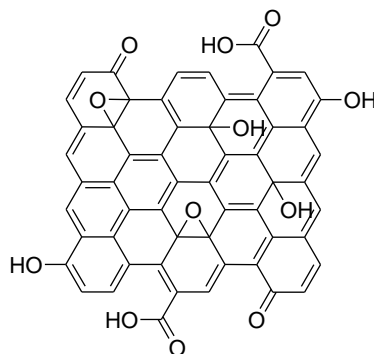


Figure 2 Chemical structure of graphene oxide (GO)

A superparamagnetic, GO-Fe₃O₄ nanoparticles hybrid was high loading capacity of doxorubicin hydrochloride. It can be rearranged in the acidic and basic condition under the external magnet force [11]. The encapsulation of graphene oxide loaded doxorubicin with folic acid conjugated chitosan (GO-DOX-CHI-FA) as drug delivery carrier via π - π stacking interaction are applied to control drug release for drug delivery system that enhanced the stability in aqueous medium [12]. GO modified with chitosan (GO-CS) via amide bond improves aqueous solubility and biocompatibility. It demonstrates high loading of camptothecin and in vitro study show cytotoxicity in HepG2 and HeLa cell lines [13]. GO-DOX as an anticancer drug nanocarrier was used to treat hematological malignancies which pure GO exhibited low cytotoxicity and did not affect the antitumor activity of DOX [14].

However, there previously was no reports about mucodhesive property of graphene oxide. Therefore, this work focus on the mucoadhesive material that is stable in acid condition and able to attach the target through mucus membrane for a long period of time. The modified covalent attachment of chitosan and its derivative with graphene oxide has been synthesized to enhance mucoadhesive property. The GO is composed of oxygen functional group which is able to form hydrogen bonding and electrostatic interaction as a non-covalent type, enable to increase mucoadhesion with mucin.

Chitosan (CS) is naturally linear cationic polysaccharide consist of *N*-acetyl-*D*-glucosamine and *D*-glucosamine units and was found to have good mucoadhesive property, biodegradability, non-toxicity and high biocompatibility. Owing to cationic and chain flexibility would be able to interact more strongly with the mucus glycoproteins via hydrogen bonds

of primary amino (NH_2) and hydroxyl (OH) groups of chitosan backbone and electrostatic effect however its poor solubility in neutral and basic pH [15, 16]. In order to improve its mucoadhesive property, the thiolated quaternized chitosan (TQCS) (Fig.3), which are partially quaternized derivatives [17, 18] and immobilized thiol groups to the primary amino groups of CS [8, 19, 20] have been synthesized. It not only interacts with the negatively charged of mucin glycoproteins but it also form covalent bonds via disulfide would be able to interact more strongly with the mucus glycoproteins. Furthermore, it increases the solubility of CS in water at neutral and basic pH values. As previous reported [21], Quaternized chitosan-homocysteine thiolactone (QCS-HT) has found good mucoadhesion, biodegradability and biocompatibility which exhibited up to 6 times stronger adherence mucus glycoprotein compared to pure chitosan at pH 1.2.

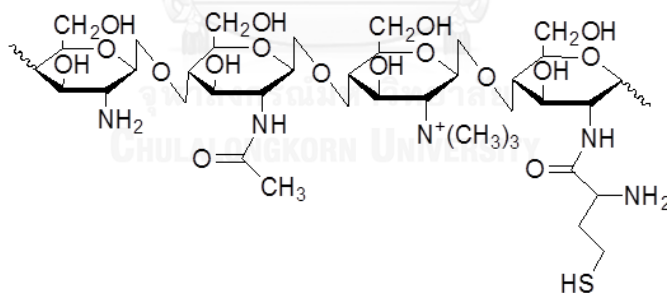
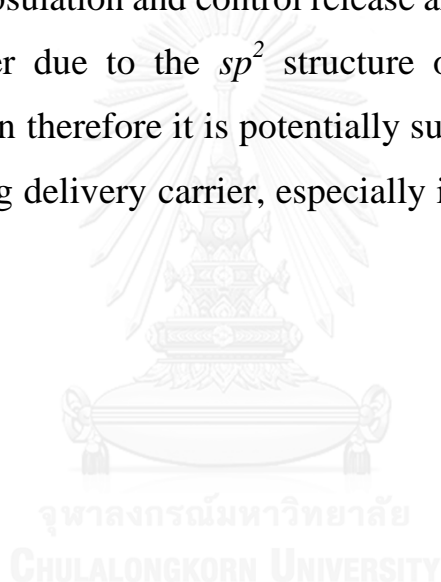


Figure 3 Chemical structure of thiolated quaternized chitosan (TQCS)

The point of this work is synthesized quaternized thiolated chitosan (TQCS) is the covalent attachment of homocysteine thiolactone (HT) to N-trimethyl chitosan (QCS) that presented the thiol group and positive

charge on the side chain. It has an active side to attach to mucus membrane. After that incorporation CS and TQCS with GO via amide linkage (Fig. 4a and b) in order to improve the aqueous solubility of GO and mucoadhesive property. The amount of thiol groups immobilized on TQCS and G-TQCS were determined by Ellman's method, Periodic acid Schiff (PAS) colorimetric method was used to quantify mucin adsorbed onto composite in the simulated gastrointestinal fluid (pH 1.2, 4.0 and 6.4). Furthermore, the GO is able to enhance the efficiency of encapsulation and control release aromatic insoluble drug on composite polymer due to the sp^2 structure of GO inducing the π - π stacking interaction therefore it is potentially suitable for application in a mucoadhesive drug delivery carrier, especially in a low pH environment.



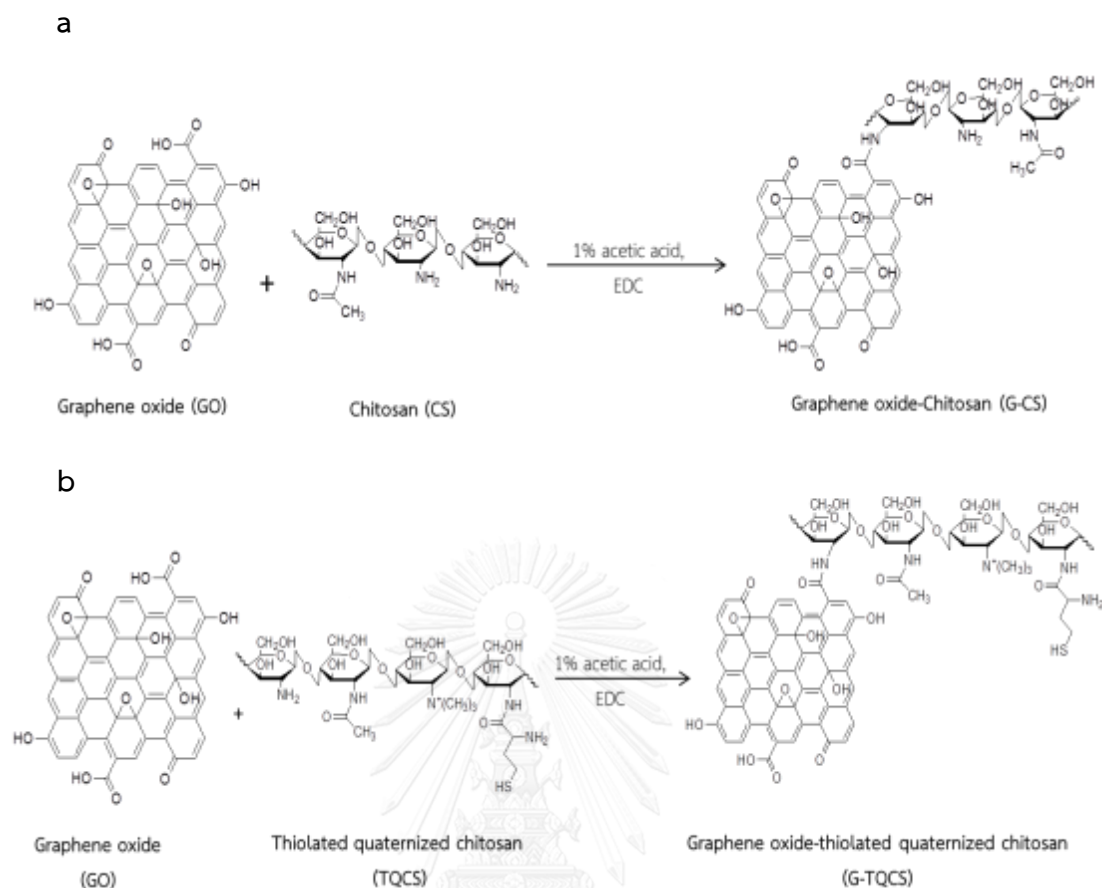


Figure 4 Synthesis scheme of incorporation CS and TQCS with GO

a) G-CS and b) G-TQCS

Curcumin (Cur) (Fig. 5), a bis- α,β -unsaturated β -diketone is a polyphenol derived from the rhizome of the herb *Curcuma longa* plant, commonly known as dietary spice turmeric. Chemically, exhibits keto-enol tautomerism form, it has a predominant keto form in acidic and neutral solutions and a stable enol form in alkaline media [22].

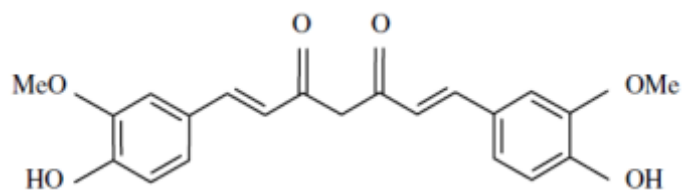


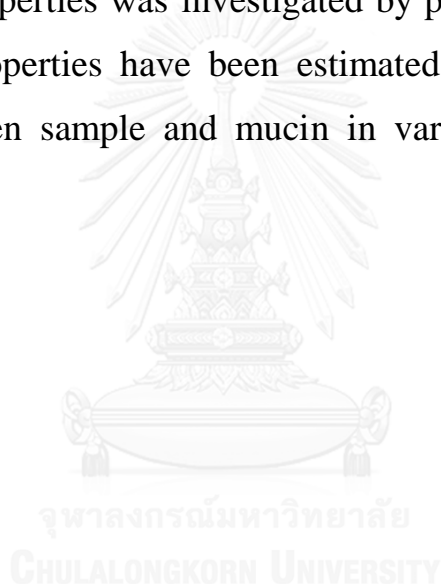
Figure 5 Chemical structure of Curcumin (Cur)

Studies of Cur have found that wide range of biological activities including anti-inflammatory [23], anti-cancer [24, 25], anti-oxidant [26] and wound healing [27]. Cur strong ability to inhibit carcinogenesis has attracted particular interests as potential cancer chemotherapy [28]. Moreover, in vivo and in vitro studies of Cur have demonstrated chemopreventive effect in animal tumor that can suppresses cancer cell proliferation, inhibits angiogenesis, induce apoptosis and inhibitor of protein kinase [29].

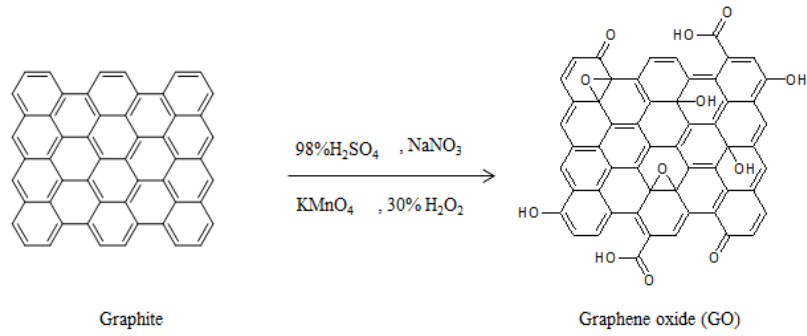
However, a major drawback of Cur limits its bioavailability in vascular and oral administration due to its extremely low solubility in aqueous solutions. Consequently, to overcome this limitation, Cur was encapsulated or loaded in some release devices (polymeric nanoparticle, biodegradable microspheres, polymeric micelles and hydrogel) [30-33]. The decomposition of Cur occurs with faster reactions at neutral to basic conditions and its stables at a pH < 6.5 [34].

Therefore, this work attempts to develop a novel nanocomposite as drug delivery carrier for biomedical application, especially at the gastrointestinal tract (GI tract). The graphene oxide-chitosan (G-CS) and graphene oxide-thiolated quaternized chitosan (G-TQCS) were synthesized. The three steps of synthesis G-CS and G-TQCS are illustrated in synthesis scheme (Fig. 6). Firstly, preparation of GO

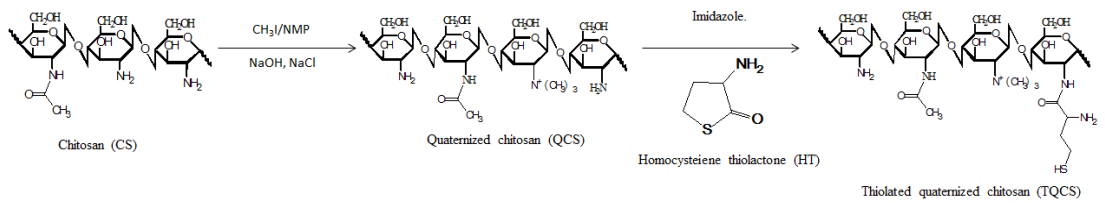
through oxidized of graphene or graphite and then prepared TQCS from CS potentially to enhance mucoadhesive property. Finally, the covalently association of GO with CS and TQCS via amide linkage to increase solubility and mucoadhesion that can achieve restrict of drug delivery carrier via oral route. The synthesized polymer and composites were characterized in terms of element analysis and morphology by FTIR, ¹H-NMR, TGA, SEM and AFM. Degree of thiol substitution was evaluated using Ellman's method. Additionally, the in vitro mucoadhesion properties was investigated by periodic acid schiff (PAS) method, these properties have been estimated from assessment of the interaction between sample and mucin in various pH buffer solution.



Step I.



Step II.



Step III.

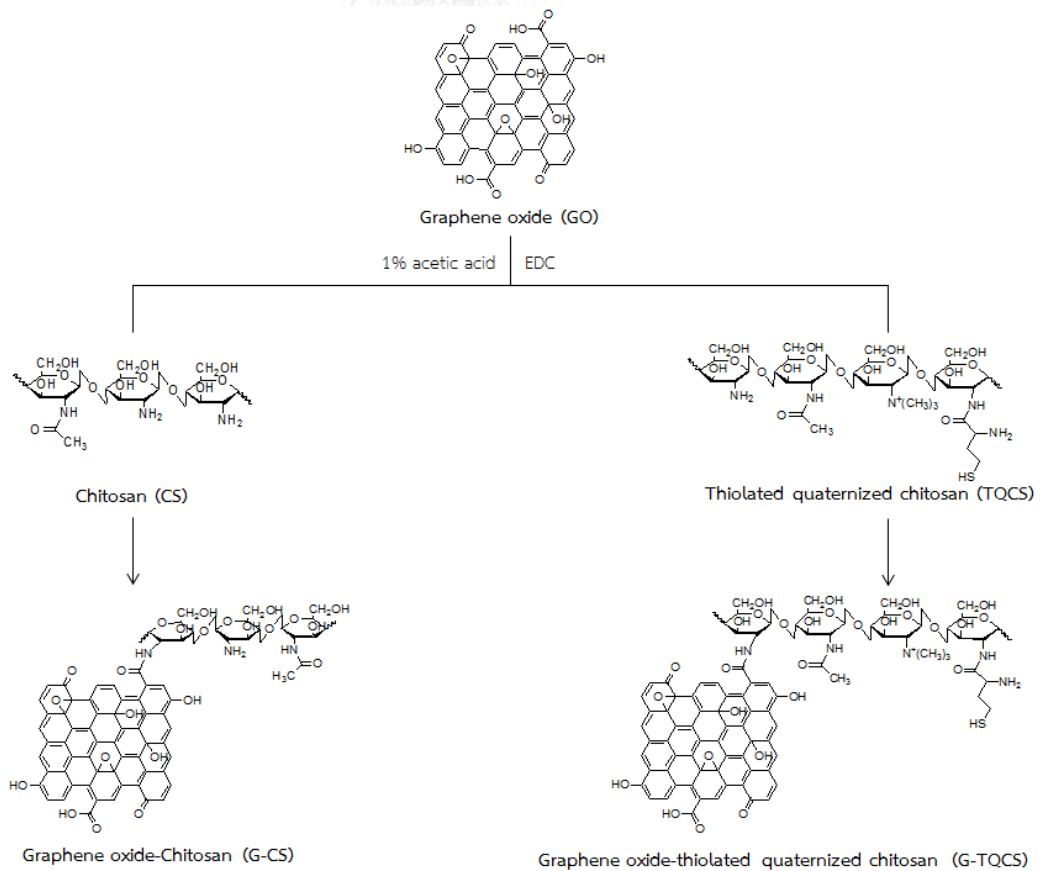


Figure 6 Synthesis scheme of G-CS and G-TQCS

Moreover, the utilization of composite film of G-CS and G-TQCS as a drug delivery carrier for natural hydrophobic drugs (curcumin) was investigated (Fig. 7a and b). The obtained drug-load composite films were characterization by FTIR and AFM. Study the in vitro release behavior and cytotoxicity against cancer cell (CHAGO and SW620) of the drug-load composite films in various pH buffers (pH1.2 and 6.4), the gastrointestinal tract environment.

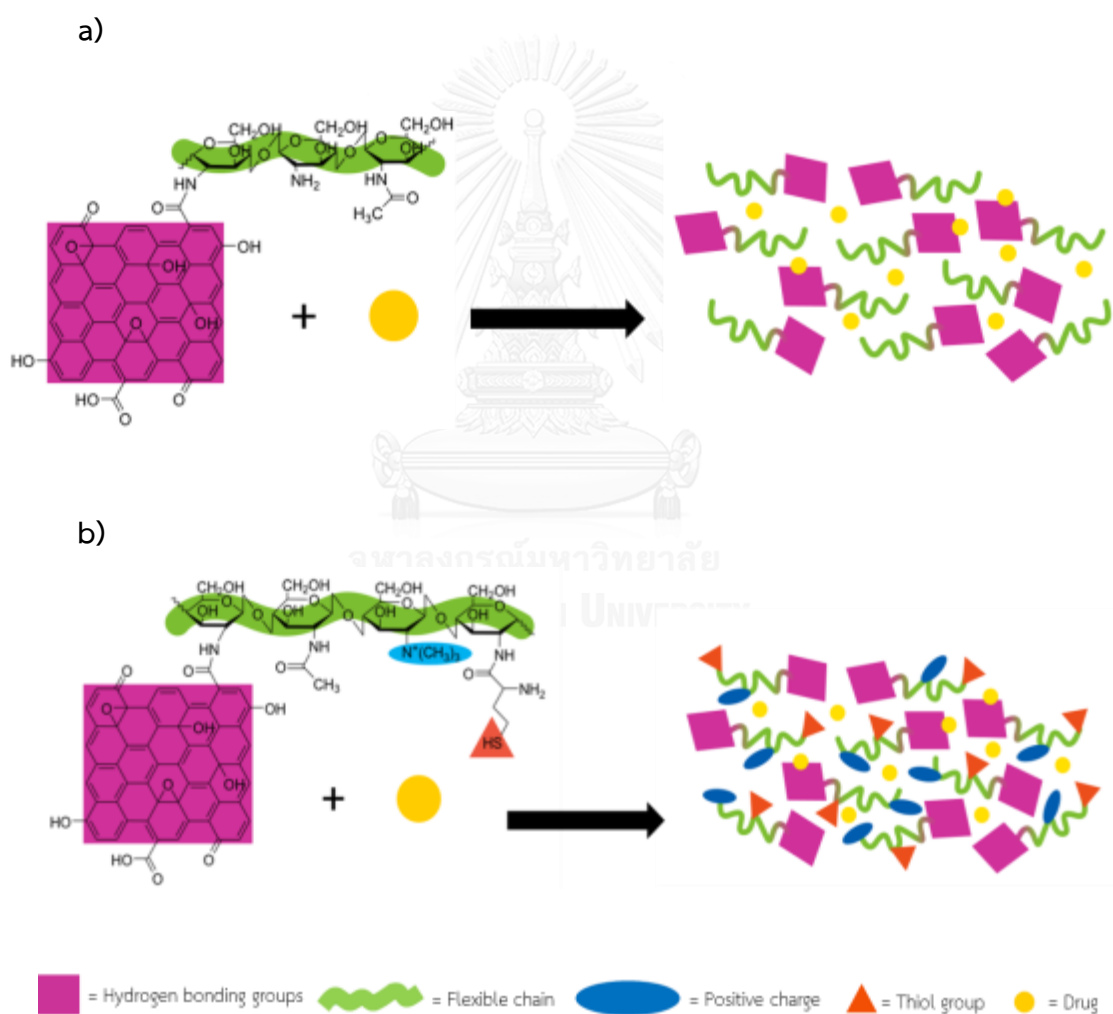


Figure 7 Illustration of drug loaded mucoadhesive nanocomposite

a) G-CS and b) G-TQCS

1.2 The objectives of this research

1) To synthesize graphene oxide modified with thiolated quaternized chitosan as anticancer drug delivery carriers at the gastrointestinal tract for oral administration.

2) To improve mucoadhesive property, biocompatible and control release efficiency of the obtained composite film (G-TQCS-Cur) that loaded aromatic structure and poor solubility anticancer drug at low pH environment.

1.3 The scope of research

The scope of this research was carried out by stepwise methodology as follows:

- 1) Review literature for related research work.
- 2) Modified graphene oxide
 - a. Preparation of thiolated quaternized chitosan, graphene oxide, graphene oxide- chitosan and graphene oxide-thiolated quaternized chitosan.
 - b. Characterization of the physical and chemical properties of graphene oxide and modified graphene oxide with chitosan and thiolated quaternized chitosan using elemental and morphology analysis, FTIR, ¹H-NMR, TGA, SEM and AFM.
 - c. Determination degree of quaternization (positive charge on side chain).
 - d. Determination degree of thiol and disulfide substitution.

e. Investigation of mucoadhesive property at pH 1.2 in simulated gastric fluid (SGF), pH 4.0 and simulated intestinal fluid (SIF) pH 6.4 by using UV-Vis spectrometry.

3) Drug-loaded composite films as drug delivery carrier

a. Preparation of the curcumin loading on composite to form drug-loaded composite films.

b. Characterization of the obtained drug-loaded composite films in terms of chemical analysis and morphology by FTIR and AFM.

c. Determination of the drug entrapment efficiency.

d. Study the In vitro release behavior of the drug-loaded composite films in simulated gastrointestinal fluid pH 1.2 and 6.4 using UV-Vis method.

4) Study *in vitro* cytotoxicity of drug-loaded composite films at various times

a. Determination of the cell viability of composite films with and without Cur by MTT assay at incubation time for 24, 48 and 72 h.

5) Report, discussion and writing up thesis.

CHAPTER II

THEORY AND LITERATURE REVIEWS

2.1 Cancer

Cancers are an evolutionary process as somatic cells mutate that untoward expansion and divide rapidly of normal cells (Fig. 8). Cancer is the crucial cause of death worldwide, according to the World Health Organization (WHO) that most of cancer deaths occurred in developing countries [1]. Cancer arises by the interaction of genetic vulnerability and environmental pollutants. The various treatment of cancer is such as dietary phytochemicals, chemotherapy, surgery, immunotherapy, photothermal therapy in order to prevent uncontrolled cell division. The possibility of reduced risk for the major cause of cancer depends on the food habit with greater fruits and vegetables in the diet [24].

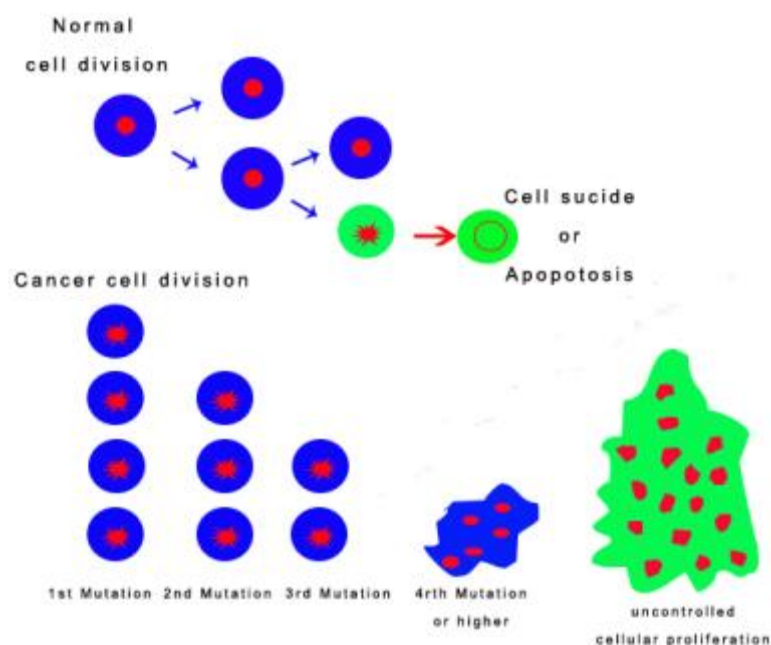


Figure 8 Cell division of normal and cancer cell [35]

2.2 Controlled release system

Controlled drug delivery system is the process as drug or other active agents entrapped within a suitable carrier that the active agent is released from the carrier in a predesigned manner to enhance efficiency of therapy (Fig. 9). The benefit of these are shielded drug from premature degradation, reduced dosage and delivered drug directly to specific target that suitable transport the drug through the part of body.

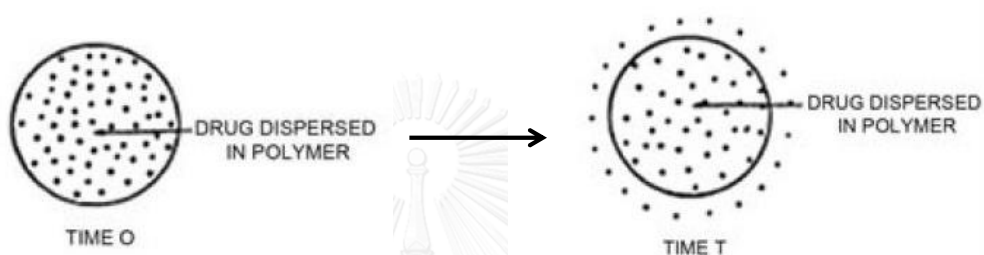


Figure 9 Presentation of controlled release system

Drug concentration at the site of action must be maintained at a level that provides maximum safe concentration (MSC) and minimum effective concentration (MEC). Figure 10 show the drug concentration in plasma profile for oral administration by conventional tablet and controlled release formulation. The pattern of drug release from controlled release formulation is purposely changed release from a conventional formulation (immediate-release) that achieved a desired therapeutic purpose or reduced side effect of drug [36].

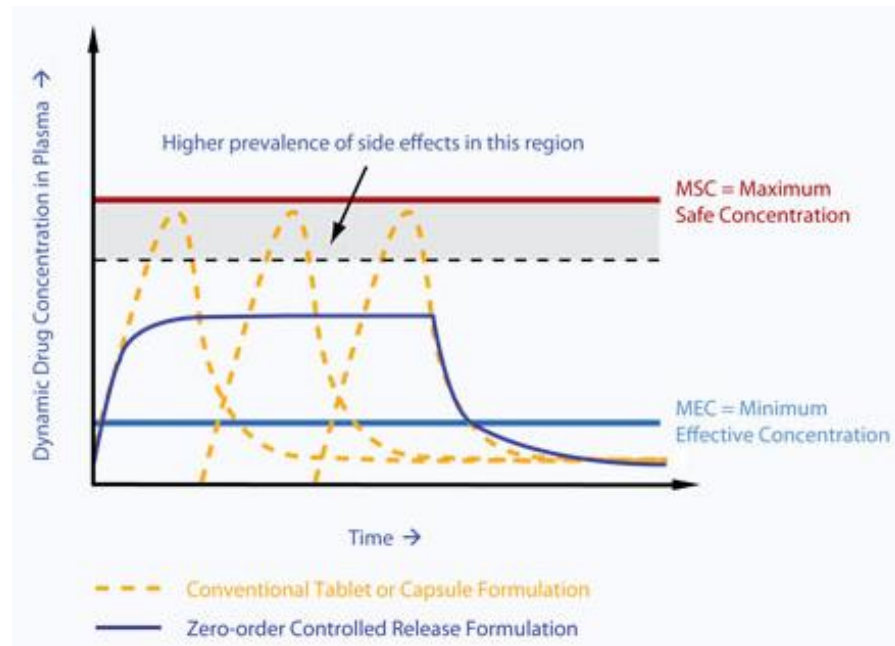


Figure 10 An illustration of the zero-order controlled drug release [37]

The drug can be released from the system by 3 mechanisms [38].

2.2.1 Diffusion-controlled drug release

Diffusion of a drug molecules occurs when it pass from the polymer matrix to the external environment. This system requires a longer diffusion time to progressively release drug through a polymeric membrane forms (Fig. 11).

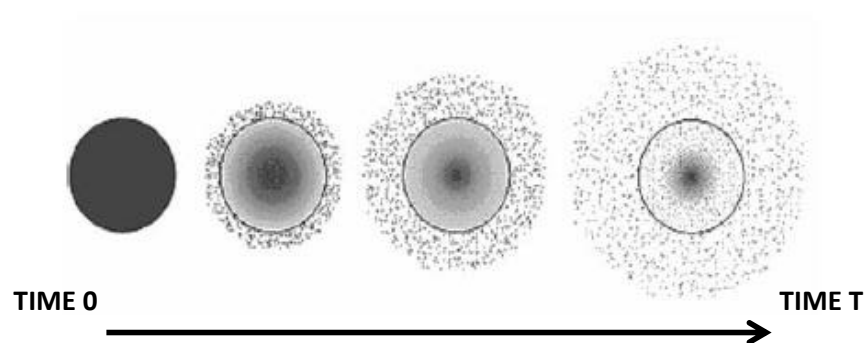


Figure 11 Presentation of diffusion controlled release

2.2.2 Swelling-controlled release

The swelling of the drug carrier occurs when diffusion of drug is faster than hydrogel swelling. The aqueous solvent content within the polymer matrix increases that enable the drug diffuse through the swollen carrier into the external environment. The factor of swelling of the drug carrier is a change of the environment surrounding such as pH, temperature, ionic strength, etc.

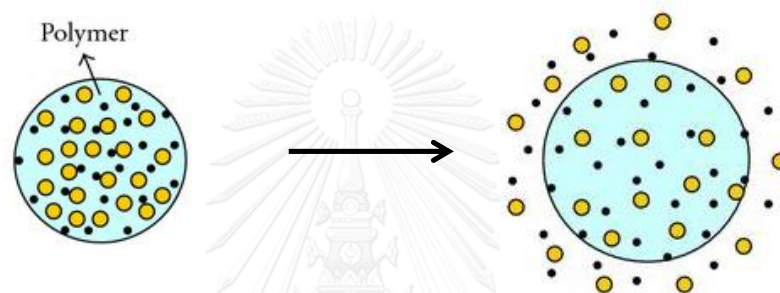


Figure 12 Presentation of swelling controlled release

2.2.3 Erosion Controlled Release

The drug can be released from the matrix due to erosion of polymers, which can be classified into 2 types.

Bulk erosion: The polymer degrades in a fairly uniform manner throughout the polymer matrix.

Surface erosion: The degradation occurs only at the surface of the polymer device.

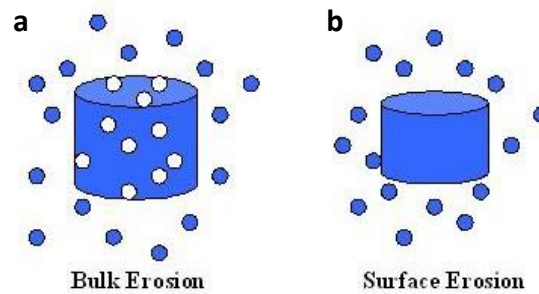


Figure 13 Presentation of erosion controlled release: a) Bulk erosion and b) Surface erosion

2.3 Mucoadhesive property

Mucoadhesion is the term of adhesion of materials that occurs on mucosal membranes in the human body for enhancing retention time at target sites and to improve the specific localization of drug delivery systems on various membranes. It has been widely promoted as a way of achieving site-specific drug delivery through the incorporation of suitable mucoadhesive polymers and drug that attach to a biological substrate (mucous layer). The advantages associated with the use of bio/mucoadhesive drug delivery systems include [3, 7, 39]:

- Increased the residence time of the dosage form at the site of absorption
- Decreased drug concentration for disease treatment at the absorption site therefore improving bioavailability of systemically delivered drugs.
- Reduced side effect that may be caused by systemic administration of drugs.
- Allowed for possible targeting of particular sites or tissues, for example the gastrointestinal tract (GI).

2.3.1 Mucous interaction

The mucus is a highly hydrated protein gel layer that covers the mucosal surfaces (gastrointestinal, pulmonary, oral and nasal). Its general function of the mucus is to protect mucosal tissues from dehydration, mechanical stress, harmful microorganisms and toxic substances. Mucus mainly consist of water (>95%) and mucins, which are highly glycosylated. Apart from glycosylated domains, mucins also contain “naked domains” with non-glycosylated (secretory IgA, lysozyme, lactoferrin, lipids, polysaccharides, and various other ionic species) and are enriched in cysteine residues. The cysteine residues can form intermolecular bonds, and in the native state mucins are often found as oligomers composed of several end-to-end linked mucin subunits (Fig. 14). A common feature of mucins is the abundance of negatively charged groups. The negative charges arise mainly from sialic acid residues ($pK_a \approx 2.6$) and in some cases from sulphated sugars ($pK_a \approx 1$) resulting in their complete ionization under physiological conditions. These acidic groups account for the low isoelectric point of mucins [40, 41].

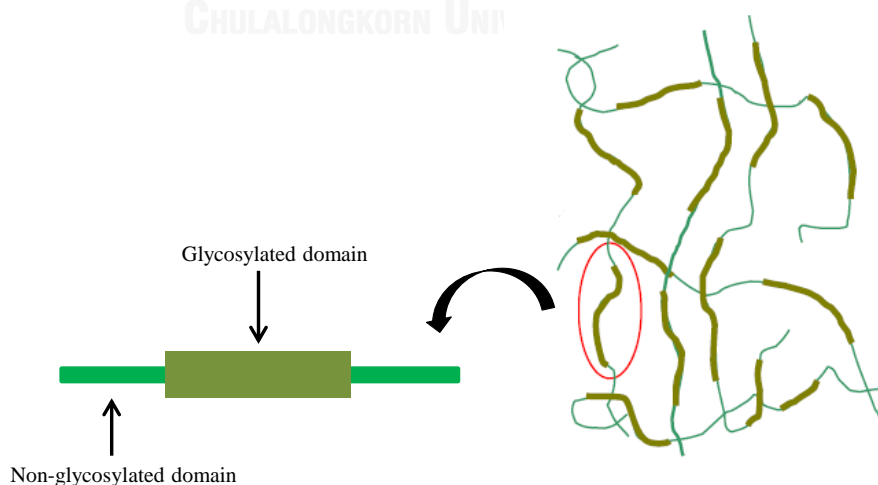


Figure 14 A proposed illustration of mucin [3]

For adhesion to occur, molecules must bond across the interface. These bonds can arise in the following way.

- Ionic bond is a bond of interaction of two oppositely charged ions via electrostatic interactions to form a strong bond.
- Covalent bond is a bond of sharing valence electrons between atoms in order to “fill” the orbitals in both. These are also strong bonds.
- Hydrogen bond is an interaction bond of hydrogen atoms covalently with electronegative atoms such as oxygen, fluorine or nitrogen, carries a slight positively charge and therefore is attracted to other electronegative atoms. The hydrogen is generally weaker than ionic or covalent bonds.
- Van-der-Waals bonds are some of the weakest forms of interaction that occurs from dipole–dipole and dipole-induced dipole attractions in polar molecules, and dispersion forces with non-polar substances.
- Hydrophobic bonds as the hydrophobic effect, these occur when non-polar groups are present in an aqueous solution. Water molecules adjacent to non-polar groups form hydrogen bonded structures, which lowers the system entropy. There is an increase in the tendency of non-polar groups to associate with each other to minimise this effect.

2.3.2 Mechanism mucoadhesion of polymer attachment

Mucoadhesion is a complex process and numerous theories include wettability, electrostatic, diffusion–interlocking, adsorption and fracture processes. These numerous theories should be considered as supplementary processes involved in the different stages of the mucus/substrate interaction, rather than individual and alternative theories. The mechanism of mucoadhesion is an adhesive process in two steps, the contact stage and the consolidation stage (Fig. 15).

- The contact stage: An intimate contact occurs between the mucoadhesive and mucous membrane, with wetting and swelling of the formulation, initiating its deep contact with the mucus layer. The gastrointestinal tract is an example of an unapproachable mucosal surface where the adhesive material cannot be placed directly onto the target mucosal surface, but an adhesion in the esophagus can occur [42].
- The consolidation stage: The mucoadhesive materials are activated by the presence of moisture, which will effectively plasticize of the system permission mucoadhesive molecules to become free and to link up by weak van der Waals and hydrogen bonding. Various physicochemical interactions occur to consolidate and strengthen the adhesive joint, leading to prolonged adhesion [43].

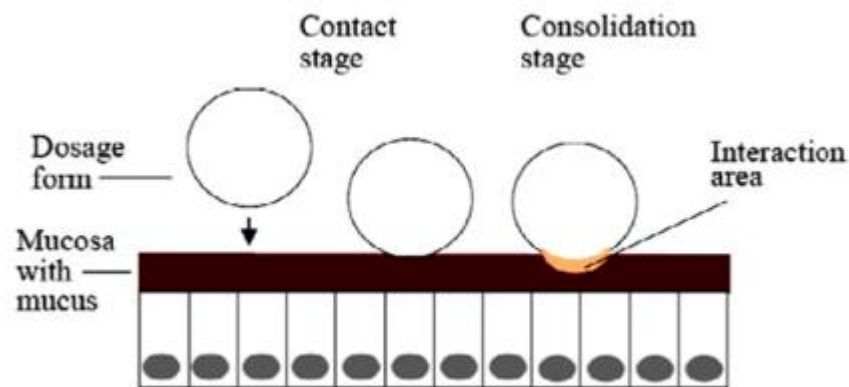


Figure 15 The two steps of the mucoadhesion [3]

2.3.3 Factors affecting mucoadhesion

The effect on the mucoadhesive properties of polymer systems have been several factors the below mentioned

1. Polymer-Related Factors

- Functional group contribution: The secondary bonding mainly arises due to hydrogen bond formation, it is well accepted that mucoadhesive polymers possessing hydrophilic functional groups such as, carboxyl (COOH), hydroxyl (OH), amide (NH₂) and sulphate groups (SO₄H) may be more favorable in formulating targeted drug delivery system.

- Degree of hydration: Adhesion is thought to be a result of a combination of capillary attraction and osmotic forces between the dry polymer and the wet mucosal surface which act to dehydrate and strengthen the mucus layer. In this situation cross-linked polymers that only permit a certain degree of hydration may be advantageous for providing a prolonged mucoadhesive effect.

- Polymer molecular weight, chain length, conformation, and degree of cross-linking: A large molecular weight is essential for entanglement; however, excessively long polymer chains lose their ability to diffuse and interpenetrate mucosal surfaces. It is generally understood that the threshold required for successful bioadhesion is least 100,000 molecular weight. The degree of cross-linking within a polymer system significantly influences chain mobility and resistance to dissolution. Chain flexibility is critical for interpenetration and entanglement with the mucus gel. Increased chain mobility leads to increased inter-diffusion and interpenetration of the polymer within the mucus network.

2. Environment Related Factors

There are numerous environmental and physiological factors that will have a marked effect on the mucoadhesive strength of polymer

systems. Macromolecular charge is affected by the pH of the physiological environment due to the dissociation of functional groups. Moreover, above the pK_a of mucin a net negative charge may result in the repulsion of anionic species. Additionally, the ionic strength of the surrounding medium may also have a significant role in defining the mucoadhesive bond force. In general mucoadhesion strength is decreased in the presence of ions due to shielding of functional sites that are pertinent for adhesion processes and importantly, gel network expansion.

2.3.4 Polymer used for oral mucoadhesive drug delivery

The mucoadhesive polymer should have high levels of mucoadhesive bonds include hydrophilicity, negative charge potential and the presence of hydrogen bond forming groups. Furthermore, it should be sufficient flexibility to penetrate the mucus network, biocompatible, non-toxic and economically favorable. Polymers with hydroxyl or carboxyl groups on their surface had been earlier claimed as the most desirable candidates for bioadhesion. The characteristics of an mucoadhesive polymer such as: [44]

- Polymer and its degradation products should be non-toxic, non-irritant and free from leachable impurities
- Good spread ability, wetting, swelling, solubility and biodegradability properties
- Form a strong non covalent bond with mucin epithelial cell surfaces
- Quickly adhere to moist tissue and possess site specificity
- Allow easy incorporation of the drug and offer no hindrance to its release

- Polymer must not decompose on storage or during shelf life of dosage form
- Cost effective.

2.4 Graphene oxide

Graphene oxide (GO) is a highly oxidized form of chemically modified graphene that consists of single atom thick layer of graphene sheets with carboxylic acid, epoxide and hydroxyl groups in the plane (Fig. 16) [9]. This gives GO good dispersibility in many solvents, particularly in water. In addition, the peripheral carboxylate group provides colloidal stability and pH-dependent negative surface charge [45]. The reactive oxygen functional groups of GO exhibits strongly hydrophilic and enhanced chemical activity compared with pristine graphene, which renders it a good candidate for use in the biomedical applications through chemical functionalizations.

The most common method adapted for large-scale production of GO is developed by Hummers et al [46]. The Hummers method uses a combination of sulfuric acid and potassium permanganate as an oxidant. These methods require extensive oxidation of aromatic structure in order to weaken Van der Waals interaction between graphene sheets followed by exfoliation of graphene and dispersion in solution.

It is well known that the surface chemistry of nanomaterials is a key to building drug carriers with good biocompatibility and controlled behavior in biological systems. Therefore, the modification of GO to build desired drug carriers is of great significance.

The chemically modified GO using various chemical reactions that provide for either covalent or non-covalent attachment. GO can be covalently functionalized using specially selected small molecules or polymers through activation and amidation or esterification of either the carboxyls or hydroxyls in GO via coupling reactions. The epoxy groups can be also used for the covalent functionalization of GO through ring-opening reactions due to a nucleophilic attack at the α -carbon. Moreover, the non-covalent functionalization of GO can also be accomplished via π - π stacking, cation- π , van der Waals interactions, or hydrogen bonding [10].

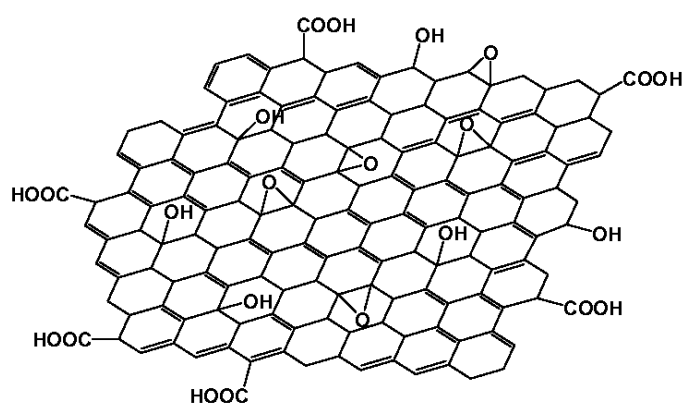


Figure 16 The structural model of graphene oxide (GO)

In order to use GO for clinical applications, it is essential to confirm their biocompatibility and toxicity through extensive in vitro and in vivo studies using cells and animal models. GO sheets contain a large amount of hydrophilic groups (carboxyl, hydroxyl and epoxy groups) on their edge or basal planes, and their hydrophilicity is significantly increased. These enhanced their biocompatibility in comparison with graphene. The surface modifications of GO can

significantly reduce their toxic interactions with living systems [14, 47, 48]. Therefore, GO may be a highly biocompatible nanomaterial.

2.5 Thiolated polymer

Thiolated polymer is a new generation of mucoadhesive polymer from hydrophilic polymers such as polyacrylates, chitosan, carboxymethylcellulose or polyvinyl alcohol. The presence of thiol groups allows the formation of covalent bonds with cysteine-rich subdomains of the mucus gel layer (Fig. 17), leading to increased residence time and improved bioavailability [3]. In this respect thiomers mimic the natural mechanism of secreted mucus glycoproteins that are also covalently anchored in the mucus layer by the formation of disulphide bonds. Disulphide bonds between thiolated polymers and cysteine-rich subdomains of mucus glycoproteins are supposed to be responsible for the enhanced mucoadhesive properties of polymer [49]. The thiolated polymer have been developed drug delivery systems, Self-assembled nanoparticles between TMC-Cys and negatively charged protein drugs could be a promising vehicle for oral delivery and enhancing mucoadhesive properties [17]. The N,N,N-trimethyl-chitosan were synthesized and then grafted with homocysteine thiolactone (HT) exerted higher mucoadhesive property [21]. This considerable improvement in the mucoadhesive properties of thiolated polymers is based on the formation of disulfide bonds between thiol-bearing side chains of the polymer and cysteine-rich subdomains of mucus glycoprotein. Furthermore, the results of this study showed that improved mucoadhesive properties of thiolated polymers are strongly pH dependent

[8, 49]. At pH > 5, thiol groups become more reactive leading to the formation of disulfide bonds already within the polymeric network itself before reacting with disulfide and/or thiol substructures of the mucus. Their thiol groups become only reactive when interpenetrating the mucus gel layer exhibiting pH 5–7. Consequently thiomers of a comparatively lower pH form likely more disulfide bonds with the mucus layer [7].

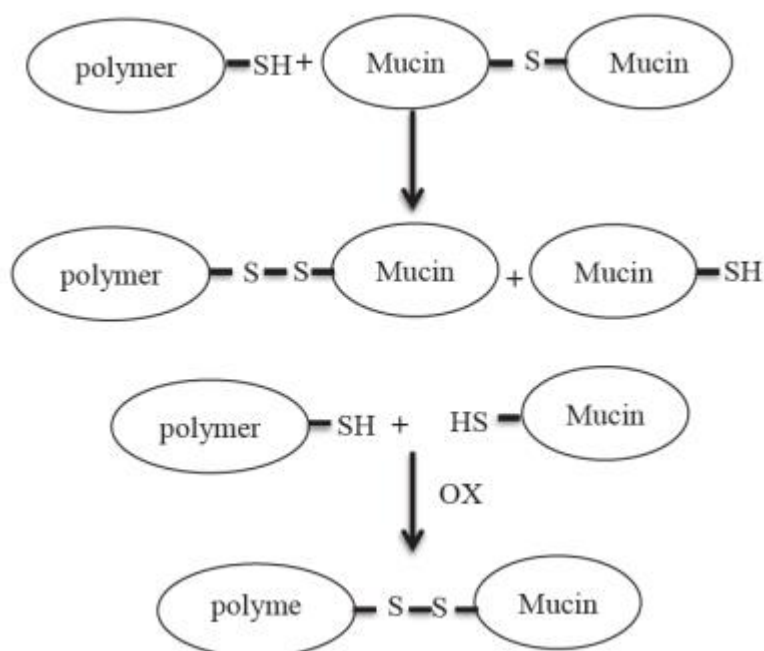


Figure 17 The formation of covalent bond between thiolated polymer and mucin [8]

2.6 Curcumin

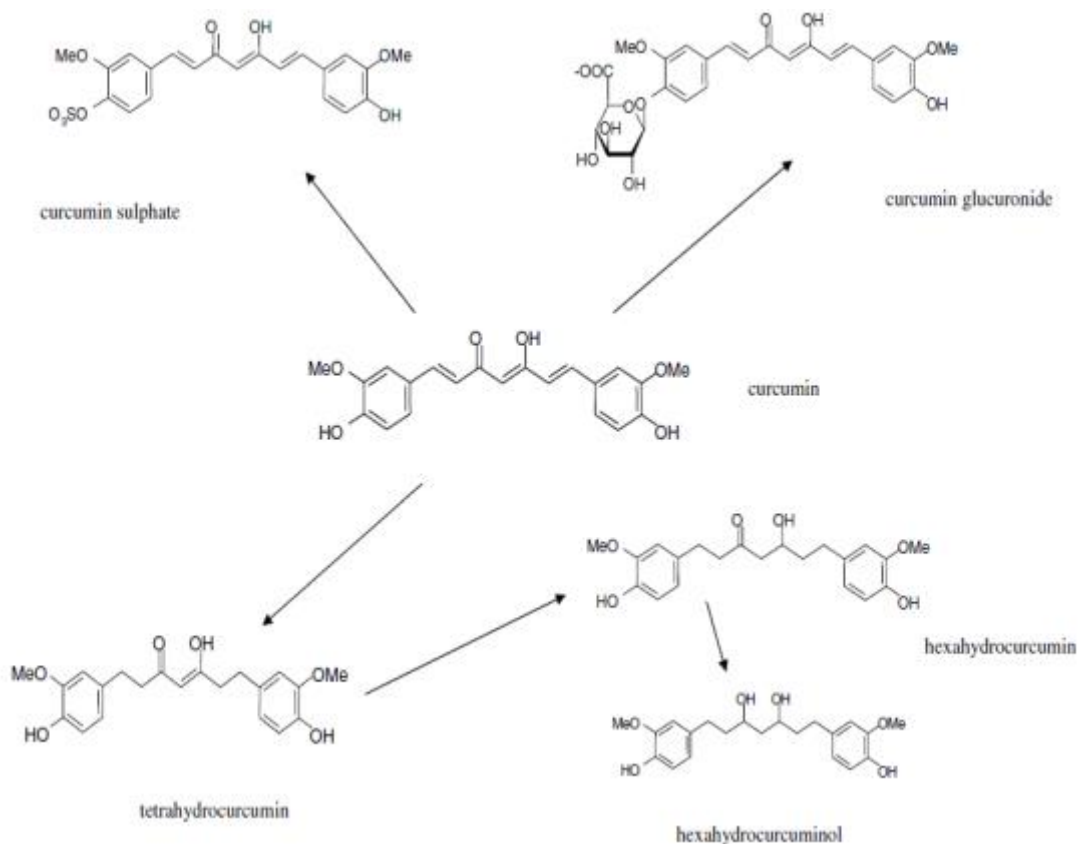
Curcumin is a hydrophobic polyphenol isolated from dried rhizome of turmeric (*Curcuma Longa* Linn), which is the herbal remedy and dietary spice. It has been used from the time immemorial as a dietary supplement, coloring agent, spice and also for curing the diseases. A vast research revealed that curcumin has a wide range of therapeutic effects

such as anti-inflammatory, antibacterial, antifungal, anticancer, antioxidant [50].

Curcumin with its proven anti-inflammatory and antioxidant properties has been exhibited a variety of beneficial effects and appears to have a significant potential in the treatment of multiple diseases that are a result of oxidative stress. It was shown to be a potent scavenger of a variety of reactive oxygen species including superoxide anion radicals, hydroxyl radicals and nitrogen dioxide radicals [29]. In vivo and in vitro studies have demonstrated curcumin's ability to inhibit carcinogenesis at three stages: tumor promotion, angiogenesis and tumor growth. Curcumin has shown growth inhibitory effects in vitro in cancer cell lines derived from human prostate, large intestine, bone and leukaemia.

Curcumin can exist in at least two tautomeric forms, keto and enol. The enol form is more energetically stable in the solid phase and in solution. Stability of curcumin increases in acidic and decreases as the pH increases. Also in the presence of light the degradation was much higher as compared to in the absence of light. It has been found that that curcumin at pH 1.2 is highly stable. On the other hand, stability of curcumin decreases and decomposed rapidly in buffer solutions, neutral-basic pH conditions [34]. Curcumin is a light sensitivity sample that should be protected from light.

Curcumin has a molecular weight of 368.37 and a melting point of 183°C. Commercial grade curcumin contains the curcuminoids desmethoxycurcumin and bis desmethoxycurcumin (Fig. 18).



Recent concerns regarding the safety of selective enzyme inhibitors in large-scale chemoprevention trials emphasise the importance of carefully evaluating any potential toxicity of agents at the preclinical and early clinical trial levels. The clinical research suggests that an oral dose of 3.6 g daily, is suitable and not associated with adverse effects in humans [51].

However, clinical usefulness of curcumin in the treatment of diseases is limited due to poor aqueous solubility, hydrolytic degradation in alkaline pH, metabolism via glucuronidation and sulfation in the liver and in intestine, and poor oral bioavailability. These limitations results in decreased therapeutic efficacy or absence of therapeutic efficacy in

in-vivo studies. Though there are many novel approaches to overcome these limitations, nanotechnology (Particle size <1000 nm) is the most recent and offer significant improvement.

2.7 MTT assay

The MTT is a colorimetric assay that measures the reduction of yellow 3-(4, 5-dimethylthiazol-2-yl)-2, 5-diphenyl tetrazolium bromide by mitochondrial succinate dehydrogenase. This assay is broadly used to measure the *in vitro* cytotoxic effects of drugs on cell lines or primary patient cells.

The MTT enters the cells and passes into the mitochondria where it is converted to an insoluble purple formazan by cleavage of the tetrazolium ring by dehydrogenase enzymes, which determines mitochondrial activity (Fig. 19). Therefore, for most cell populations the total mitochondrial activity is related to the number of viable cells. The cells are then solubilized with an organic solvent (eg. DMSO) and the released solubilized formazan reagent measure by spectrophotometer [52]. Since reduction of MTT can only occur in metabolically active cells the level of activity is a measure of the viability of the cells.

Additionally, the MTT method of cell determination is useful in the measurement of cell growth in response to mitogens, antigenic stimuli, growth factors and other cell growth promoting reagents, cytotoxicity studies, and in the derivation of cell growth curves. The use of MTT method does have limitations influenced by the physiological state of cells and variance in mitochondrial dehydrogenase activity in different cell types.

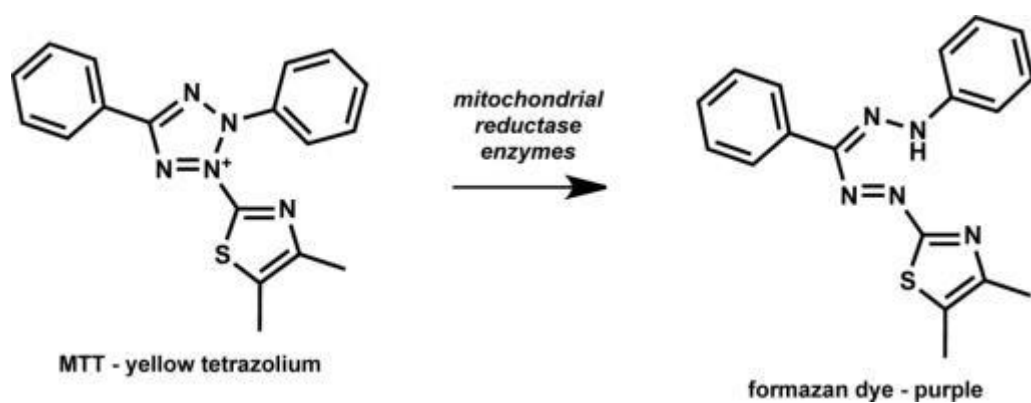


Figure 19 The principle of cytotoxicity (MTT) assay [53]



CHAPTER III

EXPERIMENTAL

3.1 Materials

3.1.1 Polymer and Material

- Chitosan, food grade, MW 500 kDa., Deacetylation 85%, Lot No. 497613, (Seafresh Industry Co. Ltd. Thailand)
- Nanographene powder, average particle size of 6-8 nm (SkySpring Nanomaterials, Inc., USA)

3.1.2 Model drug

- Curcumin powder (CAS number: 458-37-7, ~95% HPLC, Adipogen International, Inc., Thailand)

3.1.3 Cell cultures

- CHAGO and SW620 cell lines, originated from human lung and intestine carcinoma cell lines. All kinds of cells were cultured in RPMI with 10% fetal bovine serum (FBS) (X-Zell Biotech Co, Ltd)

3.1.4 Chemicals

All chemicals and organic solvents were purchased from Sigma Aldrich, Merck, Spectrum Laboratories or Lab-Scan.

- Homocysteine thiolactone (HT)
- Imidazole
- Mucin (type II) from porcine stomach
- Iodomethane
- Sodium hydroxide, analytical grade (NaOH)
- Sodium chloride, analytical grade (NaCl)
- *N*-methyl pyrrolidone (NMP)
- Basic fuchsin (pararosaniline)
- Sodium metabisphite
- *N*-(3-dimethylaminopropyl)-*N*-ethylcarbodiimide hydrochloride
- Periodic acid, analytical grade
- Acetic acid, analytical grade
- Sulfuric acid 98%, analytical grade (H₂SO₄)
- Hydrogen peroxide 30%, analytical grade
- Acetone, commercial grade
- Ethanol 95 %, commercial grade (EtOH)
- Sodium nitrate, analytical grade (NaNO₃)
- Potassium permanganate, commercial grade (KMnO₄)
- 5,5-Dithio-bis(2-nitrobenzoic acid) ; (DTNB)
- Sodium-borohydride (NaBH₄)
- Dialysis tubing (Mw cut-off 12–14 kDa)

3.2 Preparation of graphene oxide conjugated with chitosan and Thiolated quaternized chitosan (G-CS and G-TQCS)

3.2.1 Synthesis of Thiolated quaternized chitosan (TQCS)

The preparation of QCS was synthesized by methylation from CS as previously reported [21]. Briefly, the mixture of 1% (w/v) CS in 1% (v/v) acetic acid solution (100 mL), 15% (w/v) NaOH (5 mL) and 1:1 (v/v) ratio of iodomethane: NMP (30 mL) reacted at 60 °C for 45 min with stirring. For precipitation of QCS used 80% (v/v) ethanol and collected by centrifugation (12000 rpm for 2 min). The QCS precipitate was dissolved in 5% (w/v) NaCl (to exchange I⁻ with Cl⁻) then resolvated in water and precipitated with 80% (v/v) acetone. The QCS collected by centrifugation (12000 rpm for 2 min) and lyophilized at -30 °C and 0.01 mbar. The final product obtained a dry white solid of QCS.

The TQCS was an attachment covalently of QCS with HT. This was achieved by the formation of amide bonds from primary amino groups on QCS chain attack to the carbonyl group of HT. Firstly, 1% (w/v) of QCS in 1% (v/v) acetic acid solution (100 mL) was added to an imidazole solution (0.68 g in 2.5 mL water), followed by gradually drop wise of 0.1% (w/v) of HT and stirred at room temperature under a nitrogen atmosphere for 12 h. Then the mixture was adjusted pH 7, precipitated with acetone and collected by centrifugation (12000 rpm for 2 min). The precipitate was resolvated in water and dialyzed (Mw 12-14 kDa) against changes of 1 L of water for 2 days. The final product was lyophilized at -30 °C and 0.01 mbar and stored the dry white solid of TQCS at 4 °C.

3.2.2 Synthesis of graphite oxide (GO)

The GO was synthesized by a modified Hummers method as previously reported [54]. The 1:1 (v/v) ratio of nanographene or graphite powder: NaNO_3 (6 g) were added in 150 mL concentrated H_2SO_4 (reaction placed in an ice bath), followed by gradually added KMnO_4 (9 g) and stirred at 40 °C in water bath for 2 h. Then the reaction mixture was slowly diluted with de-ionized water causing an increase of temperature to 98 °C. After 20 min, the mixture was added 30% H_2O_2 solution (30 mL) and stirred for 10 min. The mixture solution was filtered and washed with DI water (after resolvated with excess DI water) at room temperature under vacuum until its neutral pH. Finally the precipitate was oven-dried at 50 °C and obtained GO black solid powder.

3.2.3 Synthesis of G-CS and G-TQCS

The G-CS and G-TQCS were prepared by the amidation of GO with CS and TQCS, respectively that used of EDC as a coupling agent [13]. In a typical process, the 10: 1 (w/w) ratio of CS or TQCS (1 g): GO (0.1 g) was dispersed in 1% (v/v) acetic acid solution (100 mL) and sonicated for 2 h to get a homogeneous colloidal suspension. Then the EDC (0.5 g) was added in mixture solution, stirred for 24 h at room temperature and sonicated for 3 h. Thereafter, the reaction mixture was precipitated with acetone and dialyzed (Mw 12-14 kDa) against DI water (1 L) for 2 days at 4 °C. Finally, these were lyophilized at -30 °C and 0.01 mbar to obtain the gray sponge-like of G-CS or G-TQCS. The route schematically summarized of G-CS and G-TQCS were synthesized following in Figure 20 *route A* and *B*, respectively.

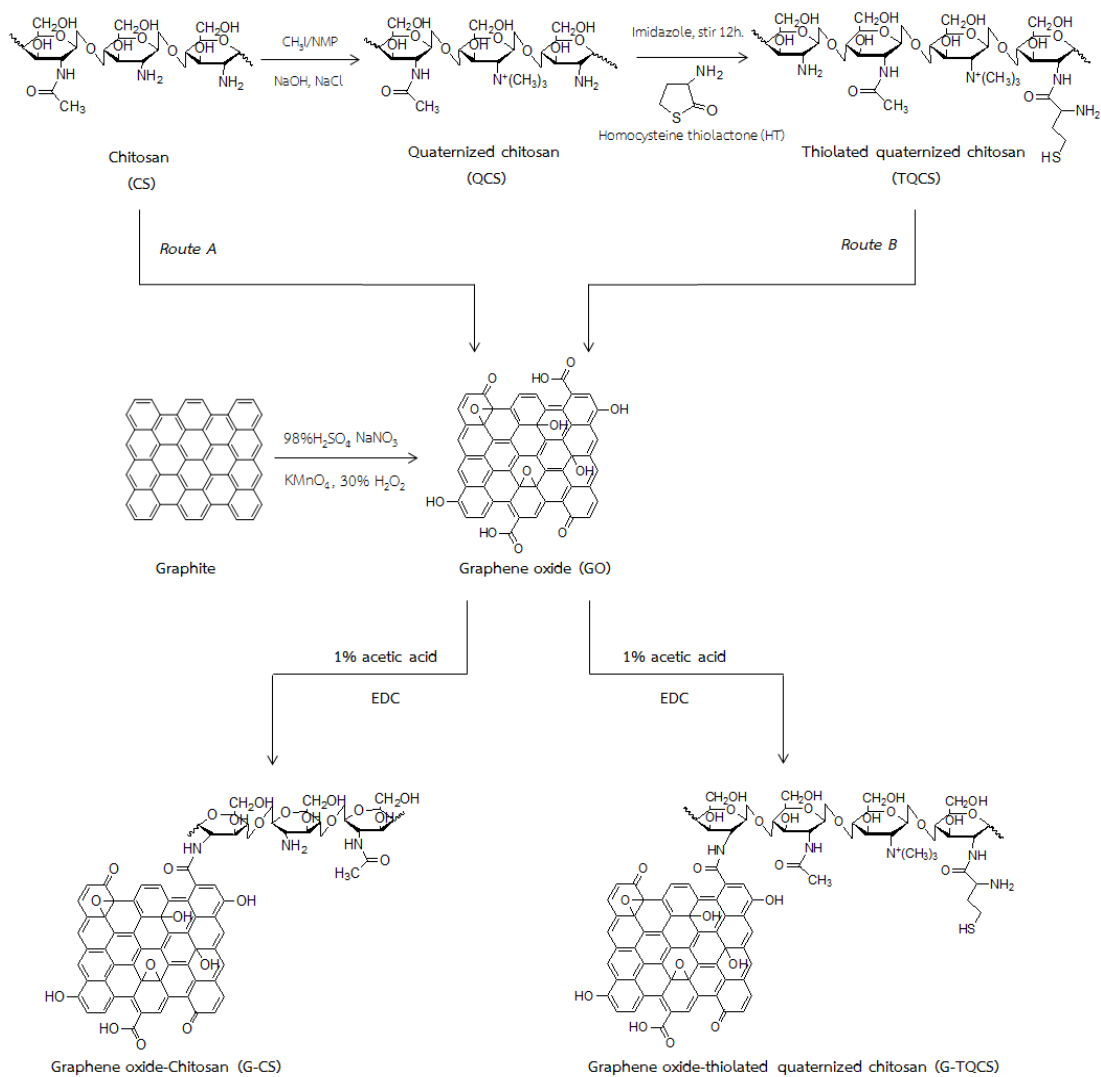


Figure 20 The schematically synthesized of Route A) G-CS and Route B) G-TQCS

3.3 Characterization

3.3.1. Fourier transformed infrared spectroscopy (FT-IR)

The FTIR spectroscopy was employed to confirm functional groups of CS, QCS, TQCS, GO, G-CS and G-TQCS. The dried samples were mixed with dry KBr and pressed into a pellet that analyzed with Nicolet 6700 spectrometer in the region from 4000 cm^{-1} to 400 cm^{-1} .

3.3.2. ^1H Nuclear Magnetic Resonance spectroscopy (NMR)

The ^1H NMR spectra of CS, QCS and TQCS were recorded on Varian XL-400 NMR spectrometer. The preparation of sample solution at concentrations 10 mg/mL was dissolved in D₂O and slightly dropped wise trifluoroacetic acid (CF_3COOH).

The degree of quaternization (DQ) was calculated using the data obtained from the ^1H NMR spectra according to Eq. (1), as previously described [55]

$$\%DQ = \frac{[N^+(\text{CH}_3)_3] / 9}{[H3-H6] / 5} \times 100 \quad (1)$$

Here, $[N^+(\text{CH}_3)_3]$ is the integral of the trimethyl amino group at δ 2.76 ppm and $[H3-H6]$ is the integral of proton in chitosan hexagonal ring in the range of δ 3.57 – 3.38 ppm.

3.3.3 Thermogravimetric analysis (TGA)

The thermal stability of the synthesized sample was evaluated by TGA analysis using a PerKinElmer Pyris Diamond TG/DTA machine under a nitrogen flow at a rate of 25 mL/min. Approximately 2 mg of samples were placed in the alumina pan, sealed and heated from 50 to 600°C.

3.3.4 Scanning Electron Microscope (SEM)

The morphology and surface appearance of GO, G-CS and G-TQCS before drug loading were investigated by SEM using Philips XL30CP. The sample was mounted onto an aluminum stub using double sided carbon adhesive tape and coated with gold-palladium at 18 mA for at least 4 min. The scanning was performed under high vacuum and ambient temperature with beam voltage of 10-20 kV.

3.3.5 Atomic Force microscopy (AFM)

The nanomaterial was confirmed of morphology and their thickness by AFM that performed in tapping-mode using Digital Instrument S3000 AFM. The GO, G-CS and G-TQCS were characterized the morphology and thickness to confirmed the attachment of polymer on GO sheet. The preparation of sample for AFM were dissolved at concentrations 0.01 mg/ml and dropped aqueous sample solution on a fresh silicon wafer, followed by dried under ambient conditions for 24 h.

3.4 Determination of the thiol group and disulfide group content

The amount of thiol groups on TQCS and G-TQCS were determined by UV-Vis spectrophotometer with Ellman's reagent [56]. First, 10 mg of conjugated samples were added in solution of 500 μ L 0.5 M phosphate buffer, pH 8.0 and 500 μ L Ellman's reagent (3 mg of 5, 5'-dithio- bis(2-nitrobenzoic acid) in 10 mL of 0.5 M phosphate buffer, pH 8). Then the samples were incubated for 2 h at room temperature. The supernatant was collected by centrifugation (3200 rpm, 5 min). Finally, 200 μ L of each supernatant were transferred to a microtitration plate and the absorbance was measured at a wavelength of 450 nm. The amount of thiol moieties was calculated from an according standard curve obtained by chitosan solution with increasing amounts of cysteine standards.

The amount of disulfide bonds within the obtained TQCS and G-TQCS were evaluated to the following test. Firstly, the TQCS and G-TQCS (10 mg) were hydrated in 1 mL of 50 mM phosphate buffer pH 8.0 for 30 min. The solution was added 3% NaBrH solution (600 μ L) and incubated for 2 h in an oscillating water bath at 37 °C. The 1M HCl (500 μ L) was added in order to destroy the remaining NaBrH. Following by the addition of acetone (100 μ L) that the mixture was agitated for 5 min. After, 1M phosphate buffer pH 8.5 (1 mL) and 0.5% (w/v) DTNB dissolved in 0.5M phosphate buffer pH 8.0 (200 μ L) were added in mixture solution. Incubation for 15 min at room temperature aliquots of 200 μ L were transferred to a 96-well microtitration plate and the free sulfhydryl groups were determined by measured at a wavelength of 450 nm. The amount of disulfide bonds was calculated by subtracting the quantity of free thiol groups as evaluated by the method described above

from the total quantity of thiol moieties present on the TQCS and G-TQCS.

3.5 In vitro bioadhesion of mucin to CS, TQCS, GO, G-CS and G-TQCS

The Periodic Acid Schiff (PAS) is the method used for both the quantitative and qualitative analysis of mucopolysaccharides in tissue and cell. The PAS colorimetric assay for the determination of the free mucin concentration was used as previously reported [44], as to evaluate the amount of mucin adsorbed onto the composites.

The preparation of Schiff reagent contained 100 mL of 1% (w/v) basic fuchsin (pararosaniline) in an aqueous solution and 20 mL of 1 M HCl. Sodium metabisulfite (1.67% (w/v) final) was added before use, and the mixture solution was incubated at 37 °C until it became colorless or pale yellow. Periodic acid reagent was freshly prepared by adding 50% (v/v) periodic acid solution (10 μ L) to 7% (v/v) acetic acid solution (7 mL). Standard calibration curves were prepared from the five mucin standard solutions in the range of 0.1 - 0.5 mg/mL in each of different buffer (at pH 1.2, 4.0 and 6.4). After adding 0.1 mL of periodic acid reagent, the solutions were incubated at 37 °C for 2 h then added 0.1 mL of Schiff reagent and incubated at room temperature for 30 min. Next 100 μ L aliquots of the solution were transferred in triplicate into a 96-well microtiter plate and the absorbance at 555 nm was recorded. The mucin contents were calculated by reference to the standard calibration curve.

A 0.5% (w/v) mucin solution in each of three buffer solutions that differ in pH, namely SGF (pH 1.2), 0.1 M sodium acetate buffer (pH 4.0) and SIF (pH 6.4) media, were prepared. The samples were dispersed at concentration 10 mg/mL in the above mucin solutions, vortexed, and shaken at room temperature for 3 h. Then the dispersions were centrifuged at 12000 rpm for 2 min. The supernatant was harvested and used for the measurement the absorbance at 555 nm of the free mucin content. The mucin concentration was calculated by reference to the calibration curve. The amount of mucin adsorbed onto the CS, TQCS, GO, G-CS and G-TQCS were calculated as the difference between the total amount of mucin added and the free mucin content in the supernatant.

3.6 Pharmaceutical applications

A pharmaceutical application potential of the covalent functionalization of GO with CS and TQCS (G-CS and G-TQCS) as drug delivery carriers, the curcumin (Cur) was the representation model anticancer natural drug for studying the drug delivery carrier. The properties of drug loaded composite film such as characterization, morphology, entrapment efficiency, drug release profiles and in vitro cytotoxic effect on cancer cell were investigated.

3.6.1 Preparation of curcumin loaded composite films

In order to study pharmaceutical application potential of samples (CS, TQCS, GO, G-CS and G-TQCS) as drug delivery carriers, Cur was used as a model anticancer natural drug. CS, TQCS, GO and modified

GO were used to prepared composite film due to high mucoadhesion especially at low pH environment. The composite films loaded 10% (w/w) Cur were prepared by combination of Cur solution with CS, TQCS, GO or modified GO solution. The physical entrapment of Cur in CS, TQCS, GO, G-CS and G-TQCS were carried out as follows firstly preparation of a stock solution of Cur (20 mg) was dissolved in small quantity of ethanol for loaded in each of sample. 200 mg of CS, TQCS, GO, G-CS and G-TQCS were dissolved in 1% (v/v) acetic acid solution (50 mL) under stirring. Cur was loaded into each of sample solution by drop wise of Cur solution under continuous stirring for 3 h. The mixture solution was decanted to the film mould and air dried for 24 h resulting in the formation of Cur-loaded composite films.

3.6.2 Characterization of the Cur-loaded composite films

3.6.2.1 Fourier Transform Infrared (FTIR) Spectroscopy

The FTIR spectra of the Cur-loaded composite films were examined by using the Attenuated Total Reflection (ATR) mode with a Fourier transform infrared (FTIR) spectrometry (Nicolet 6700) in the range of 4000-400 cm^{-1} .

3.6.2.2 Atomic Force microscopy (AFM)

The thickness and phase image of Cur-loaded GO, G-CS and G-TQCS films were analyzed by AFM with Digital Instrument S3000 AFM that used in tapping-mode. The preparation of Cur-loaded GO, G-CS and G-TQCS films for AFM analysis, These were dissolved in 1% (v/v) acetic acid solution at concentrations 0.01 mg/ml and dropped aqueous

sample solution on a fresh silicon wafer, followed by dried under ambient conditions for 24 h.

3.6.3 Study of the drug behavior of the Cur-loaded composite films

3.6.3.1 Calibration curve of Cur in Ethanol (EtOH)

The standard stock Cur solution was prepared in ethanol at concentration 10 $\mu\text{g/mL}$. 1 mg Cur was dissolved in 1 mL ethanol and adjusted volume to 100 mL. The standard Cur solution was diluted to 8, 6, 4 and 2 $\mu\text{g/mL}$ with ethanol. The absorbance of standard solution was determined by UV-Vis spectrophotometer at 428 nm. The ethanol was used as a reference solution. The absorbance and calibration curve of Cur in ethanol was shown in appendix 1C

3.6.3.2 Calibration curve of Cur in various PBS buffers (pH 1.2 and 6.4)

The standard stock Cur solution was prepared in mixture solvent of the 80:20 (v/v) ratio of PBS buffer (at pH 1.2 and 6.4): EtOH. Cur (1 mg) was dissolved in mixture solvent (1 mL) and adjusted to volume 100 mL at concentration 10 $\mu\text{g/mL}$. The stock Cur solution was diluted to 8, 6, 4 and 2 $\mu\text{g/mL}$ with mixture solvent of two different buffers in volumetric flask. The absorbance of standard solution was determined by UV-Vis spectrophotometer at 428 nm. The mixture solvent of the 2:1 (v/v) ratio of PBS buffer (at pH 1.2 and 6.4): EtOH was used as a reference solution.

The absorbance and calibration curve of Cur in mixture solvent was shown in appendix 2C-3C.

3.6.3.3 Determination of drug loading and entrapment efficiency

To determine the loading and entrapment efficiency of Cur immobilized onto CS, TQCS, GO, G-CS and G-TQCS that 5mg of composite films were immersed in 10 mL of EtOH. The mixture solution was stirred at room temperature for 1 h. A yellowish supernatant was collected and determined by UV-Vis spectrophotometer at 428 nm. All experiments were performed in triplicate. The percentage of loading and entrapment efficiency of Cur was calculated from the following Eq. (2) and (3), respectively:

$$\text{Loading efficiency (\%)} = \frac{\text{Original-unbound Cur (mg)}}{\text{Total amount of composite film (mg)}} \times 100 \quad (2)$$

$$\text{Entrapment efficiency (\%)} = \frac{\text{Total amount of Cur (mg)-unbound Cur (mg)}}{\text{Total amount of Cur (mg)}} \times 100 \quad (3)$$

3.6.3.4 *In vitro* drug release

The Cur release from composite films (CS-Cur, TQCS-Cur, GO-Cur, G-CS-Cur and G-TQCS-Cur) was studied at two different pH values (1.2 and 6.4). The Cur has low solubility in pure water and aqueous acid solutions, but has good solubility in solvents such as ethanol, acetone and dimethylsulfoxide therefore we used the mixture

solvent containing 80:20 (v/v) ratio in each of the different buffer solution at pH 1.2 (SGF) and pH 6.4 (SIF) : ethanol to determine quantities of cur release from composite films [57]. 10 mg of the Cur-loaded composite film was immersed into 5 mL of a mixture solvent in a tube. Tubes were incubated at 37 °C under gentle shaking at speed of 100 rpm. The incubated solution was collected in each for a time-dependent release study at time intervals of 0.5, 1, 3, 6, 9, 11 and 24 h and equal volume of mixture solvent was compensated. The supernatant of released Cur was analyzed by UV-Vis spectrophotometer at 428 nm. The amount of Cur released was calculated using standard calibration curve of Cur in various PBS buffers (pH 1.2 and 6.4). The percentage of cumulative Cur release was calculated from Eq. (4).

$$Release (\%) = \frac{Amount\ of\ released\ Cur\ (mg)}{Total\ amount\ of\ Cur\ (mg)} \times 100 \quad (4)$$

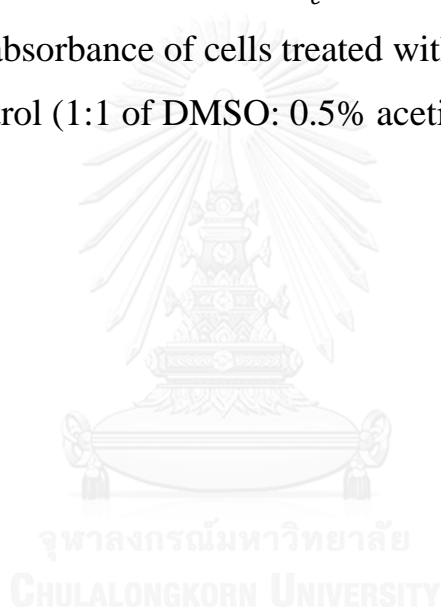
3.7 Cytotoxicity assay

Cytotoxicity studies of sample (CS, TQCS, GO, G-CS and G-TQCS) before and after loaded Cur against cancer cell lines (CHAGO and SW620) were determined by MTT assay. The MTT assay is a colorimetric test based on the selective ability of viable cells to reduce the tetrazolium component of MTT to purple formazan crystals. For each kind of cells at a density of 5×10^3 cells (200 μ L/well) were seeded into 96-well plates and incubated at 37 °C for 24 h. The cells were incubated with 2 μ L of different concentration of sample solutions (300, 100, 10, 5, 1 μ g/mL) and free Cur (20, 5, 1, 0.5, 0.1 μ g/mL) for various period of

time 24, 48 and 72 h. 10 μL of MTT solution (5 mg/mL in NSS) was added to each well and incubated at 37 $^{\circ}\text{C}$ and 5% CO_2 for 4 h. Then, the medium were removed and the formazan crystals were solubilized with 150 μL DMSO. The percentage of cell viability was determined by measuring absorbance at 540 nm and calculated using the following Eq. (5). Triplicate samples were analyzed for each experiment.

$$\text{Cell viability (\%)} = \frac{N_t}{N_c} \times 100 \quad (5)$$

Where N_t is the absorbance of cells treated with sample and N_c is the absorbance of control (1:1 of DMSO: 0.5% acetic acid)



CHAPTER IV

RESULT AND DISCUSSION

4.1 Synthesis of GO, TQCS and G-TQCS

In this work, I attend to synthesize the modified mucoadhesive composite of graphene oxide (GO) and thiolated quaternized chitosan (TQCS) as drug delivery carrier, particularly at low pH environment. Firstly, the GO was prepared by oxidizing purified natural graphite or graphene powder *via* modified Hummers method [54]. Secondly, the TQCS was prepared by the amidation process of quaternized chitosan (QCS) and homocysteine thiolactone (HT) that using imidazole to produce reactive intermediate of HT *via* ring-opened reaction [21]. Finally, the G-TQCS was synthesized by covalent attachment of GO to TQCS *via* coupling the carboxylic acid group (-COOH) of GO to primary amine group (-NH₂) of TQCS that using N-(3 Dimethylaminopropyl)-N'-ethylcarbodiimide hydrochloride (EDC) as a coupling agent (Fig. 21). The final G-TQCS obtained a dark gray spongy-like tissue after that it was characterized to confirm the chemical structure.

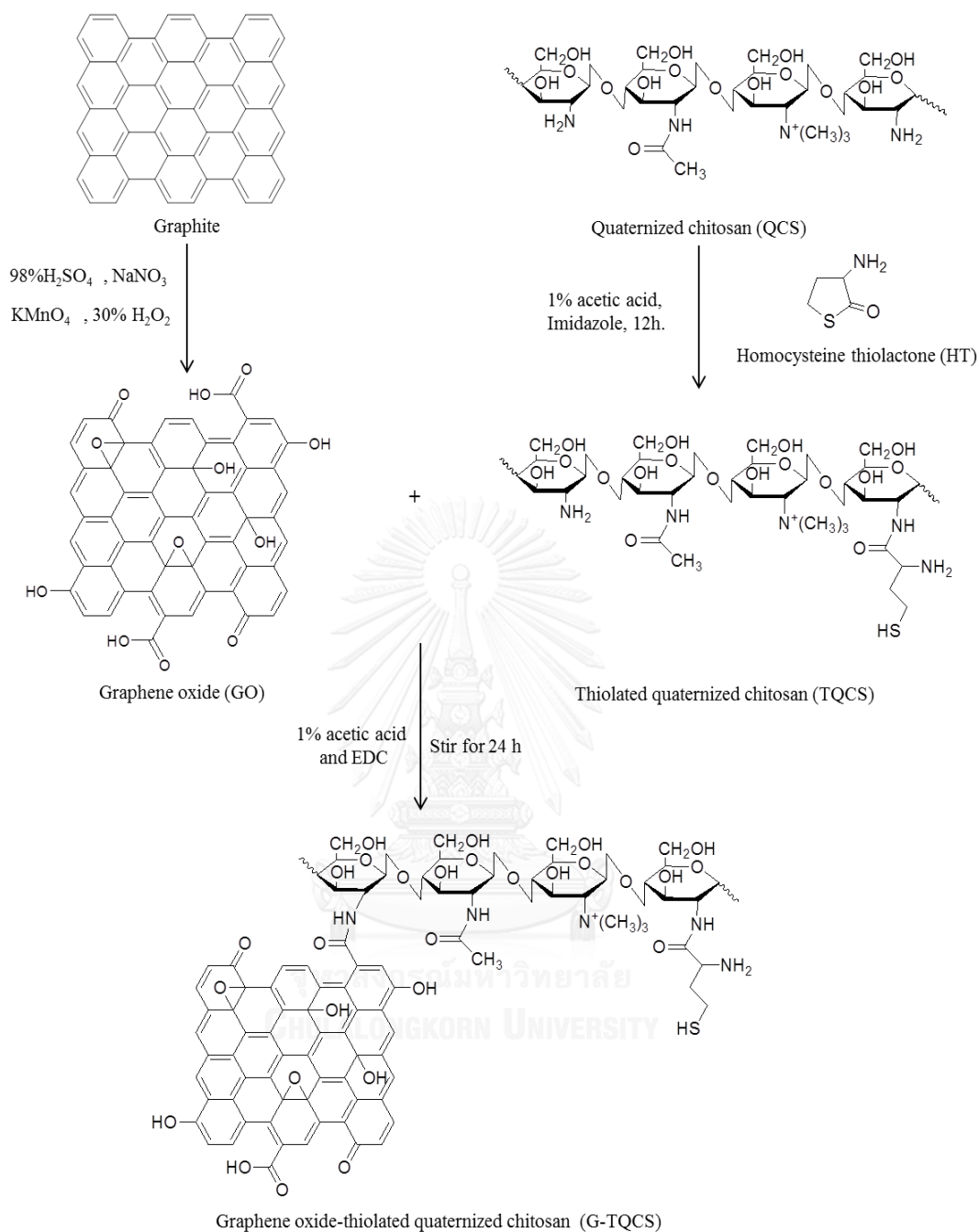


Figure 21 Synthesis scheme of graphene oxide-thiolated quaternized chitosan (G-TQCS)

4.2 Characterization and thermal properties of CS, CS derivatives and GO conjugated with CS or TQCS

4.2.1 Fourier Transform Infrared Spectroscopy (FTIR)

FTIR was used to identify the functional group of synthesized samples. The FTIR spectra of GO, CS, QCS, TQCS, G-CS and G-TQCS were showed in Figure 4.2 and 4.3. The spectrum of chitosan (Fig. 22a) showed the characteristic absorption bands at 3420 cm^{-1} , 1639 cm^{-1} , 1596 cm^{-1} and 1078 cm^{-1} attributed to vibration of O-H that overlapped with N-H stretching, carbonyl group of secondary amide (amide I), N-H (amide II) bending and C-O stretching, respectively.

For quaternized of chitosan (QCS), the peaks at 1458 cm^{-1} and 1372 cm^{-1} correspond to the vibration of C-H bending of trimethylammonium group ($-\text{N}^+(\text{CH}_3)_3$) were observed as showed in Figure 22b. In addition, the peaks of C=O (amide I) vibration was observed at 1658 cm^{-1} . It was suggested that the quaternization was immobilized on chitosan backbone.

The spectrum of TQCS (Fig. 22c) showed a new peak at 671 cm^{-1} attributed to thiol groups ($-\text{SH}$) of the side chain of HT. Additionally, the absorption bands at 1636 cm^{-1} and $1461, 1378\text{ cm}^{-1}$ were corresponded to C=O (amide I) and C-H bending of QCS backbone, respectively. It was indicated that HT was successfully conjugated on the QCS chain.

The absorption bands of GO (Fig. 22d) at $3406, 1723, 1624, 1227$ and 1058 cm^{-1} were assigned to the stretching vibration of C=O (carboxylic group), C=C (sp^2 carbon), C-OH (hydroxyl group) and C-O-C (epoxy group), respectively. These confirmed the decoration of

oxygen functional groups on both the basal plane and edges of GO. After conjugated GO with CS and TQCS, FTIR spectra of G-CS and G-TQCS (Fig. 22e and f) did not show the vibration of carbonyl group of carboxylic group on GO at 1723 cm^{-1} . In addition we used the ratio of peak area to determine the covalently attachment via amide bond of G-CS and G-TQCS. The ratio of peak area between $1700\text{-}1500\text{ cm}^{-1}$ (C=O (amide I) stretching) and $1270\text{-}900\text{ cm}^{-1}$ (C-O stretching) was 0.32 of G-CS and 0.25 of G-TQCS that higher than 0.22 of CS and 0.20 of TQCS, respectively. Therefore, these results suggested that CS and TQCS were conjugated on the surface of GO *via* amide bond.



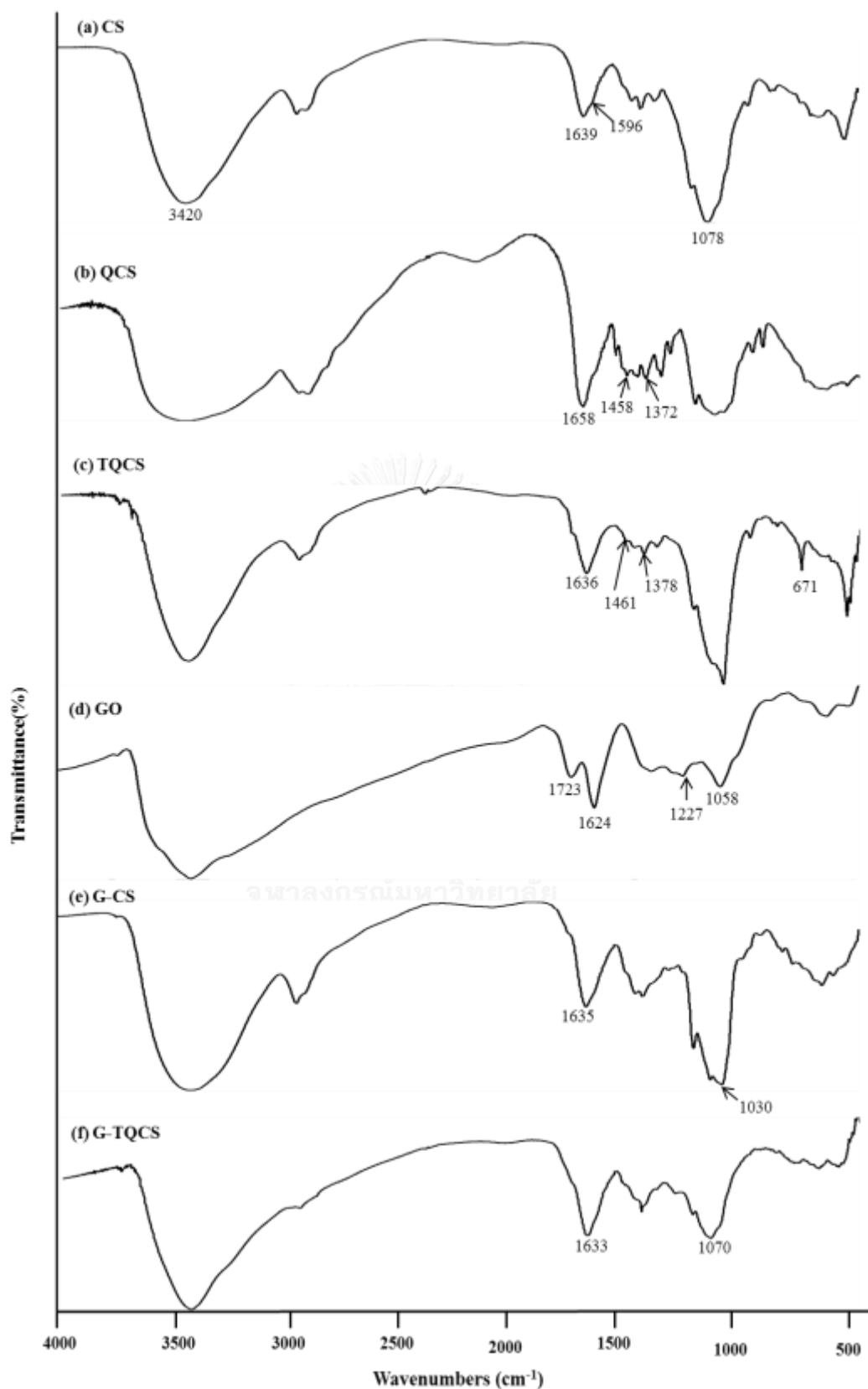


Figure 22 FTIR spectra of a) chitosan, b) quaternized chitosan and c) thiolated quaternized chitosan d) graphene oxide, e) G-CS and f) G-TQCS

4.2.2 Nuclear Magnetic Resonance Spectroscopy ($^1\text{H-NMR}$)

The second technical ascertain synthesized products is $^1\text{H NMR}$. The chemical structure of CS, QCS and TQCS were characterized by $^1\text{H NMR}$ as showed in Figure 23. The chemical shifts at 4.53, 3.57 – 3.38, 2.84 and 1.73 ppm were associated to the H1, H3-H6, H2 and N-acetylglucosamine (NHAc) in chitosan skeleton, respectively (Fig. 23a). The QCS exhibited new proton positions at 3.20-3.03, 2.76 and 2.54 ppm which assigned to 3-,6- OCH_3 , $\text{N}^+(\text{CH}_3)_3$ and $\text{N}^+\text{H}(\text{CH}_3)_2$ in QCS backbone, respectively (Fig. 23b). It was suggested that the quaternization of CS did not only interact with amine group but also interact with hydroxyl group. The preparation process of QCS was not dialyzed due to its act as an intermediate of TQCS therefore it might contain of solvent residual as showed the chemical shifts at 3.24 and 2.18 correspond to CH_2 in N-methylpyrrolidone [58] and acetone solvent [59], respectively. Additionally, $^1\text{H NMR}$ analysis was used to determine the degree of quaternization (DQ) of QCS that calculated from the Eq. (1) in section 3.3.2 was 13.25 %. Moreover, TQCS (Fig. 23c) showed new chemical shift at 2.62 ppm correspond to Hd from the ring opened side chain of HT that overlapped with $\text{N}^+\text{H}(\text{CH}_3)_2$. These results confirmed that the modification of CS to form QCS and TQCS were successful. In order to confirm that HT was attached to chitosan, the amount of grafted thiol groups will be evaluated by the Ellman's methods [56].

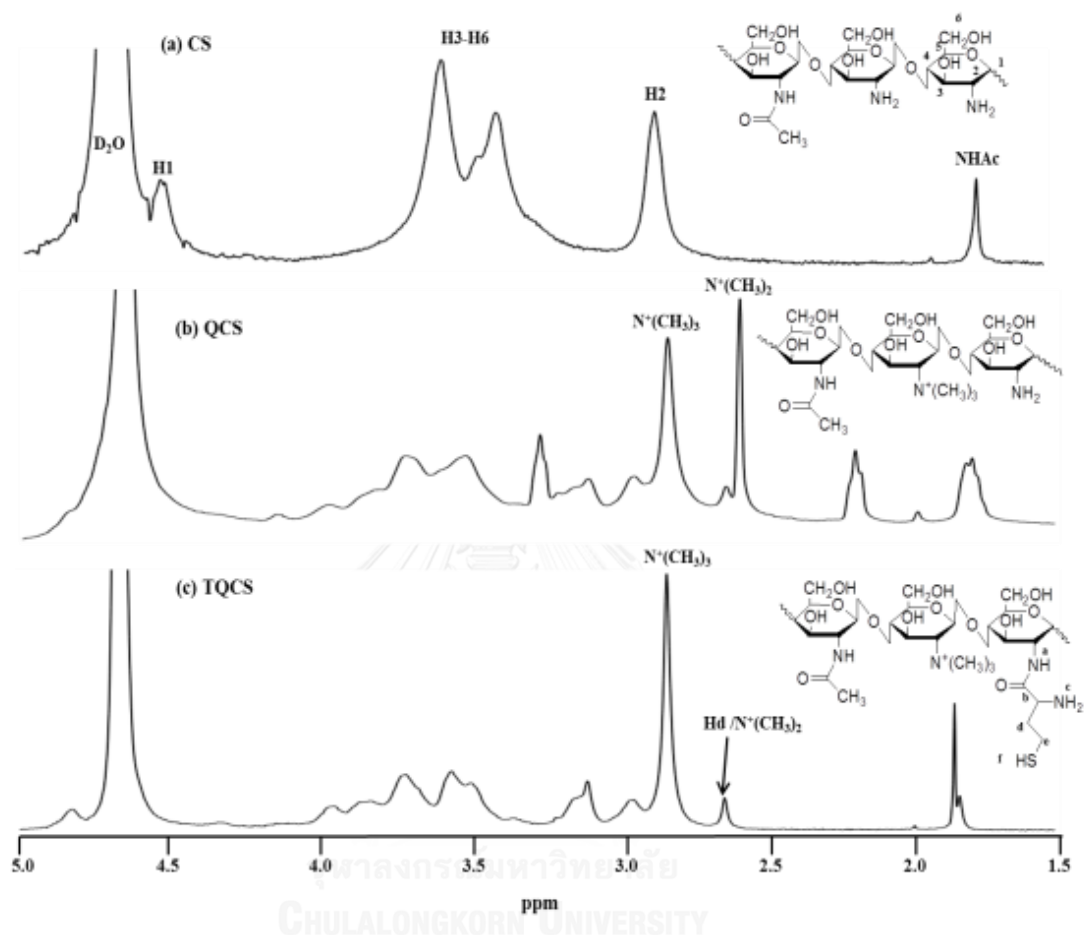


Figure 23 ^1H NMR spectra of a) chitosan, b) quaternized chitosan and c) thiolated quaternized chitosan

4.2.3 Thermogravimetric analysis (TGA)

TGA is a technique used to investigate the thermal properties of samples. The TGA and DTG curves of CS, QCS, HT, TQCS, GO, G-CS and G-TQCS were presented in Figure 4.4 and 4.5, respectively.

The thermal decomposition of CS (Fig. 24a) showed DTG at 333 °C, accounting for a weight loss of 60% due to chitosan backbone degradation. The QCS (Fig. 24b) showed DTG at 313 °C (56% of weight loss) that have lower thermal stability than CS corresponded to interference of close packing of chitosan chains because of the repulsion between the positive charges of quaternary ammonium groups.

For the TQCS (Fig. 24c) showed TG curve that was overlapped of two stages of decomposition at 169 °C to 453 °C. The first stage showed DTG at 233 °C associated with the thermal degradation of HT grafted on side chain. The second stage showed DTG at 327 °C, accounting for 55% weight loss because of the degradation of CS backbone. Additionally, the thermal stability of TQCS was lower than CS due to the HT side chain decreased the crystallinity of CS [21].

TGA data of GO (Fig. 25a) showed DTG at 231 °C with 62% weight loss due to the pyrolysis of oxygen functional group on GO surface. In contrast, G-CS and G-TQCS (Fig. 25b and c) showed two stages, the first stage showed DTG at 243 °C (11% of weight loss) and 226 °C (4% of weight loss), respectively assigned to the degradation of oxygen-containing group of GO. The second stage showed DTG at 341 °C (32% of weight loss) and 337 °C (44% of weight loss), respectively associated with the degradation of chitosan skeleton. The total weight loss of G-CS and G-TQCS were 43% and 48%, respectively

which were lower than unmodified GO. These suggested that after conjugated GO with CS and TQCS enhanced the thermal stability of GO, which indicate the existence of interfacial bonding between GO and TQCS [13, 60].

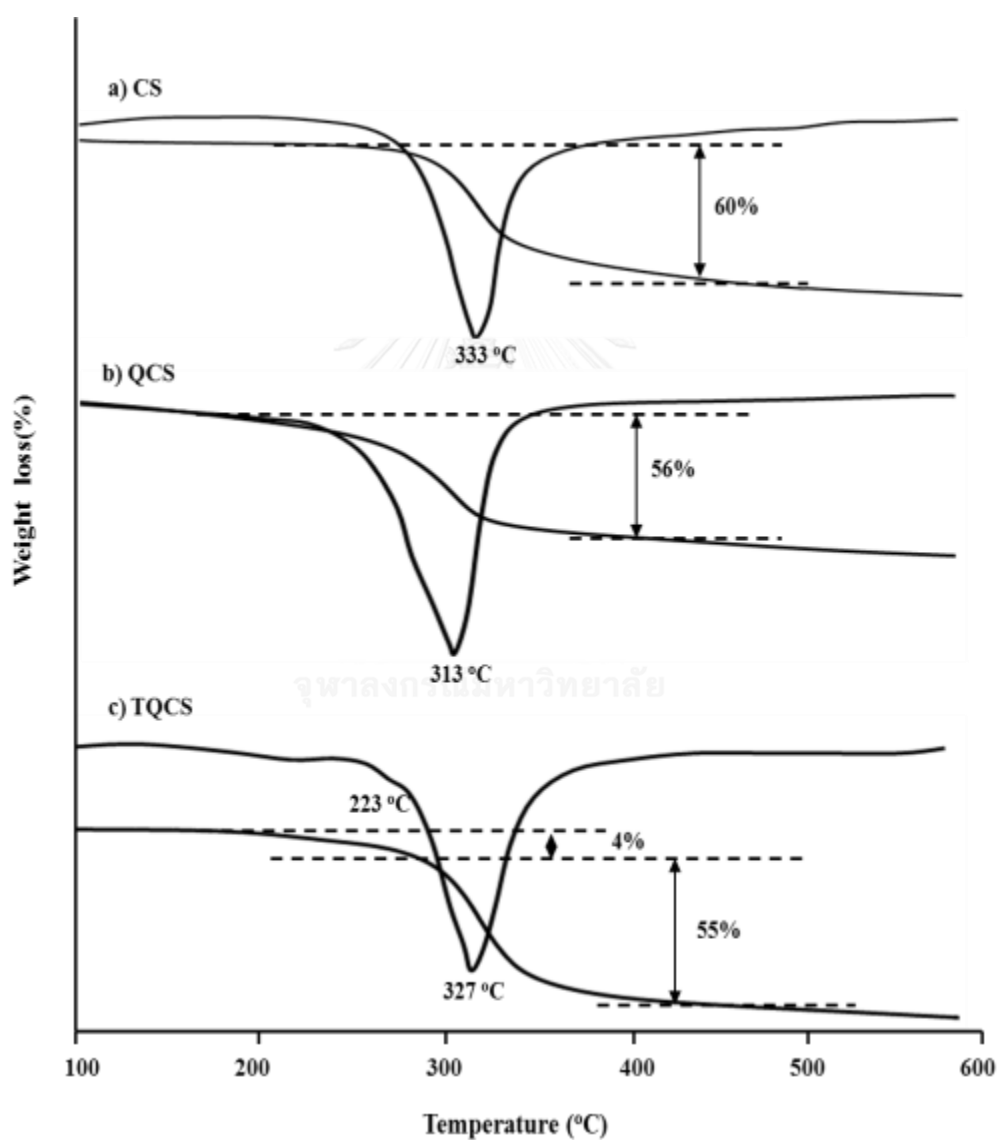


Figure 24 TGA and DTG data of a) chitosan, b) quaternized chitosan and c) thiolated quaternized chitosan

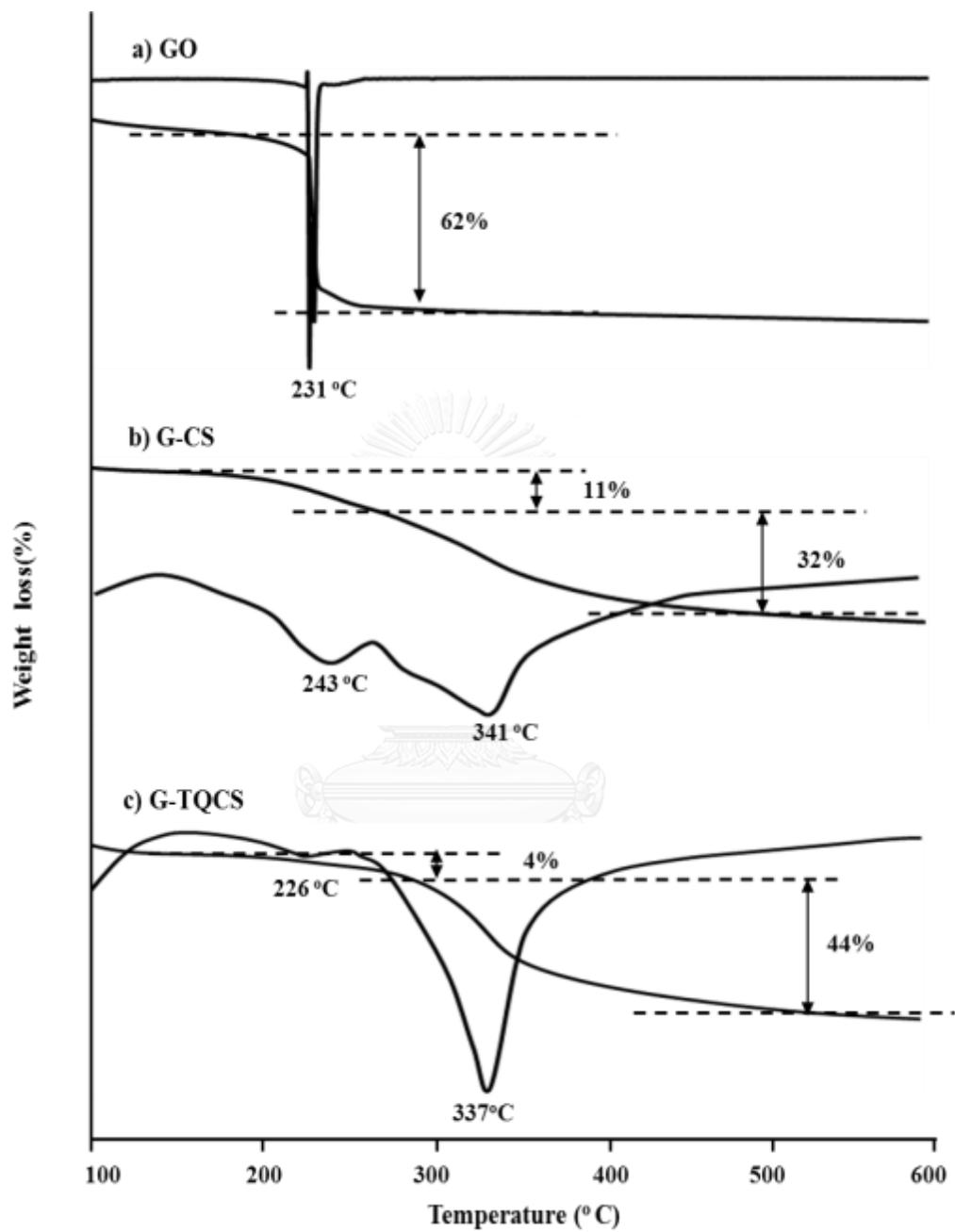


Figure 25 TGA and DTG data of a) graphene oxide, b) G-CS and c) G-TQCS

4.2.4. Scanning Electron Microscope (SEM)

SEM was performed to ascertain the morphology of synthesized samples. SEM images (Fig. 26) showed the morphology of GO, G-CS and G-TQCS (1:10 w/w). The phase of GO (Fig 4.6a) formed deflated shape, while GO conjugated with CS and TQCS (Fig 4.6b and c) exhibited the rough surface because the polymer chains were immobilized on the surface of GO [54]. Therefore, these results assured that the GO was conjugated with CS and TQCS.

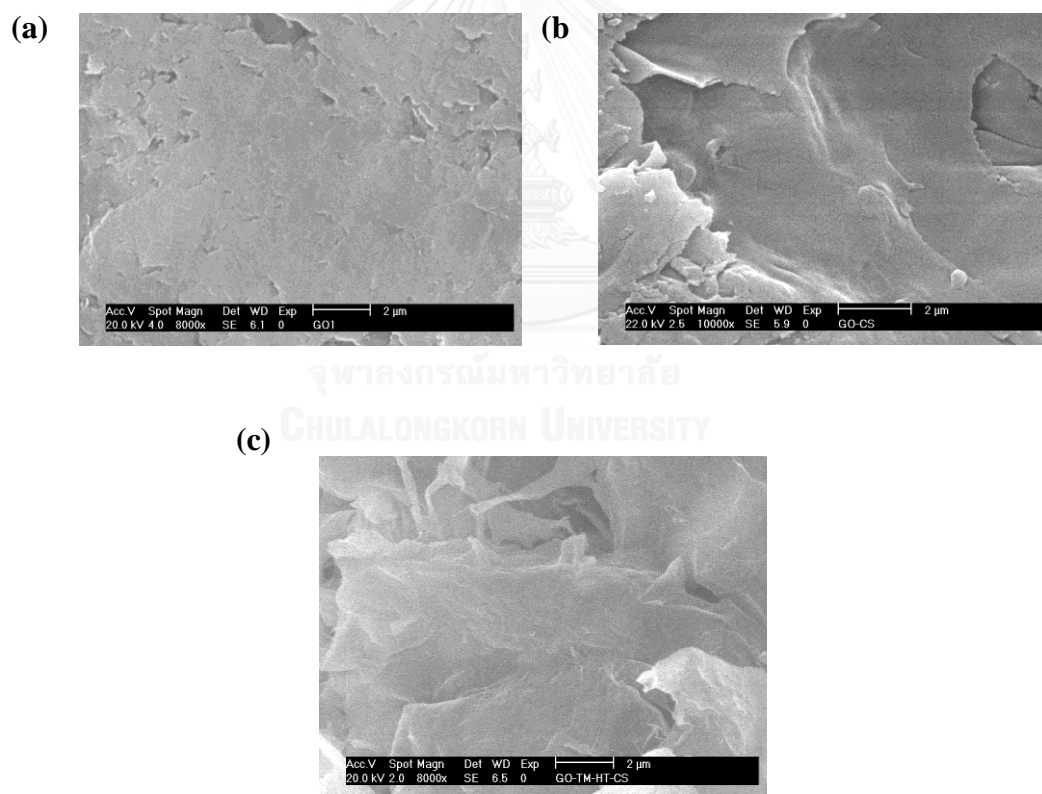


Figure 26 SEM images (a) GO, (b) G-CS and (c) G-TQCS (scale bar 2.0 μm)

4.2.5. Atomic Force Microscope (AFM)

The AFM is a technique to observe the thickness and surface topographic structure of depositions. The samples were prepared by dissolved in aqueous and deposited on a silicon wafer and dried in oven. AFM images of GO, G-CS and G-TQCS (1:10 w/w) represented in Figure 4.7 that showed topographic (left) to evaluate the thickness and phase graphic (right). The thickness of GO was 1.4 nm, whilst it dramatically increased after modified GO by conjugated with CS and TQCS, which were 20.9 and 35.0 nm, respectively. The phase image of GO (Fig. 27a) exists flat and rather roughness due to the stacked layer of graphene oxide. In contrast, the phase of G-CS and G-TQCS (Fig. 27b and c) were presented coarse surface assigned to the folding of polymer. These suggested that CS and TQCS were successfully conjugated on GO surface.



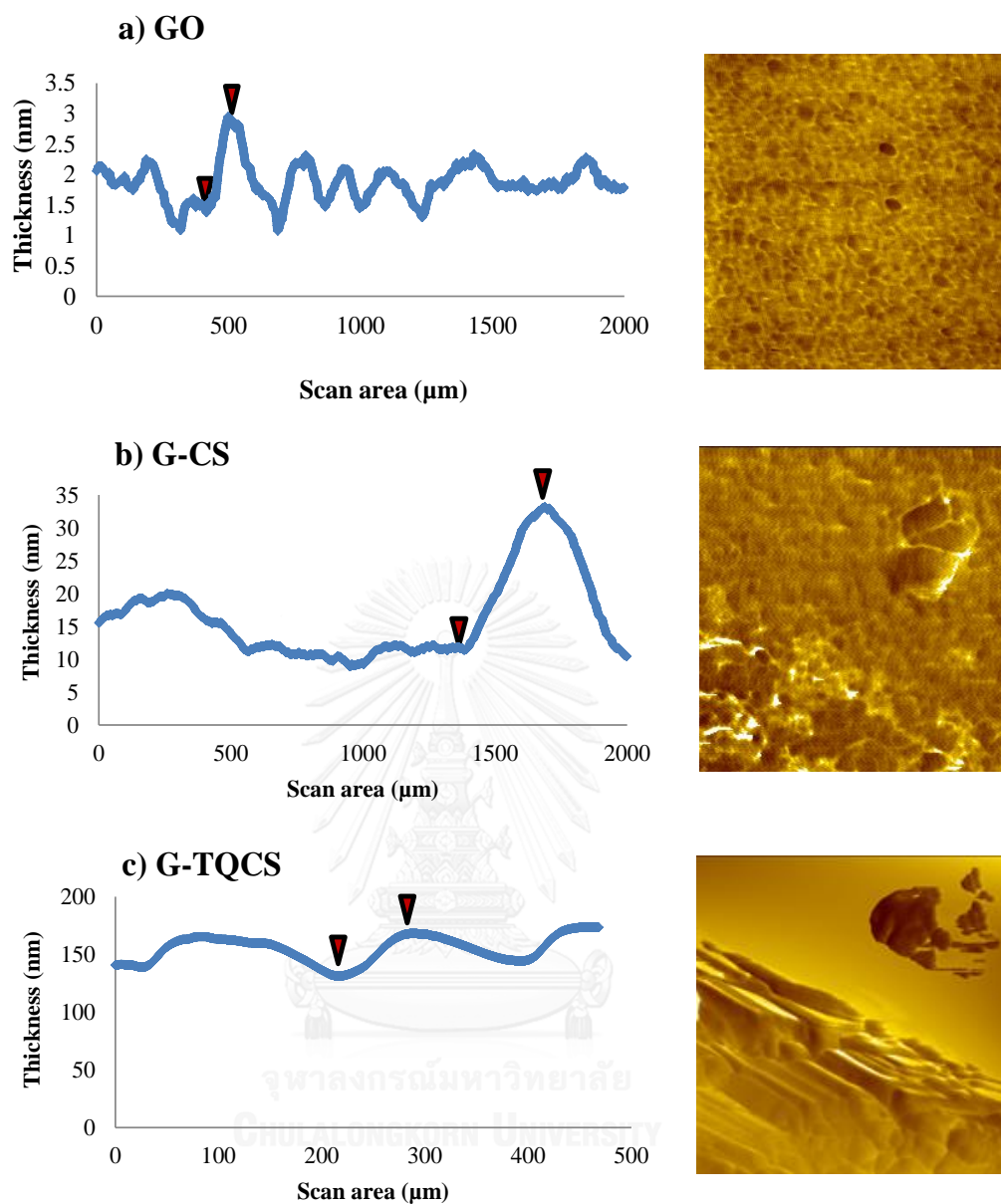


Figure 27 AFM images (tapping mode) of (a) GO, (b) G-CS (c) G-TQCS with concentrations of 0.01 mg/ml. Image dimensions are $2.0\mu\text{m} \times 2.0\mu\text{m}$

4.3 Degree of substitution of thiol and disulfide contents in TQCS and G-TQCS

The amount of free thiol group and disulfide bonds immobilized in TQCS and G-TQCS were investigated by photometrically with Ellman's reagent [56] as summarized in Table 4.1. The Ellman's reagent is widely used for quantitating free sulfhydryl group in solution. Its specificity for thiol group at neutral pH and rapidly forms a disulfide bond with thiol group and releases a thiolate ion that caused colored solution. The content of thiol groups and disulfide bond of TQCS were 324 and 57.08 $\mu\text{mol/g}$, respectively. A 1:10 (w/w) ratio of GO:TQCS exhibited 104.50 $\mu\text{mol/g}$ which lower than unmodified TQCS. Moreover, the higher level of disulfide groups of G-TQCS (63.83 $\mu\text{mol/g}$) compared to TQCS. We proposed that the moiety of thiol group (-SH) which acts as a good nucleophile that can attack to epoxy group on GO surface via ring opening. It forms C-S bond between GO and TQCS side chain. These implied that this effect reduces interaction of Ellman's reagent and thiol group from G-TQCS.

Table 1 Amounts of thiol groups and disulfide bonds on TQCS and G-TQCS (1:10 w/w)

Sample	Total thiol groups ($\mu\text{mol/g}$) ($\pm\text{SD}$, $n=3$)	Total disulfide groups ($\mu\text{mol/g}$) ($\pm\text{SD}$, $n=3$)
TQCS	324.00 \pm 0.06	57.08 \pm 0.01
G-TQCS	104.50 \pm 0.02	63.83 \pm 0.04

4.4 Mucoadhesive properties

4.4.1 Mucus glycoprotein assay

Mucoadhesion has been widely promoted as procedure in developing novel delivery system for enhanced bioavailability. Mucoadhesive drug delivery system provide a means of achieving site-specific drug delivery and increased retention time at target sites [61].

The mucoadhesion usually depends on the consequence of electrostatic, wetting, adsorption, diffusion, mechanical between polymer and mucin in mucus glycoprotein. The interaction between mucin with polymer or composite can be spontaneously adsorption.

Periodic Acid Schiff (PAS) method is most commonly used to accentuate molecules that rich contain of carbohydrate content such as mucin, glycogen and fungi. The PAS method works by the periodic acid that is oxidized some of the tissue carbohydrates to produce aldehyde groups that interact with Schiff's reagent forming a bright red solution. It demonstrates the attachment of carbohydrate on tissue component [62].

In this study, we selected porcine mucin type II which is a commercial powder as a mucus glycoprotein agent, typically used to study in mucoadhesion assays. The mucoadhesive property of the CS, TQCS, GO, G-CS and G-TQCS estimated by the residue of free mucin in their aqueous solutions which evaluated the amount of absorbed mucin on polymer and composite at different pH, in simulated gastric fluid (SGF, pH 1.2), 0.1 N sodium acetate buffer (pH 4.0) and simulated intestinal fluid (SIF, pH 6.4) media.

The UV-Visible spectrophotometric detection method used to measurement of standard solutions of mucin (100-500 $\mu\text{g/mL}$). A linear relationship of the amount of mucin at wavelength 555 nm, with the linear regression equations obtained by the least square method being $y = 0.4957x + 0.0058$, $y = 1.0897x + 0.0218$ and $y = 0.8318x - 0.0170$ for the assay in pH 1.2, pH 4.0 and pH 6.4, respectively.

4.4.2 Adsorption of mucin on polymer or composites

The amount of mucin was adsorbed onto the CS, TQCS, GO, G-CS and G-TQCS, as a measure of their mucoadhesiveness (Table 4.2) decreased at low pH values and increased at high pH because of the degree of the ionization of sialic acid or the different forms of the glycoprotein depend on the pH value of the environment. The absorption of mucin on polymer or composite was pH dependent. Sialic acid (pK_a 2.6) is a saccharide acid, and mucin is a glycoprotein. Therefore, when the pH value decreases, the amount of ionized sialic acid also decreases, so the potential interaction with polymer or composite was reduced[41]. In contrast, the adsorption of G-TQCS on mucin were decreased at pH 6.4 due to the thiol groups on the side chain of G-TQCS were oxidized, lead to the formation of intramolecular disulide bonds already within the composite before reacting with thiol substructure on mucin [7]. Moreover, at high pH the thiol groups become more reactive as a nucleophile to attack the residual of epoxy group on GO surface. These reduced the binding of G-TQCS on mucin.

The comparative relation of the adsorption of TQCS, GO, G-CS and G-TQCS on mucin were higher than pure CS at all three pH value

(Fig. 28) hence the absorption of derivative CS or composites on mucin was sensitive to pH. The interaction of mucin with G-CS and G-TQCS are presented in Figure 29a and b, respectively.

The TQCS, thiolated derivative CS significantly increased the mucin adsorption level to compare with CS in all three pH mediums evaluated. The results observed that the TQCS absorbed mucin about 8.0-, 1.5- and 2.2- fold more than CS at pH 1.2, 4.0 and 6.4, respectively. Moreover, the GO obviously and significantly increased the adsorption of mucin about 13.2-, 1.7- and 2.5-fold more than CS, whilst the corresponding G-CS showed 12.6-, 1.6- and 2.5-fold higher mucoadhesion than CS at pH 1.2, 4.0 and 6.4, respectively. For G-TQCS composite, at pH 1.2 showed 10.7- and 1.4-fold higher mucoadhesion level than CS and TQCS, respectively. However, it showed the lower adsorption of mucin about 1.2- and 1.4-fold which compared to TQCS at pH 4.0 and 6.4, respectively. These results suggested that the amount of adsorption of polymer and composites on mucin was more marked in the more acidic media.

At pH 1.2, the acidic condition in stomach, a statistically significant increase in the level of adsorbed mucin in TQCS, GO, G-CS and G-TQCS more than unmodified CS were observed. The mucoadhesive ability of TQCS was increased by the amine and HT on the side chains associated to the electrostatic and hydrophobic effects. Moreover, the GO, G-CS and G-TQCS were significantly higher mucoadhesion not only by hydrophobic effects of conjugated hydrocarbon on GO and $-CH_2$ moieties of CS and TQCS chains but also interaction of hydrogen bonding and sulfide bond from ring opening of epoxy with thiol group on mucin to increase the mucoadhesiveness of

composites. The electrostatic effect, this is due to the amine (NH_2) groups of both the CS backbone (pK_a 5.6) and HT side chain that mostly protonated to the ammonium cation (NH_3^+) in an acidic media and trimethylammonium ($^+\text{N}(\text{CH}_3)_3$) on TQCS chain being able to interact with either the carboxylate (COO^-) or sulfonate (SO_3^-) groups on the mucin carbohydrate side chain. For the hydrophobic effect, the $-\text{CH}_2$ moieties of HT and the sp^2 carbon base structure of GO interact in part with the $-\text{CH}_3$ groups on the mucin side chains that lead to a high mucoadhesive adsorption. The hydrogen bonding according to hydroxyl ($-\text{OH}$) and carbonyl groups ($\text{C}=\text{O}$) of GO interacted with carboxylic (COOH) and hydroxyl group (OH) on sialic acid, which is a subdomain of mucus, result in enhancement of absorbed mucin on GO, G-CS and G-TQCS. Furthermore, the thiol group ($-\text{SH}$) on mucin side chain, as a good nucleophile was able to attack the epoxy group ($\text{C}-\text{O}-\text{C}$) on GO surface via ring opening interaction and formed of C-S bond between GO and mucin lead to increase the mucoadhesion.

Therefore, both effects of electrostatic and hydrophobic influenced on the mucoadhesion of CS and TQCS, in addition the effect of hydrogen bonding and thiol group on mucin side chain also impact on GO, G-CS and G-TQCS in the lower pH range.

At pH value in small intestine (pH 4.0 and 6.4) observed higher mucoadhesiveness of CS, TQCS, GO, G-CS and G-TQCS. For TQCS, at high pH value increased concentration of the reactive form of thiolate anions ($-\text{S}^-$) that lead to a greater extent of oxidation and nucleophilic. So not only electrostatic, hydrophobic effects and hydrogen bonding are influenced but also the level of covalently disulfide bond between the TQCS and cysteine-rich subdomains of mucus glycoprotein is a

considerable determinant of its mucoadhesiveness. But the mucoadhesion of TQCS, GO and G-CS are slight higher than CS when compared the adsorption on mucin at lower pH (pH1.2). Conversely, for G-TQCS at pH 6.4 showed lower adsorption of mucin due to thiolate anions, $-S^-$ on mucin side chain are more reactive nucleophile than thiol group, $-SH$ which effortlessly interact by ring opening of epoxy group on GO before reacting with thiol groups on mucin. Additionally, the strong hydrogen bonding of GO and CS or TQCS resulting in the entanglement of polymer chains that is difficult to adsorb composites on mucin.

These results suggest that G-CS and G-TQCS represented high mucoadhesive property that good attach with mucosa membrane, preferably at low pH in gastric fluid (pH 1.2) that produced they are suitable for drug delivery carrier. These mucoadhesive graphene oxide composite carriers enhance the retention time of drug release at defined sites (low pH environment) that improved patient convenience and compliance due to less frequent drug administration.

Table 2 The amount of adsorption of mucin on CS, TQCS, GO, GO-CS and G-TQCS (ratio of GO: CS or CS derivatives are 1:10 w/w) at pH 1.2, 4.0 and 6.4 PBS buffer

Batch	Adsorbed of mucin at pH 1.2 (mg) \pm SD	Adsorbed of mucin at pH 4.0 (mg) \pm SD	Adsorbed of mucin at pH 6.4 (mg) \pm SD
CS	0.03 \pm 0.08	0.30 \pm 0.04	0.17 \pm 0.06
TQCS	0.22 \pm 0.01 ^a	0.46 \pm 0.01 ^b	0.37 \pm 0.01 ^b
GO	0.37 \pm 0.04 ^a	0.51 \pm 0.02 ^b	0.43 \pm 0.01 ^a
G-CS	0.35 \pm 0.04 ^{a,c}	0.49 \pm 0.01 ^{b,c}	0.43 \pm 0.01 ^{a,c}
G-TQCS	0.32 \pm 0.02 ^{a,c,d}	0.39 \pm 0.04 ^{b,c,d}	0.28 \pm 0.02 ^{a,c,e}

^a The mean difference is significant ($P < 0.05$) compared to CS using LSD method.

^b The mean difference is not significant ($P > 0.05$) compared to CS using LSD method.

^c The mean difference is significant ($P < 0.05$) compared to GO using LSD method.

^d The mean difference is significant ($P < 0.05$) compared to TQCS using LSD method.

^e The mean difference is not significant ($P > 0.05$) compared to TQCS using LSD method.

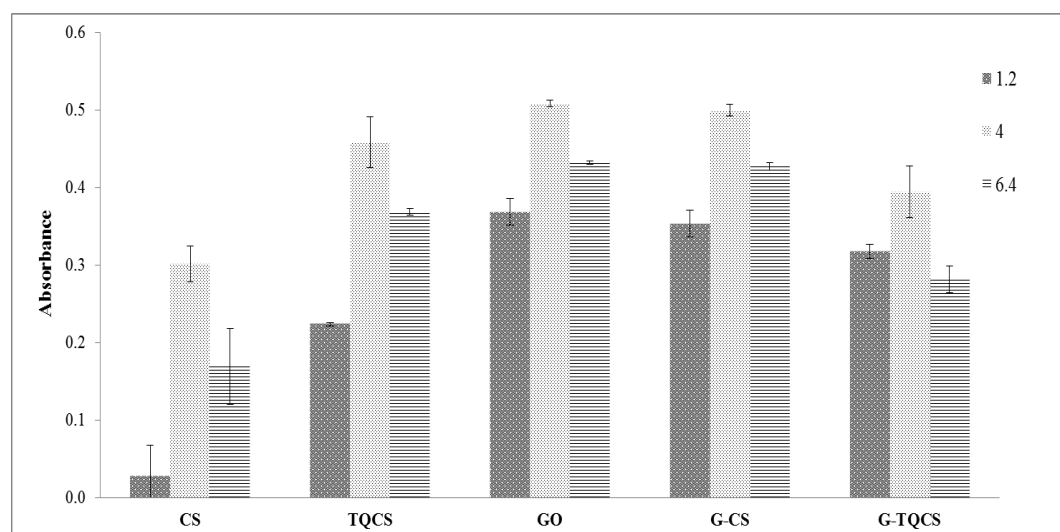
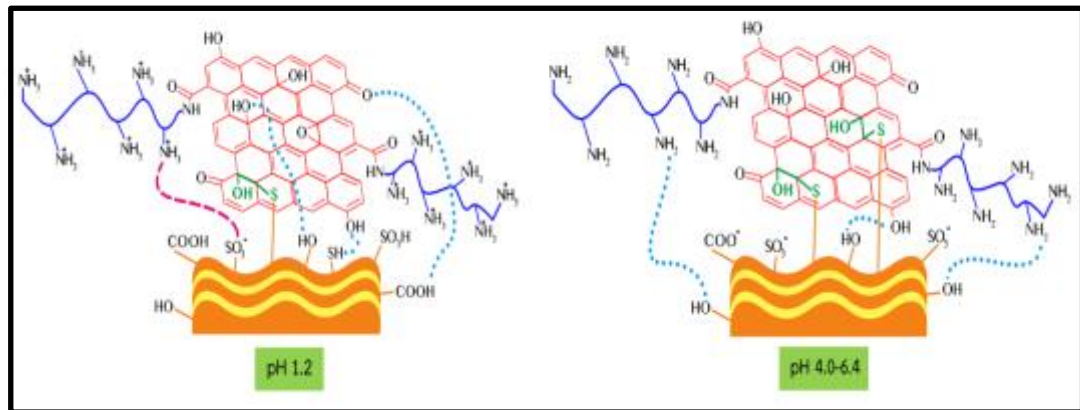


Figure 28 Adsorption of mucin on CS, TQCS, GO, G-CS and G-TQCS at pH 1.2, 4.0 and 6.4 PBS buffer

a)



b)

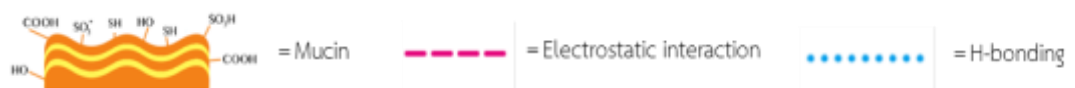
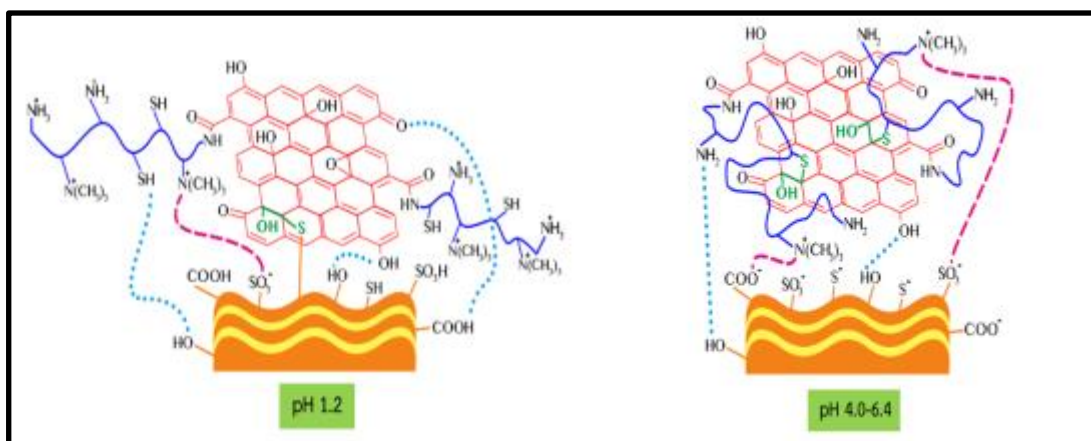


Figure 29 Representative the interaction between a) G-CS and b) G-TQCS with mucin at pH value rang in stomach (pH 1.2) and small intestine (pH4.0 and 6.4)

4.5 Characterization of CS, TQCS, GO, G-CS and G-TQCS loaded curcumin

4.5.1 Fourier Transform Infrared Spectroscopy (FTIR)

In the previously part, we successfully synthesized the mucoadhesive composites of G-CS and G-TQCS. The next step curcumin (Cur), a natural anticancer drug were loaded in CS, GO, G-CS or G-TQCS that expected to use for a model of anticancer drug carrier.

FTIR spectroscopy was performed to determine the combination of curcumin and CS, GO, G-CS or G-TQCS in the composites as shown in Figure 4.10 and 4.11. The FTIR spectrum of curcumin (Fig. 30a) exhibited an absorption band at 3501 cm^{-1} due to the phenolic O-H stretching vibration. Additionally, sharp peaks at 1624, 1602, 1509 and 1426 cm^{-1} are associated with stretching vibration of C=C of alkene, benzene ring, C=O of carbonyl and olefinic bending vibration of C-H, respectively. Moreover, peaks at 1273 and 856 cm^{-1} assigned for aromatic C-O stretching vibration and vibration of -C-OCH₃ of phenyl ring.

In the spectrum of CS and TQCS (Fig. 30b and c) the characteristic peaks showed O-H stretching at $3000\text{-}3500\text{ cm}^{-1}$, C-H stretching at 2916 and 2869 cm^{-1} , C=O stretching at 1654 cm^{-1} (amide I), N-H bending at 1588 cm^{-1} , C-H bending at 1418 (CH₂) and $1380\text{ (CH}_3\text{) cm}^{-1}$ and C-O-C stretching at 1027 cm^{-1} of CS skeletal respectively. Additionally, TQCS spectrum showed that area peak of C=O stretching (amide I) at $1700\text{-}1600\text{ cm}^{-1}$ and -CH₃ bending at $1400\text{-}1330\text{ cm}^{-1}$ increased from the side chain of HT and trimethylammonium group (N⁺(CH₃)₃) on CS chain.

After loading curcumin in CS and TQCS, both of CS-Cur and TQCS-Cur (Fig. 30d and e), were observed the new peaks of C=C benzene ring (1582 cm^{-1} and 1579 cm^{-1}) and carbonyl group (1506 and 1504 cm^{-1}). In addition, the peaks of C=O (amide I) at 1654 and 1652 cm^{-1} shifted to 1623 and 1626 cm^{-1} in CS-Cur and TQCS-Cur, respectively due to intermolecular hydrogen bonding between hydroxyl group of curcumin and carbonyl group of polymer chain. Moreover, TQCS showed peak at 1283 cm^{-1} assign to C-O aromatic of curcumin confirming that curcumin and CS or TQCS were bound together.

The FTIR spectrum of GO (Fig. 31a) showed The absorption band at 3406 , 1723 , 1618 , 1225 and 1058 cm^{-1} associated with O-H, C=O (carboxyl), C=C (alkene), C-OH and C-O (epoxy) stretching vibration indicating that the oxygen functional groups on GO. For the FTIR of G-CS and G-TQCS (Fig. 31b and c) showed peaks associated with C-H stretching, C=O (amide I), C-H bending and C-O-C stretching of CS skeletal respectively. Additionally, the area peak of C=O (amide I) increased compared to CS and TQCS indicating that GO were conjugated with CS and TQCS via amide bond.

After loading curcumin in composites, peaks shifted from 1602 to 1579 cm^{-1} (C=C benzene ring) and from 1426 to 1381 cm^{-1} (C-H bending vibration) in GO-Cur. For G-CS-Cur and G-TQCS-Cur (Fig. 31d, e and f), the stretching vibration of C=O (amide I) were shifted because of hydrogen bonding effect. Moreover, the new peaks corresponding to C=C stretching of benzene ring (1599 cm^{-1}), carbonyl group (1506 and 1512 cm^{-1}) and aromatic C-O stretching (1276 and 1274 cm^{-1}) showed in G-CS-Cur and G-TQCS-Cur, ascertaining that curcumin and CS or TQCS have bound together.

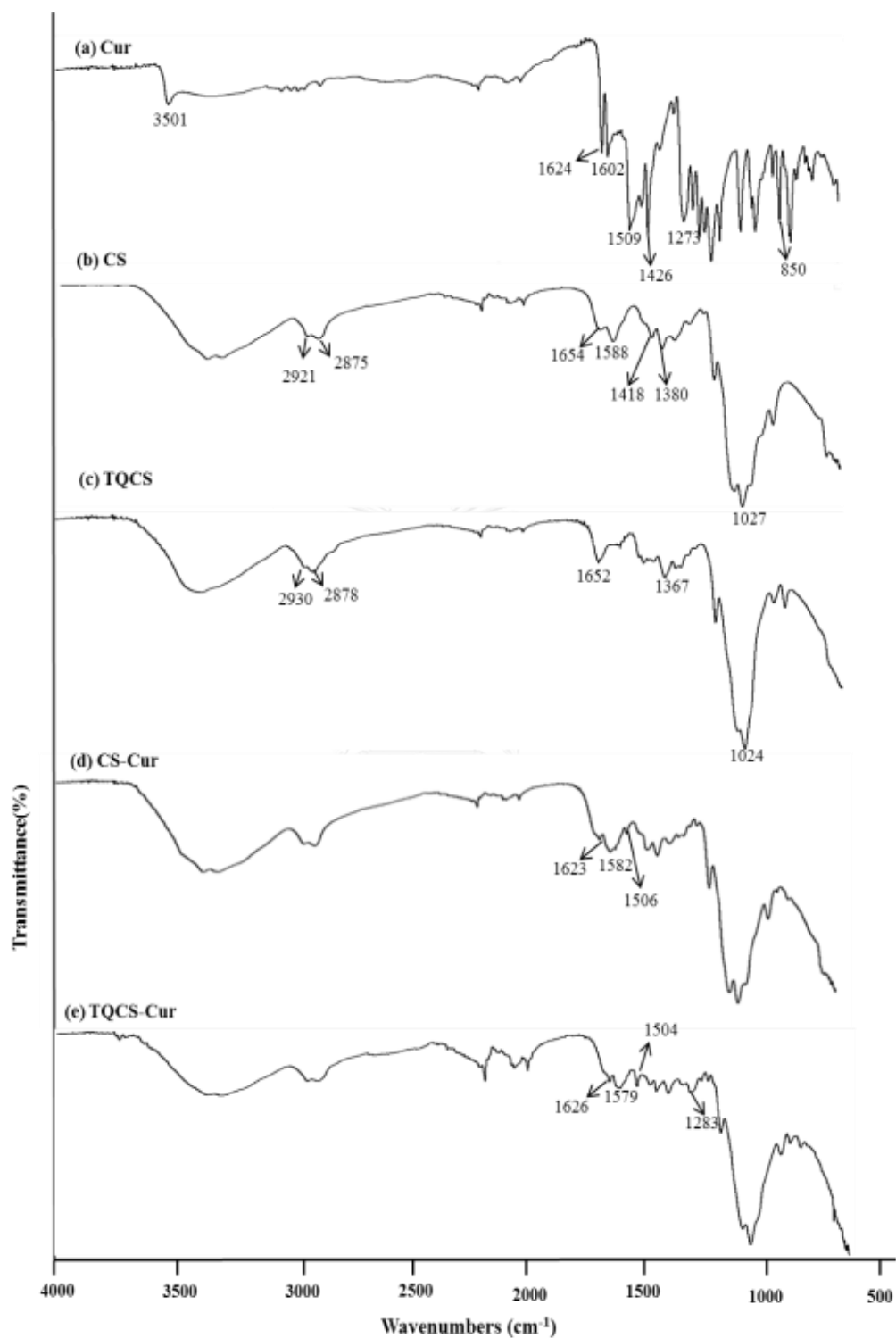


Figure 30 FTIR spectra of a) curcumin, b) chitosan, c) thiolated quaternized chitosan, d) chitosan-curcumin and e) thiolated quaternized chitosan-curcumin

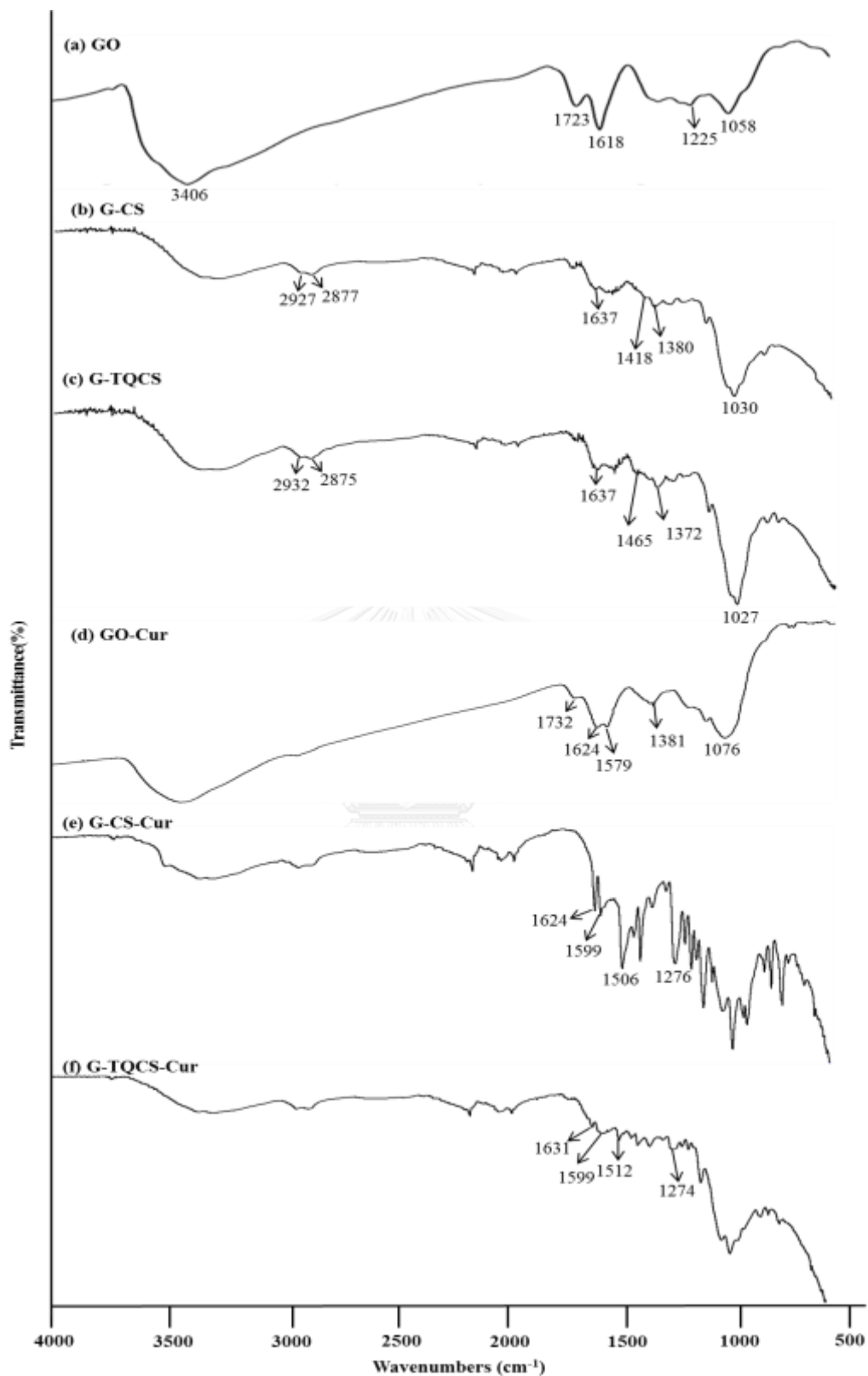


Figure 31 FTIR spectra of a) graphene oxide, b) G-CS, c) G-TQCS, d) GO-Cur, e) G-CS-Cur and f) G-TQCS-Cur

4.5.2. Atomic Force Microscope (AFM)

The thickness and morphology of curcumin-loaded modified GO which forms the composite films (GO-Cur, G-CS-Cur and G-TQCS-Cur) were observed by AFM. The preparation of test samples were dissolved in aqueous and dropped on a silicon wafer then dried in oven. AFM images of GO-Cur, G-CS-Cur and G-TQCS-Cur (10% w/w drug loading) demonstrated topographic (left) to evaluate the thickness and phase graphic (right) as shown in Figure 32. The thickness of GO-Cur was 3.02 nm while in curcumin-loaded modified GO its significantly increased that exhibited 11.81 (G-CS-Cur) and 12.30 nm (G-TQCS-Cur) because of the polymer and curcumin were immobilized on GO sheet. The phase image of GO-Cur (Fig. 32a) showed smooth surface. However, the phase of G-CS-Cur and G-TQCS-Cur (Fig. 32b and c) were displayed irregular surface attribute to the crumple of polymer chain and untreated curcumin deposit on surface of composite films. These results implied that the curcumin was totally entrapped on modified GO surface after form the curcumin-loaded composite films.

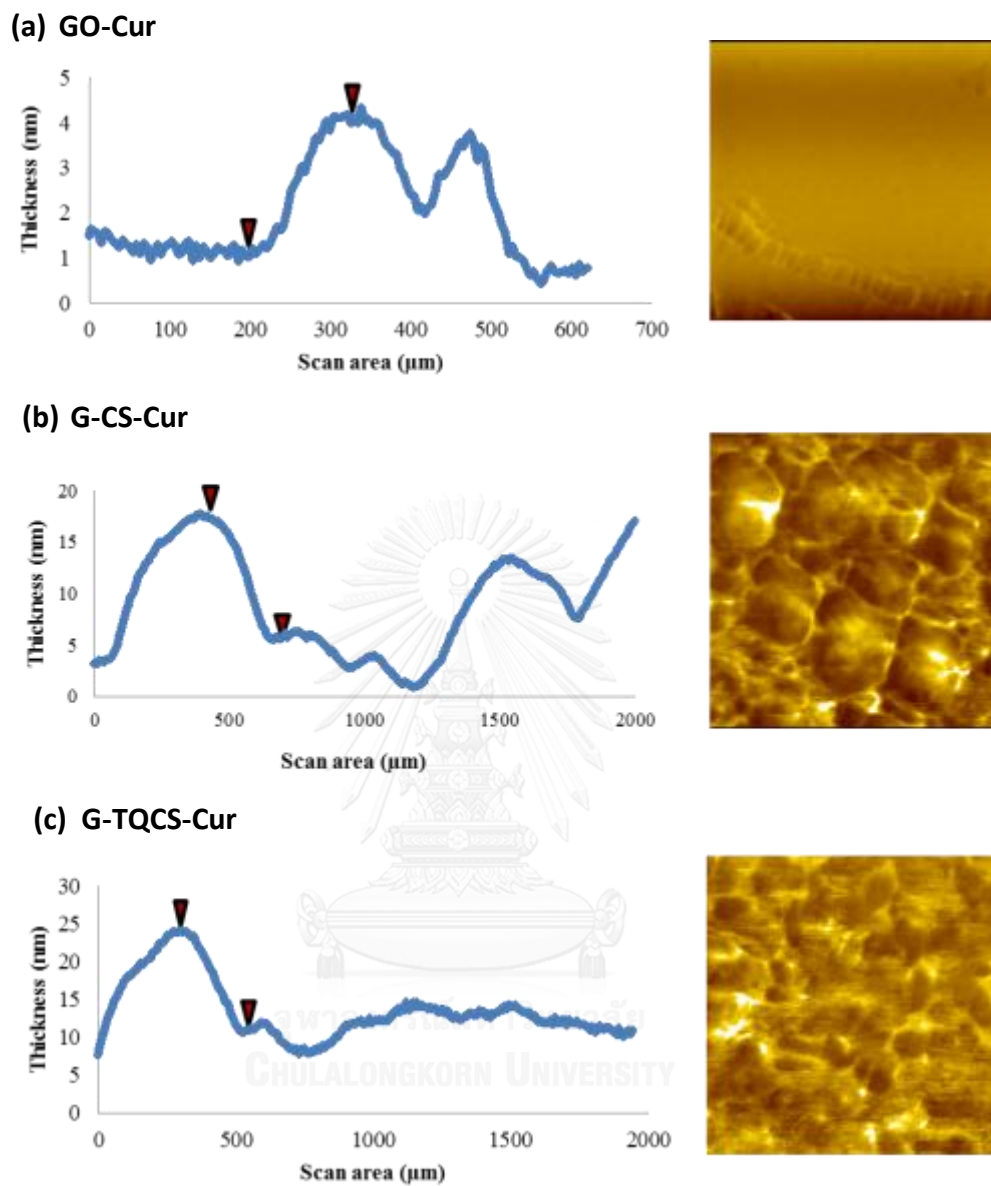


Figure 32 AFM images (tapping mode) of (a) GO-Cur, (b) G-CS-Cur (c) G-TQCS-Cur with concentrations of 0.01 mg/ ml. Image dimensions are $2.0\mu\text{m} \times 2.0\mu\text{m}$

4.6 Evaluation of drug entrapment efficiency (%EE)

The percentages of drug loading efficiency and entrapment efficiency (%EE) of the curcumin loaded on CS, TQCS, GO, G-CS and G-TQCS, which form the composite films were showed in Table 4.3. The entrapment efficiency was determined by UV/Vis spectroscopy analysis by measuring the absorbance of the characteristic peak of curcumin at $\lambda_{\max} = 428$ nm.

The entrapment efficiency of composite film 10% curcumin loaded CS, TQCS, GO, G-CS and G-TQCS were 91.92%, 94.60%, 92.46%, 92.97% and 92.05%, respectively. This result explained that preparation of composite films can produce high percentage entrapment at about 90% of encapsulation. This could be due to hydrogen bonding and hydrophobic interaction between curcumin and composite films. For hydrophobic effect results in sp^2 conjugated carbon of GO via π - π interaction and $-CH_2$ moieties of HT onto the side chain of CS and TQCS. In addition, hydrogen bonding from hydroxyl, carbonyl and carboxylic groups of GO surface interact with hydrogen bonding group on curcumin structure. Therefore, this ensures strong entrapment of curcumin in polymer and composite films that make a suitable carrier for drug delivery system.

Table 3 The percentages of loading and entrapment of curcumin loaded polymer and composites

Formulations	% Loading efficiency	% EE \pm SD
CS-Cur	8.35	91.92 \pm 0.08
TQCS-Cur	8.59	94.60 \pm 0.03
GO-Cur	8.41	92.46 \pm 0.03
G-CS-Cur	8.45	92.97 \pm 0.03
G-TQCS-Cur	8.57	92.05 \pm 0.06

4.7 *In vitro* curcumin release profiles

The curcumin released profile of the CS-Cur, TQCS-Cur, GO-Cur, G-CS-Cur and G-TQCS-Cur loaded with 10% (w/w) of curcumin was investigated as a function of time at pH 1.2 (simulated gastric; SGF) and 6.4 (intestinal fluids; SIF). These two pH buffers were chosen because they simulated curcumin-loaded composites to pass oral administration. From the cumulative drug release percentage were clear that the formulations had a differentiated pattern of release. After 12 h, at pH 1.2 (Fig. 33) there showed higher release of the curcumin in comparison with pH 6.4 (Fig. 34) and after 72 h the percentage of curcumin release showed in appendix D.

The percentage of curcumin released was calculated using a calibration curve from the standard curcumin (2, 4, 6, 8 and 10 μ g/mL) that measured by UV-Visible spectrophotometer at wavelength 428 nm. The linear equations of standard curcumin were pH 1.2: $y = 0.0611x - 0.0197$ and pH = 6.4: $y = 0.0867x - 0.0421$.

In the first 30 min, a burst release of curcumin was observed in all samples at both pH conditions (SGF and SIF). It could be inferred that the initial burst release might be relative to the adsorption of curcumin on composite surfaces. For 1-12 h the amount of curcumin was released in a sustained manner according to the gradual release of curcumin within composites, excepted of GO-Cur. Most of curcumin released from the curcumin-loaded composite films in the first 12 h.

At pH 1.2 (SGF), initial curcumin released from CS-Cur and TQCS-Cur, there were 54% and 86%, while at pH 6.4 (SIF) of that showed at 36% and 23%, respectively after 12 h. The amount of curcumin released was faster in SGF than SIF, as in acidic environment the part of CS and TQCS chain swell through the electrostatic repulsions due to the protonation of amine group of CS backbone [63]. Moreover, TQCS had more hydrophilic groups (-SH) that increases chain expansion [21]. On the other hand, at pH 6.4 (SIF) the swelling of CS and TQCS were reduced due to the almost complete deprotonation of amine group on CS and TQCS chain that occurring of inter-chain hydrogen bond leading to decreases swelling behavior. Additionally, thiol groups on TQCS formed disulfide bonds within polymer chain that cause the cross-link structure leading to slow release rate.

The GO-Cur was not shown significantly released of curcumin 3% and 6% at pH 1.2 and 6.4, respectively after 12 h. The curcumin diffusing away from GO based on the interaction between GO and curcumin, there could be hydrogen bonds and hydrophobic effect (including π - π stack) at different pH values. At pH 1.2, GO sheets are strong π - π stacking and hydrogen bonding with curcumin due to the -COOH on GO surface are not deprotonized that can interact with -OH group on curcumin leading to

more attachment of curcumin on GO sheets. Consequently, the incomplete release of curcumin from GO sheet was corresponded to the strong bonding of GO with curcumin.

For G-CS-Cur and G-TQCS-Cur not only showed cumulative release 48% and 60% at pH 1.2 but also presented 15% and 18% at pH 6.4, respectively after 12 h. At pH 1.2, the amount of curcumin within G-CS and G-TQCS were released by diffusion controlled drug release. The swelling of G-CS and G-TQCS chains occurred by the repulsive force of ammonia cation (NH_3^+) and hydrophilic groups (-SH). Conversely, at pH 6.4 the swelling behavior of composite films was limited as the above discussion and occurrence of interaction between epoxy and thiol groups within G-TQCS caused increased amount of entanglement in composite structure, thus these inhibited the diffusion of drug. In addition, the hydrogen bond and π - π stacking between regions of GO sheet and curcumin influenced the rate of drug release, as low pH the interaction are stronger than high pH environment. Therefore, the curcumin loaded composite films could be effectively control released in the stomach (pH 1.2).

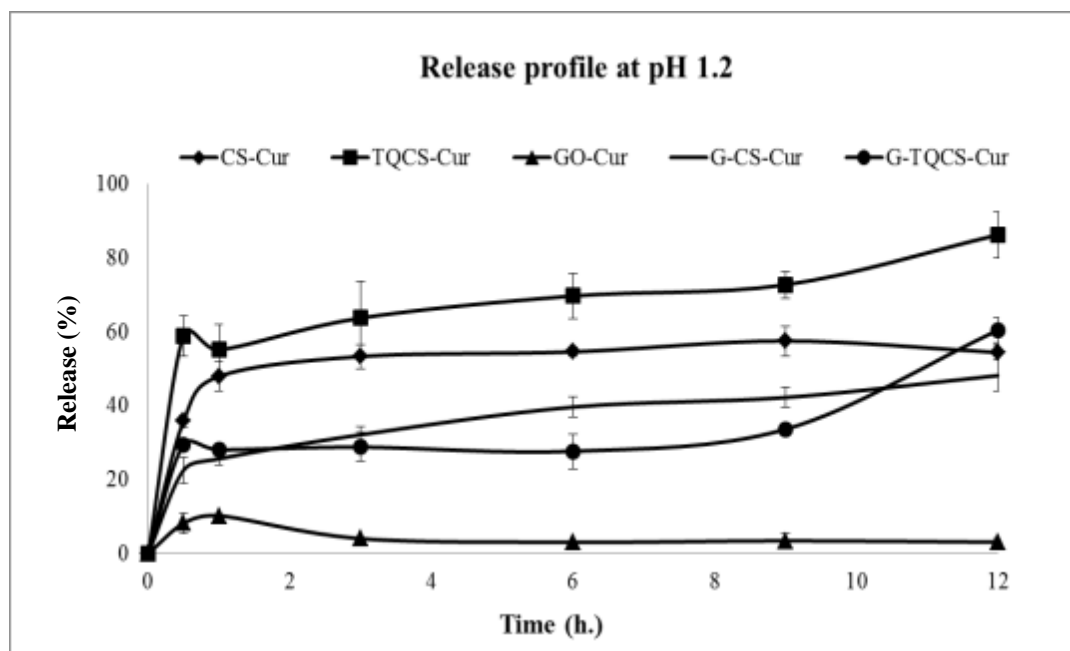


Figure 33 Release profiles of CS-Cur, TQCS-Cur, GO-Cur, G-CS-Cur and G-TQCS-Cur at pH 1.2

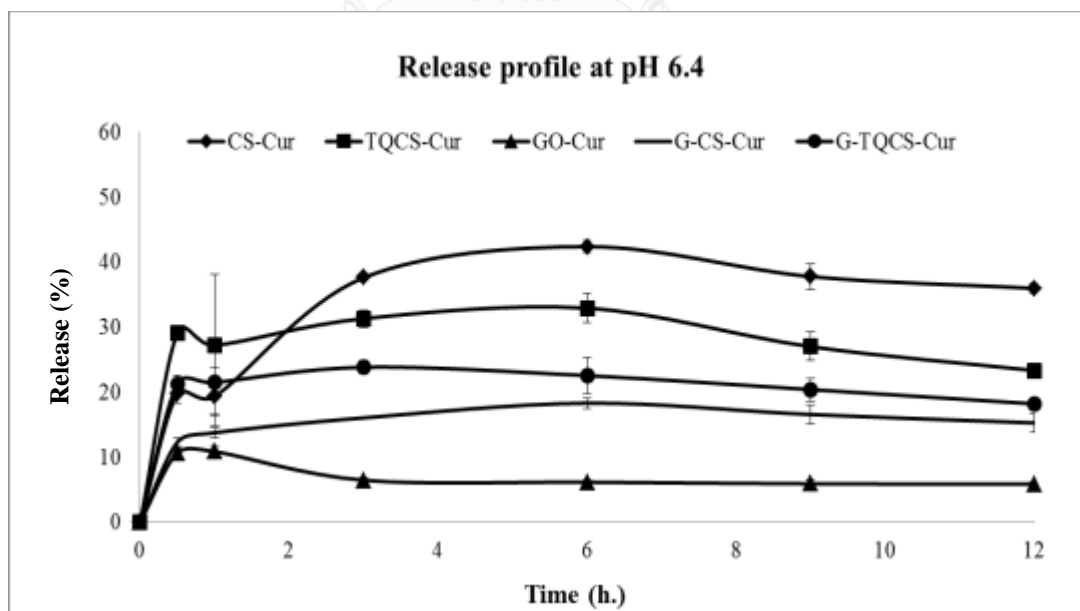


Figure 34 Release profiles of CS-Cur, TQCS-Cur, GO-Cur, G-CS-Cur and G-TQCS-Cur at pH 6.4

4.8 In Vitro Cytotoxicity Studies of Curcumin and Curcumin-loaded composite films

The cytotoxicity of pure curcumin, empty polymer and composites, curcumin-loaded polymer and composite films and control solvent (1:1 ratio of DMSO: 0.5% (v/v) acetic acid) were studied using MTT assay against two cancer cell lines (CHAGO and SW620). The cytotoxicity of pure curcumin showed the effect of increasing concentration of curcumin that presented high toxicity against two cancer cell lines (Fig. 35a and b).

The empty polymer and composite (CS, TQCS, GO, G-CS and G-TQCS) were demonstrated high cells viability (>80%) relative to the non-toxicity after 24, 48 and 72 h incubation. This suggested that within a concentration 100 $\mu\text{g}/\text{mL}$ remained low cytotoxic effect towards both of cancer cell lines (Fig. 36a and b). In contrast, the Cur-loaded polymer and composite films showed low cell viability within concentration range of 300-1 $\mu\text{g}/\text{mL}$ after all period of incubation against CHAGO and SW620 (appendix E). Hence the growth of two cancer cell lines was inhibited by increasing concentration and time of incubation of curcumin-loaded polymer and composite films.

Moreover, the cytotoxic activity of composite films with and without curcumin-loaded (concentration 300 $\mu\text{g}/\text{mL}$) tested in various of incubation time (24, 48 and 72 h) against two cancer cell lines as shown in Figure 37a and b, respectively. These results represented obviously and significantly different cytotoxicity profile in comparison to with and without curcumin-loaded within polymer and composite after all incubation times. For the curcumin-loaded polymer and composite films (Fig. 37b) exhibited high toxicity when increasing time of incubation due

to the accumulation of some dead cells lead to the acidic media which suitable condition for release curcumin from polymer and composite films as previously result of release profile. However, GO-Cur showed high cell viability in both dose and time dependent inhibition of cancer cell lines because of the strong interaction between GO and curcumin that lead to curcumin not release to media, consequently it was less effective.

The 50% growth inhibition concentration (IC_{50}) of pure curcumin and curcumin within polymer and composite films against CHAGO and SW620 after 72 h incubation were showed in Figure 38a and b, respectively. The CS-Cur and TQCS-Cur represented low amount of IC_{50} than pure curcumin ($IC_{50} = 1.07 \mu\text{g/mL}$) while G-CS-Cur and G-TQCS-Cur were higher towards the CHAGO cells (Fig. 38a). On the other hand, the similar decreasing IC_{50} value of CS-Cur ($IC_{50} = 0.83 \mu\text{g/mL}$) and G-TQCS-Cur ($IC_{50} = 0.80 \mu\text{g/mL}$) were observed in comparison with pure curcumin ($IC_{50} = 1.07 \mu\text{g/mL}$) in SW620 cells (Fig. 38b). These results indicated that after loaded curcumin into composite, the amount of curcumin which used for inhibit of cancer cell was reduced in order to improve the effective of anticancer activity.

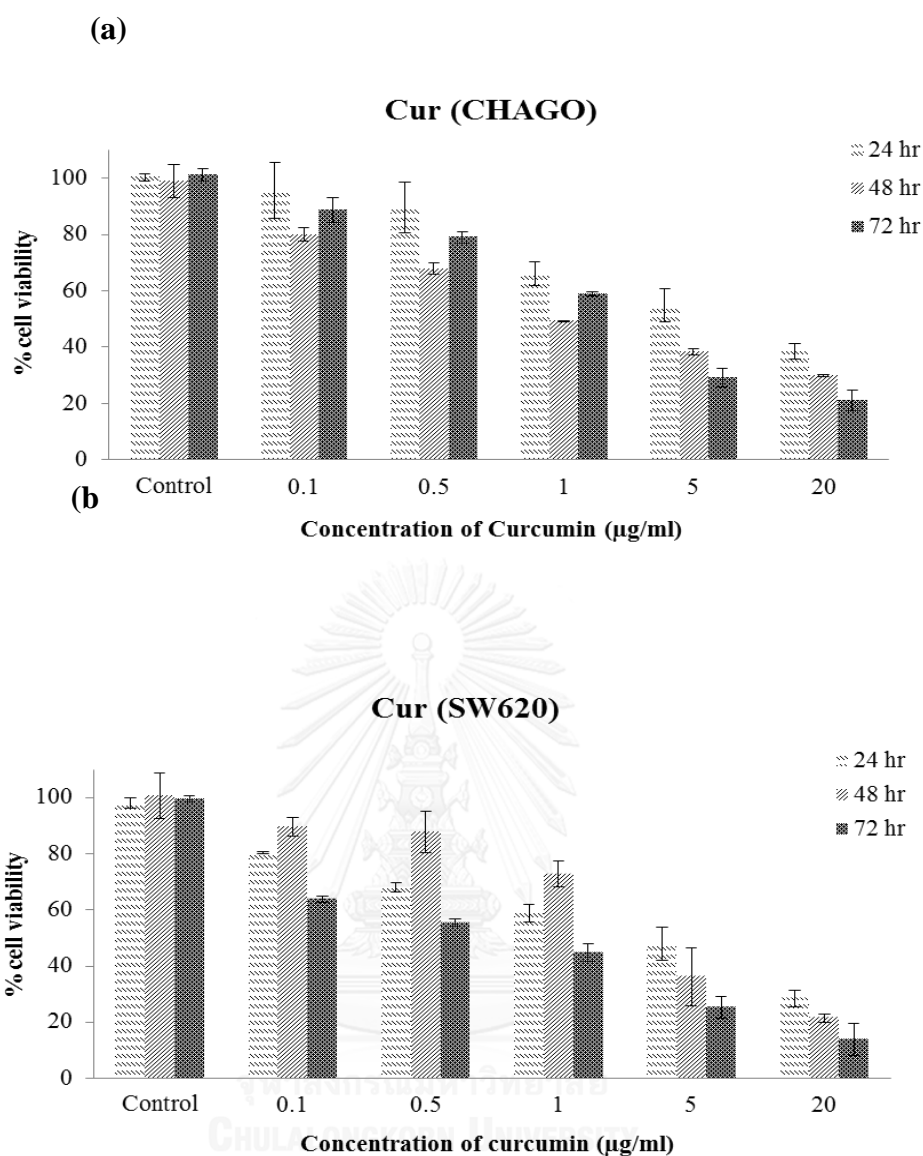


Figure 35 Cell viability of (a) CHAGO (lung cancer cell) and (b) SW620 (colon cancer cell) treated with Curcumin (Cur) for 24, 48 and 72 h (MTT assay)

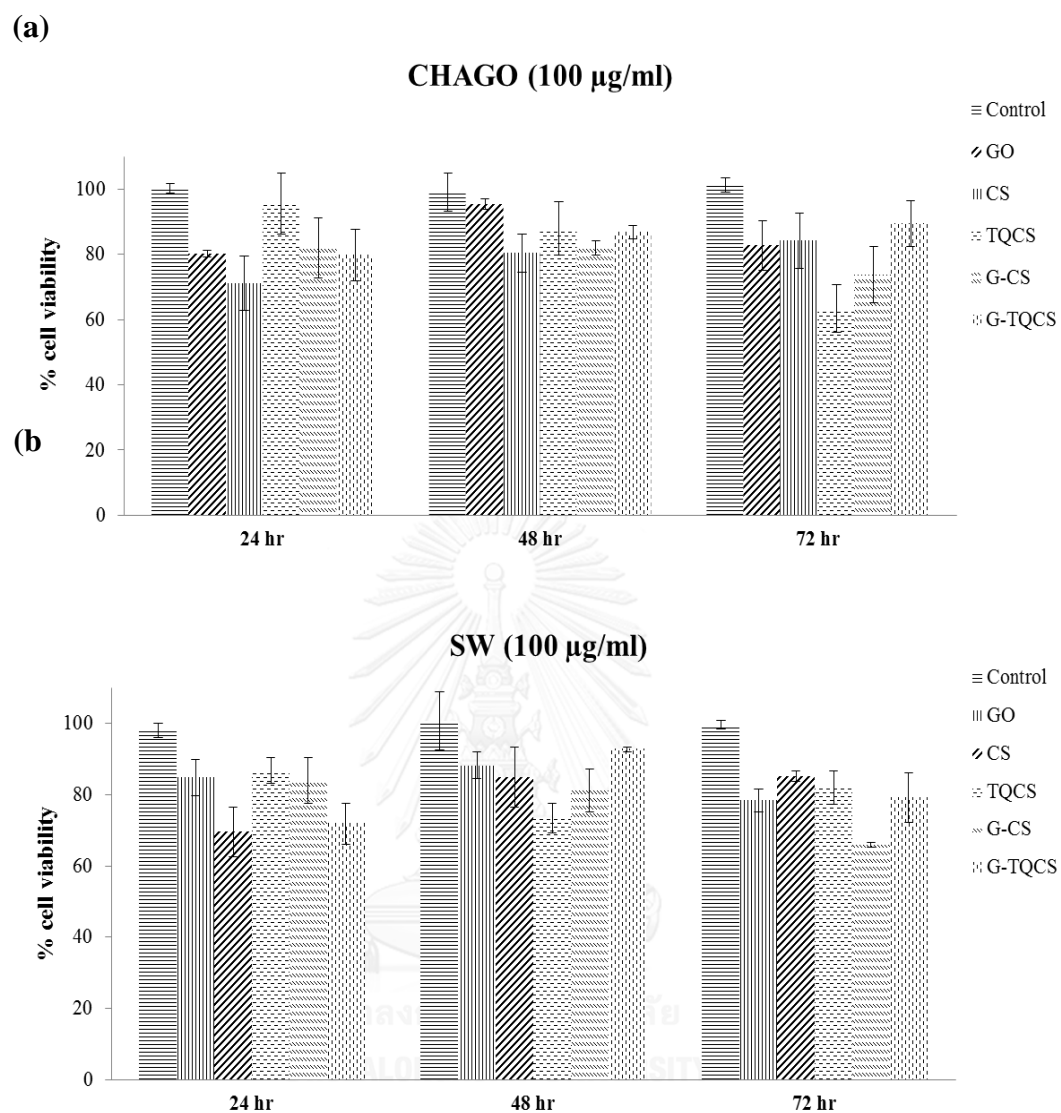
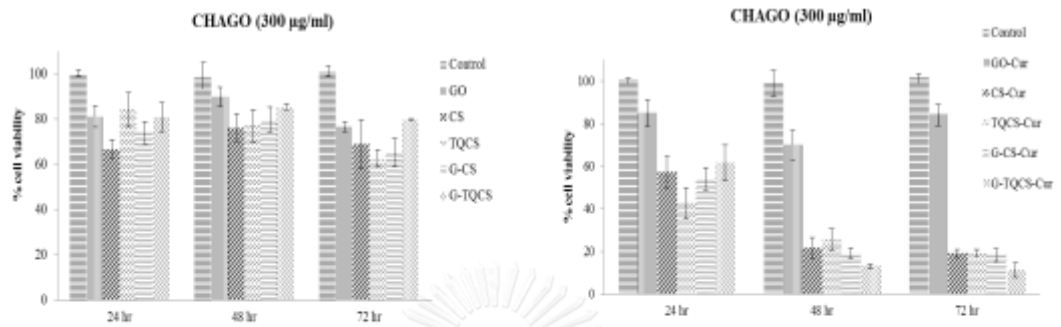


Figure 36 Cell viability of (a) CHAGO (lung cancer cell) and (b) SW620 (colon cancer cell) treated with 100 $\mu\text{g/ml}$ of CS, TQCS, GO, G-CS and G-TQCS for 24, 48 and 72 h (MTT assay)

(a)



(b)

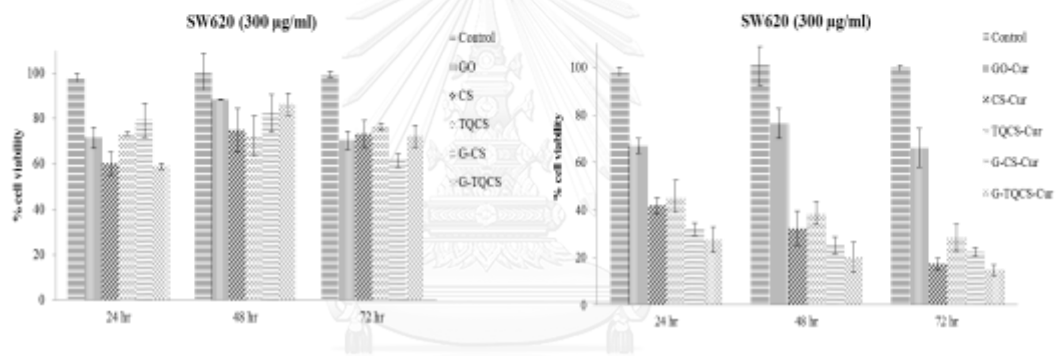


Figure 37 Cell viability of (a) CHAGO (lung cancer cell) and (b) SW620 (colon cancer cell) treated with 300 µg/mL of free (right) and Cur-loaded (left) composite films for 24, 48 and 72 h (MTT assay)

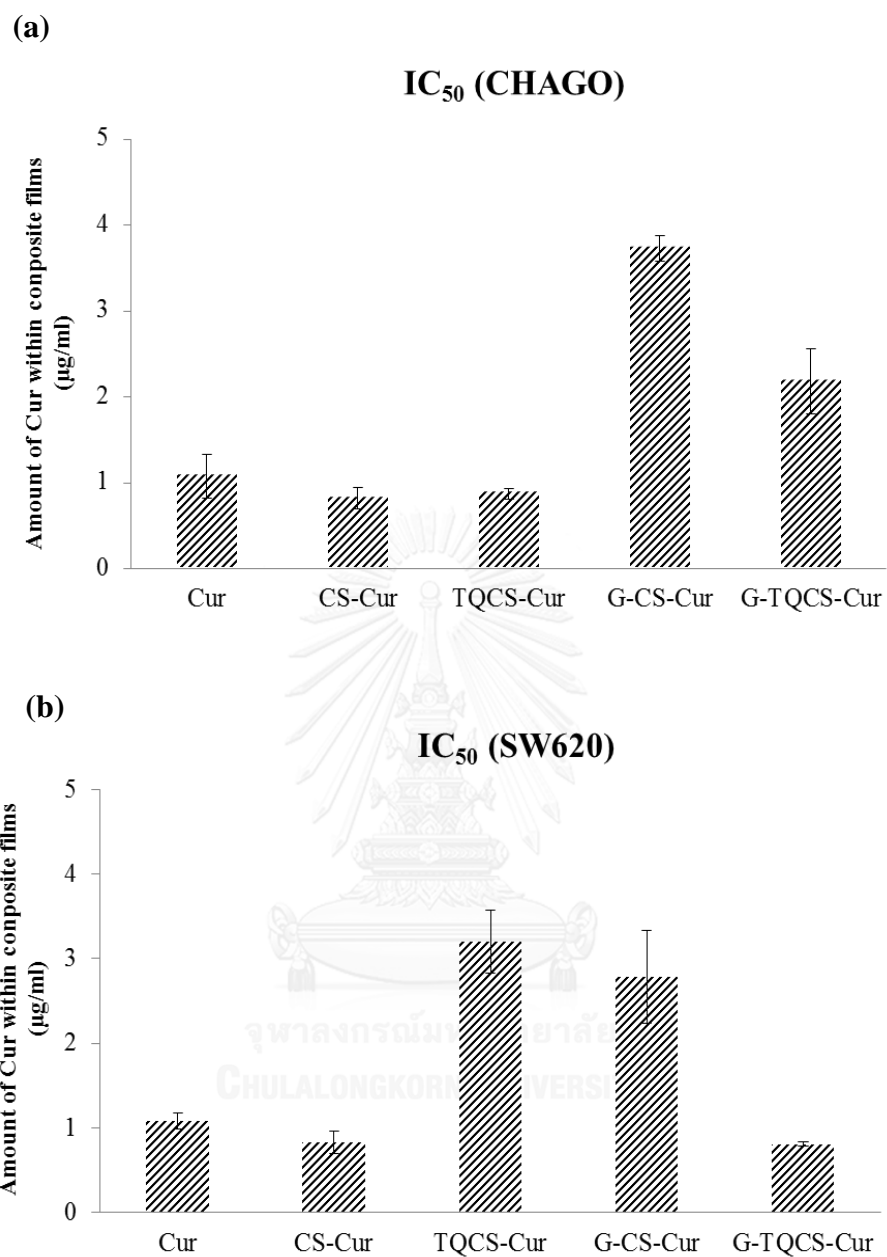


Figure 38 IC₅₀ of (a) CHAGO (lung cancer cell) and (b) SW620 (colon cancer cell) treated with CS-Cur, TQCS-Cur, GO-Cur, G-CS and G-TQCS for 72 h (MTT assay)

CHAPTER V

CONCLUSION

The graphene oxide-thiolated quaternized chitosan (G-TQCS) was modified *via* amide linkage which using EDC as a coupling agent. The modification of GO with TQCS in order to improve the aqueous solubility and enhance biocompatible of GO through gastrointestinal tract (GI). The mucoadhesive property of TQCS and GO was higher than pure CS in PBS buffer solution at stimulates GI tract (pH 1.2 and 6.4). At pH 1.2, the G-TQCS exhibited 10.7 and 1.4-fold stronger mucoadhesiveness than CS and TQCS, respectively, attribute to either interaction of electrostatic, hydrophobic effect, hydrogen bonding or thiol groups between G-TQCS and active groups on mucin that influenced on mucoadhesive properties. In contrast, at pH 6.4 the mucoadhesion of G-TQCS was reduced due to the less effectively interaction with mucin. Therefore, G-TQCS appropriately was a preferable choice to use as mucoadhesive drug delivery carrier in gastric fluid.

For the pharmaceutical application, curcumin (Cur) as a model natural anticancer drug was 10% (w/w) loaded in G-TQCS via hydrogen bonding and π - π stacking interaction between Cur and G-TQCS and formed drug-loaded composite film that showed about 90% of encapsulation efficiency. G-TQCS-Cur represented efficiently control released at pH 1.2, condition in the stomach, via the diffusion controlled drug release that exhibited 60% of cumulative release after 12 h. For the cytotoxicity of G-TQCS-Cur displayed decreasing percentage of cell viability in two cancer cell lines (CHAGO and SW620) with increasing

of concentration and time of treatment up to 72 h. The G-TQCS-Cur showed reducing of IC_{50} ($0.80 \mu\text{g/mL}$) comparing with pure Cur in SW620 cells. Consequently, G-TQCS is an innovative model composite as the mucoadhesive anticancer drug delivery carrier, especially for utilization in low pH environment.

For the future work of this research, the ratio of GO and TQCS will be optimized that presents the suitable value of mucoadhesiveness for used as mucoadhesive anticancer drug delivery carrier.



REFERENCES

1. <http://www.who.int/mediacentre/factsheets/fs297/en/index.html>, WHO. (Accessed on August 20, 2014).
2. Thanki, K., et al., *Oral delivery of anticancer drugs: challenges and opportunities*. J Control Release, 2013. **170**(1): p. 15-40.
3. Andrews, G.P., T.P. Lavery, and D.S. Jones, *Mucoadhesive polymeric platforms for controlled drug delivery*. Eur J Pharm Biopharm, 2009. **71**(3): p. 505-18.
4. Salamat-Miller, N., M. Chittchang, and T.P. Johnston, *The use of mucoadhesive polymers in buccal drug delivery*. Advanced Drug Delivery Reviews, 2005. **57**(11): p. 1666-1691.
5. Hornof, M.D., C.E. Kast, and A. Bernkop-Schnurch, *In vitro evaluation of the viscoelastic properties of chitosan-thioglycolic acid conjugates*. Eur J Pharm Biopharm, 2003. **55**(2): p. 185-90.
6. Lai, S.K., et al., *Micro- and macrorheology of mucus*. Adv Drug Deliv Rev, 2009. **61**(2): p. 86-100.
7. Grabovac, V., D. Guggi, and A. Bernkop-Schnurch, *Comparison of the mucoadhesive properties of various polymers*. Adv Drug Deliv Rev, 2005. **57**(11): p. 1713-23.
8. Bernkop-Schnurch, A., *Thiomers: a new generation of mucoadhesive polymers*. Adv Drug Deliv Rev, 2005. **57**(11): p. 1569-82.
9. Chen, D., H. Feng, and J. Li, *Graphene Oxide: Preparation, Functionalization, and Electrochemical Applications*. Chemical Reviews, 2012. **112**(11): p. 6027-6053.
10. Dreyer, D.R., et al., *The chemistry of graphene oxide*. Chemical Society Reviews, 2010. **39**(1): p. 228-240.

11. Yang, X., et al., *Superparamagnetic graphene oxide-Fe₃O₄nanoparticles hybrid for controlled targeted drug carriers*. Journal of Materials Chemistry, 2009. **19**(18): p. 2710-2714.
12. Depan, D., J. Shah, and R.D.K. Misra, *Controlled release of drug from folate-decorated and graphene mediated drug delivery system: Synthesis, loading efficiency, and drug release response*. Materials Science and Engineering: C, 2011. **31**(7): p. 1305-1312.
13. Bao, H., et al., *Chitosan-functionalized graphene oxide as a nanocarrier for drug and gene delivery*. Small, 2011. **7**(11): p. 1569-78.
14. Wu, S., et al., *Cytotoxicity of graphene oxide and graphene oxide loaded with doxorubicin on human multiple myeloma cells*. Int J Nanomedicine, 2014. **9**: p. 1413-21.
15. Jayakumar, R., R.A.A. Muzzarelli, and M. Prabakaran, *Chitosan for Biomaterials II Preface*. Chitosan for Biomaterials Ii, 2011. **244**.
16. Smart, J.D., *The basics and underlying mechanisms of mucoadhesion*. Advanced Drug Delivery Reviews, 2005. **57**(11): p. 1556-1568.
17. Yin, L., et al., *Drug permeability and mucoadhesion properties of thiolated trimethyl chitosan nanoparticles in oral insulin delivery*. Biomaterials, 2009. **30**(29): p. 5691-700.
18. Jintapattanakit, A., et al., *Physicochemical properties and biocompatibility of N-trimethyl chitosan: Effect of quaternization and dimethylation*. European Journal of Pharmaceutics and Biopharmaceutics, 2008. **70**(2): p. 563-571.

19. Schmitz, T., et al., *Synthesis and characterization of a chitosan-N-acetyl cysteine conjugate*. International Journal of Pharmaceutics, 2008. **347**(1-2): p. 79-85.
20. Margit D. Hornof, C.E.K., Andreas Bernkop-Schnürch, *In vitro evaluation of the viscoelastic properties of chitosan–thioglycolic acid conjugates*. European Journal of Pharmaceutics and Biopharmaceutics, 2003. **55**: p. 185–190.
21. Juntapram, K., et al., *Synthesis and characterization of chitosan-homocysteine thiolactone as a mucoadhesive polymer*. Carbohydrate Polymers, 2012. **87**(4): p. 2399-2408.
22. Sharma, R.A., A.J. Gescher, and W.P. Steward, *Curcumin: the story so far*. Eur J Cancer, 2005. **41**(13): p. 1955-68.
23. Okudan, N., et al., *Protective effects of curcumin supplementation on intestinal ischemia reperfusion injury*. Phytomedicine, 2013. **20**(10): p. 844-8.
24. Sa, G. and T. Das, *Anti cancer effects of curcumin: cycle of life and death*. Cell Div, 2008. **3**: p. 14.
25. Sharma, R.A. and P.B. Farmer, *Biological relevance of adduct detection to the chemoprevention of cancer*. Clin Cancer Res, 2004. **10**(15): p. 4901-12.
26. Mohan, R., et al., *Curcuminoids inhibit the angiogenic response stimulated by fibroblast growth factor-2, including expression of matrix metalloproteinase gelatinase B*. J Biol Chem, 2000. **275**(14): p. 10405-12.
27. Jagetia, G.C. and G.K. Rajanikant, *Curcumin treatment enhances the repair and regeneration of wounds in mice exposed to*

- hemibody gamma-irradiation*. Plastic and reconstructive surgery, 2005. **115**(2): p. 515-528.
28. Tang, H., et al., *Curcumin polymers as anticancer conjugates*. Biomaterials, 2010. **31**(27): p. 7139-49.
 29. Maheshwari, R.K., et al., *Multiple biological activities of curcumin: a short review*. Life Sci, 2006. **78**(18): p. 2081-7.
 30. Kumar, A., et al., *Subcellular localization of the yeast proteome*. Genes Dev, 2002. **16**(6): p. 707-19.
 31. *In vitro combinatorial anticancer effects of 5-fluorouracil and curcumin loaded N,O-carboxymethyl chitosan nanoparticles toward colon cancer and in vivo pharmacokinetic studies*. European Journal of Pharmaceutics and Biopharmaceutics, 2014.
 32. Bisht, S., et al., *Polymeric nanoparticle-encapsulated curcumin ("nanocurcumin"): a novel strategy for human cancer therapy*. J Nanobiotechnology, 2007. **5**: p. 3.
 33. Muller, R.H. and C.M. Keck, *Challenges and solutions for the delivery of biotech drugs--a review of drug nanocrystal technology and lipid nanoparticles*. J Biotechnol, 2004. **113**(1-3): p. 151-70.
 34. Wang, Y.J., et al., *Stability of curcumin in buffer solutions and characterization of its degradation products*. J Pharm Biomed Anal, 1997. **15**(12): p. 1867-76.
 35. <http://www.radiotherapy.in/what-is-cancer.html>, *Cancer*. (Accessed on September 16, 2013).
 36. *Applied Biopharmaceutics and Pharmacokinetics*. Annals of Internal Medicine, 1981. **94**(6): p. 826-826.
 37. http://www.vitaldose.com/utilizing/delivery_systems.htm, *Control release*. (Accessed on September 20, 2014).

38. Son, Y.J., et al., *Biodistribution and anti-tumor efficacy of doxorubicin loaded glycol-chitosan nanoaggregates by EPR effect*. Journal of Controlled Release, 2003. **91**(1): p. 135-145.
39. Abruzzo, A., et al., *Mucoadhesive chitosan/gelatin films for buccal delivery of propranolol hydrochloride*. Carbohydrate Polymers, 2012. **87**(1): p. 581-588.
40. Zambito, Y., et al., *Mucoadhesive nanoparticles made of thiolated quaternary chitosan crosslinked with hyaluronan*. Carbohydrate polymers, 2013. **92**(1): p. 33-39.
41. Svensson, O., Malmö högskola., *Interactions of Mucins with Biopolymers and Drug Delivery Particles*. Malmö University, 2008: p. 1-82.
42. Sogias, I.A.W., A. C.; Khutoryanskiy, V. V., , *Chitosan-based mucoadhesive tablets for oral delivery of ibuprofen*. International Journal of Pharmaceutics 2012. **436**(1-2): p. 602-610.
43. Khutoryanskiy, V.V., *Advances in mucoadhesion and mucoadhesive polymers*. Macromolecular bioscience, 2011. **11**(6): p. 748-764.
44. Salamat-Miller N, C.M., Johnston TP., *The use of mucoadhesive polymers in buccal drug delivery*. Advance DrugDelivery Review, 2005. **57**(11): p. 1666-1691.
45. Goenka, S., V. Sant, and S. Sant, *Graphene-based nanomaterials for drug delivery and tissue engineering*. Journal of Controlled Release, 2014. **173**(0): p. 75-88.
46. Hummers, W.S. and R.E. Offeman, *Preparation of Graphitic Oxide*. Journal of the American Chemical Society, 1958. **80**(6): p. 1339-1339.

47. Guo, X. and N. Mei, *Assessment of the toxic potential of graphene family nanomaterials*. Journal of Food and Drug Analysis. **22**(1): p. 105-115.
48. Liu, J., L. Cui, and D. Losic, *Graphene and graphene oxide as new nanocarriers for drug delivery applications*. Acta Biomater, 2013. **9**(12): p. 9243-57.
49. Kast, C.E., & Bernkop-Schnurch, A. Biomaterials. , *Thiolated polymers–thiomers: Development and in vitro evaluation of chitosan–thioglycolic acid conjugates*. . 2001. **22**(17): p. 2345–2352.
50. Suresh D.Kumavat. *, Y.S.C., Priyanka Borole, Preetesh Mishra., Khusbu Shenghani, Pallavi Duvvuri., *DEGRADATION STUDIES OF CURCUMIN*. International Journal of Pharmacy Review & Research, 2013. **3**(2): p. 50-55.
51. Sharma, R.A., et al., *Phase I clinical trial of oral curcumin: biomarkers of systemic activity and compliance*. Clin Cancer Res, 2004. **10**(20): p. 6847-54.
52. van Meerloo, J., G.J. Kaspers, and J. Cloos, *Cell sensitivity assays: the MTT assay*. Methods Mol Biol, 2011. **731**: p. 237-45.
53. Ebada, S.S., et al., *Methods for isolation, purification and structural elucidation of bioactive secondary metabolites from marine invertebrates*. Nat. Protocols, 2008. **3**(12): p. 1820-1831.
54. H. Huating , W.X., W. Jingchao , L. Fangming , Z. Min , X. Chunhui *Microwave-assisted covalent modification of graphene nanosheets with chitosan and its electrorheological characteristics*. Carbohydrate Polymers, 2011. **84**: p. 1158–1164.

55. Sieval, A.B., Thanou, M., Kotzé, A.F., Verhoef, J.C., Brussee, J., Junginger, H.E., *Preparation and NMR characterization of highly substituted N-trimethyl chitosan chloride*. Carbohydrate Polymers, 1998. **36**(2-3): p. 157-165.
56. Schmitz T, G.V., Palmberger TF, Hoffer MH, Bernkop-Schnürch A., *Synthesis and characterization of a chitosan-N-acetyl cysteine conjugate*. International journal of pharmaceutics, 2008. **347**(1-2): p. 79-85.
57. Parize, A.L., et al., *Evaluation of chitosan microparticles containing curcumin and crosslinked with sodium tripolyphosphate produced by spray drying*. Química Nova, 2012. **35**: p. 1127-1132.
58. Ajithkumar, M., M. Yashoda, and S. Prasannakumar, *Copolymerization of N-Vinyl pyrrolidone with methyl methacrylate by Ti (III)-DMG redox initiator*. Turkish Journal of Chemistry, 2012. **36**: p. 397-409.
59. Fulmer, G.R., et al., *NMR Chemical Shifts of Trace Impurities: Common Laboratory Solvents, Organics, and Gases in Deuterated Solvents Relevant to the Organometallic Chemist*. Organometallics, 2010. **29**(9): p. 2176-2179.
60. Shen, J., et al., *Synthesis of graphene oxide-based biocomposites through diimide-activated amidation*. J Colloid Interface Sci, 2011. **356**(2): p. 543-9.
61. Yandrapu, S.K., et al., *Development and optimization of thiolated dendrimer as a viable mucoadhesive excipient for the controlled drug delivery: an acyclovir model formulation*. Nanomedicine, 2013. **9**(4): p. 514-22.

62. <http://stainsfile.info/StainsFile/stain/schiff/reaction-pas.htm>, *Periodic Acid Schiff*. (Accessed on July 11, 2013).
63. Anitha, A., et al., *Preparation, characterization, in vitro drug release and biological studies of curcumin loaded dextran sulphate–chitosan nanoparticles*. *Carbohydrate Polymers*, 2011. **84**(3): p. 1158-1164.



APPENDIX



จุฬาลงกรณ์มหาวิทยาลัย
CHULALONGKORN UNIVERSITY

APPENDIX A

Standard curve of L-cysteine Hydrochloride

The concentrations versus peak absorbance of L-cysteine are presented in Table 1A. The plot of calibration curve of L-cysteine hydrochloride is illustrated in Figure 1A.

Table 1A Absorbance of various concentrations of L-cysteine Hydrochloride by UV

Concentration ($\mu\text{mol/g}$)	Absorbance (Avg.)
100	0.018
200	0.165
400	0.534
600	0.902
800	1.290
1000	1.642

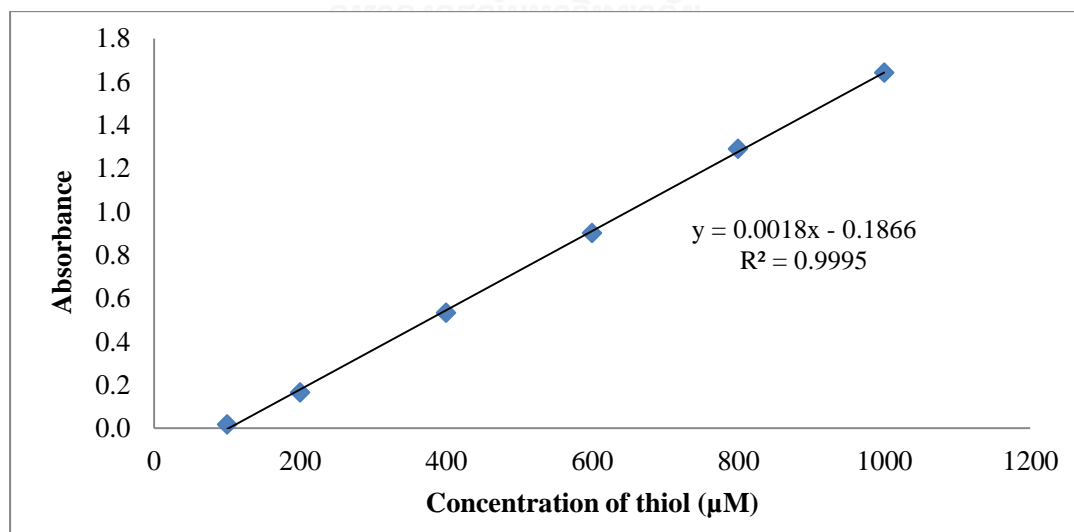


Figure 1A. Standard curve of L-cysteine Hydrochloride by UV spectrometer

Table 2A Absorbance thiol groups by UV spectrometer

Compound	Abs.	Abs.	Abs.	Thiol (μM)	SD
TQCS	0.456	0.524	0.582	324.00	0.02
G-TQCS	0.069	0.073	0.103	104.50	0.06

Table 3A Absorbance disulfide groups by UV spectrometer

Compound	Abs.	Abs.	Abs.	Thiol (μM)	SD
TQCS	0.099	0.096	0.108	57.08	0.01
G-TQCS	0.17	0.125	0.089	63.83	0.04

APPENDIX B

Calibration curve of mucin (type II)

The concentration versus peak absorbance mucin glycoprotein (type II) determined by UV is presented in Table 1B. The plot of calibration curve of mucin is illustrated in Figure 1B.

Table 1B Absorbance concentrations of mucin (type II) at pH 1.2, 4.0 and 6.4 by UV spectrometer

Concentration (mg/ 2mL)	HCl (pH 1.2)	Acetate buffer (pH 4.0)	PBS (PH 6.4)
0.2	0.108	0.254	0.159
0.4	0.205	0.439	0.326
0.6	0.296	0.658	0.455
0.8	0.402	0.930	0.631
1.0	0.505	1.100	0.839

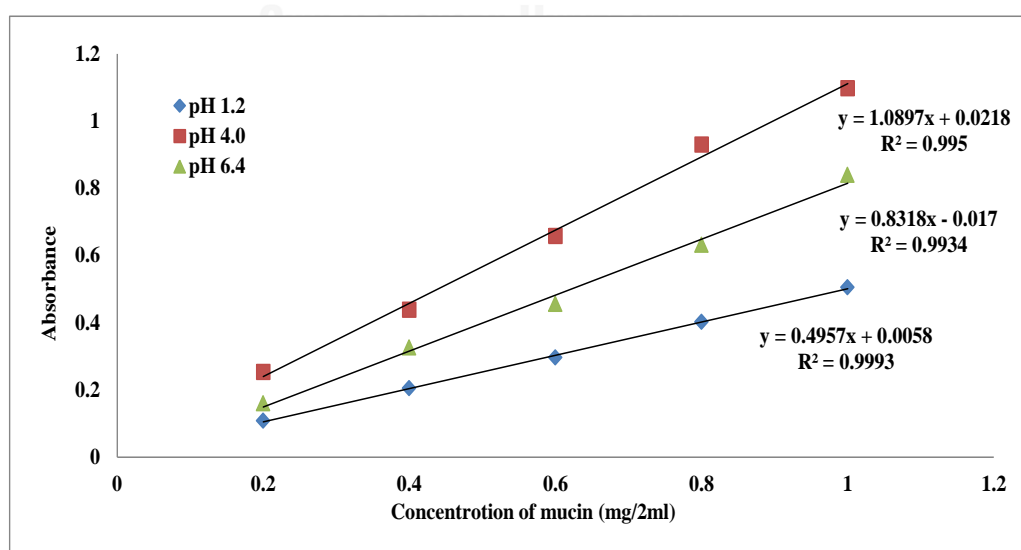


Figure 1B. Standard curve of mucin at pH 1.2, 4.0, and 6.4

Table 2B Absorbance of adsorbed mucin of CS, TQCS, GO, G-CS and G-TQCS at pH 1.2 by UV spectrophotometer

Compound	Abs.	Abs.	Abs.	Adsorbed mucin (mg/2ml)	SD
CS	0.571	0.631	0.556	0.03	0.08
TQCS	0.391	0.395	0.39	0.22	0.01
GO	0.236	0.267	0.24	0.37	0.04
G-CS	0.255	0.252	0.283	0.35	0.04
G-TQCS	0.292	0.294	0.309	0.32	0.02

Table 3B Absorbance of adsorbed mucin of CS, TQCS, GO, G-CS and G-TQCS at pH 4.0 by UV spectrophotometer

Compound	Abs.	Abs.	Abs.	Adsorbed mucin (mg/2ml)	SD
CS	0.625	0.592	0.581	0.30	0.04
TQCS	0.235	0.244	0.296	0.46	0.01
GO	0.147	0.144	0.153	0.51	0.02
G-CS	0.177	0.164	0.164	0.49	0.01
G-TQCS	0.371	0.434	0.386	0.39	0.04

Table 4B Absorbance of adsorbed mucin of CS, TQCS, GO, G-CS and G-TQCS at pH 6.4 by UV spectrophotometer

Compound	Abs.	Abs.	Abs.	Adsorbed mucin (mg/2ml)	SD
CS	0.733	0.639	0.662	0.17	0.06
TQCS	0.349	0.349	0.341	0.37	0.01
GO	0.239	0.243	0.24	0.43	0.01
G-CS	0.25	0.244	0.253	0.43	0.01
G-TQCS	0.477	0.485	0.51	0.28	0.02



APPENDIX C

Calibration curve of curcumin (Cur)

Table 1C Absorbance of curcumin drug in ethanol determined in 428 nm

Concentration of Cur ($\mu\text{g/mL}$)	Absorbance (Avg.)
10	1.629
8	1.292
6	0.914
4	0.684
2	0.375

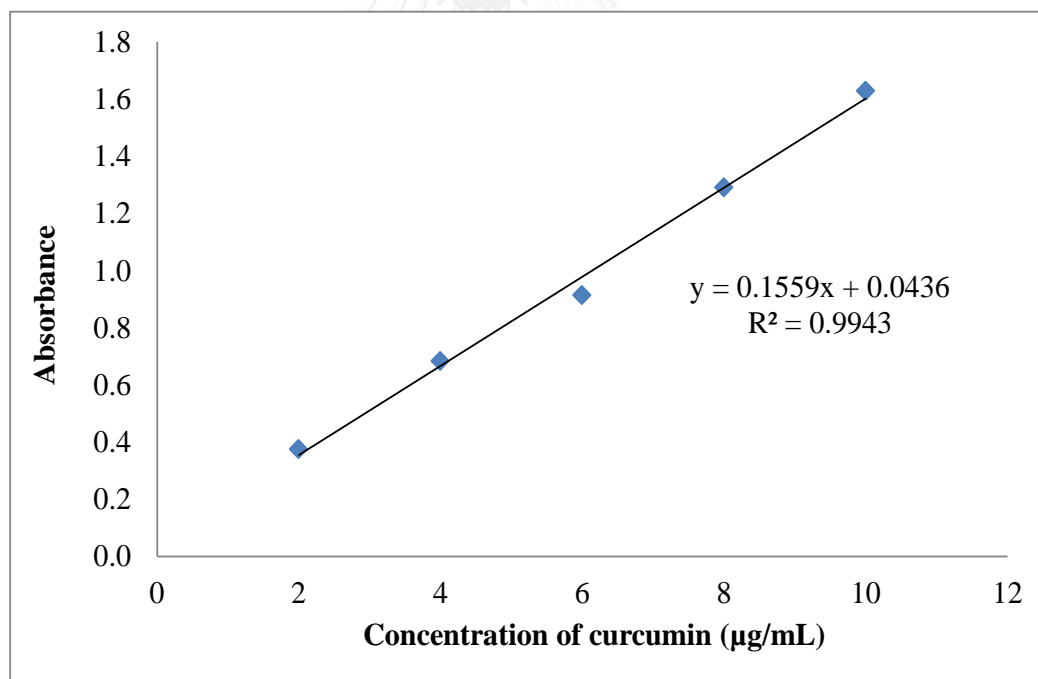
**Figure 1C.** Calibration curve of curcumin in ethanol

Table 2C Absorbance of curcumin drug in pH 1.2 determined in 428 nm

Concentration of Cur ($\mu\text{g/mL}$)	Absorbance (Avg.)
10	0.598
8	0.463
6	0.332
4	0.246
2	0.096

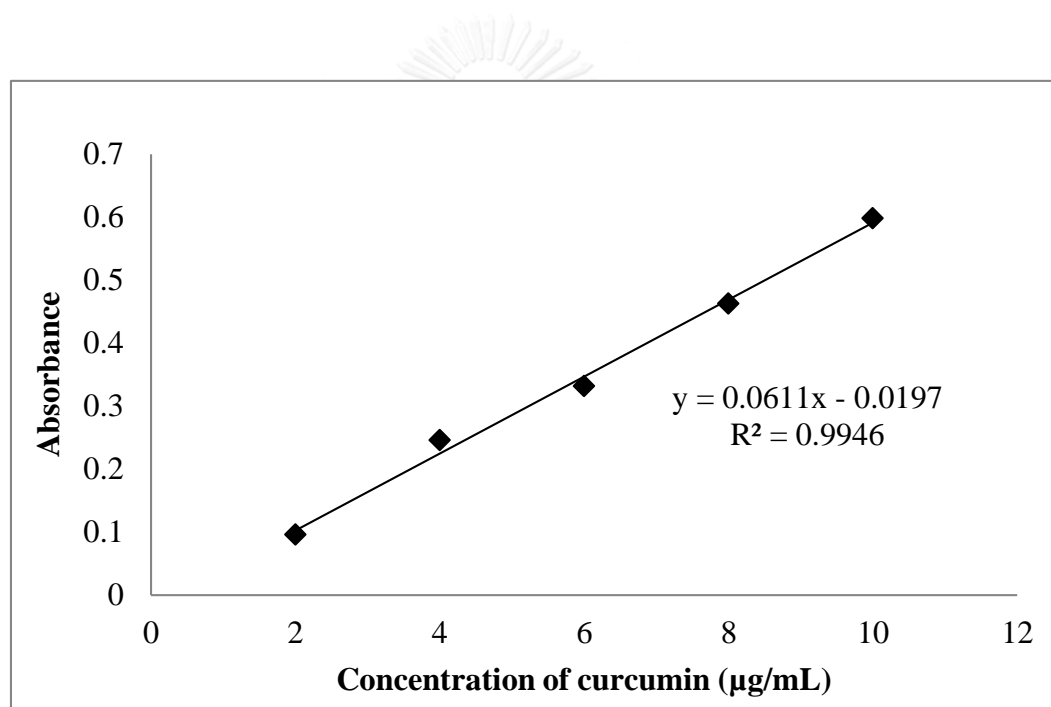
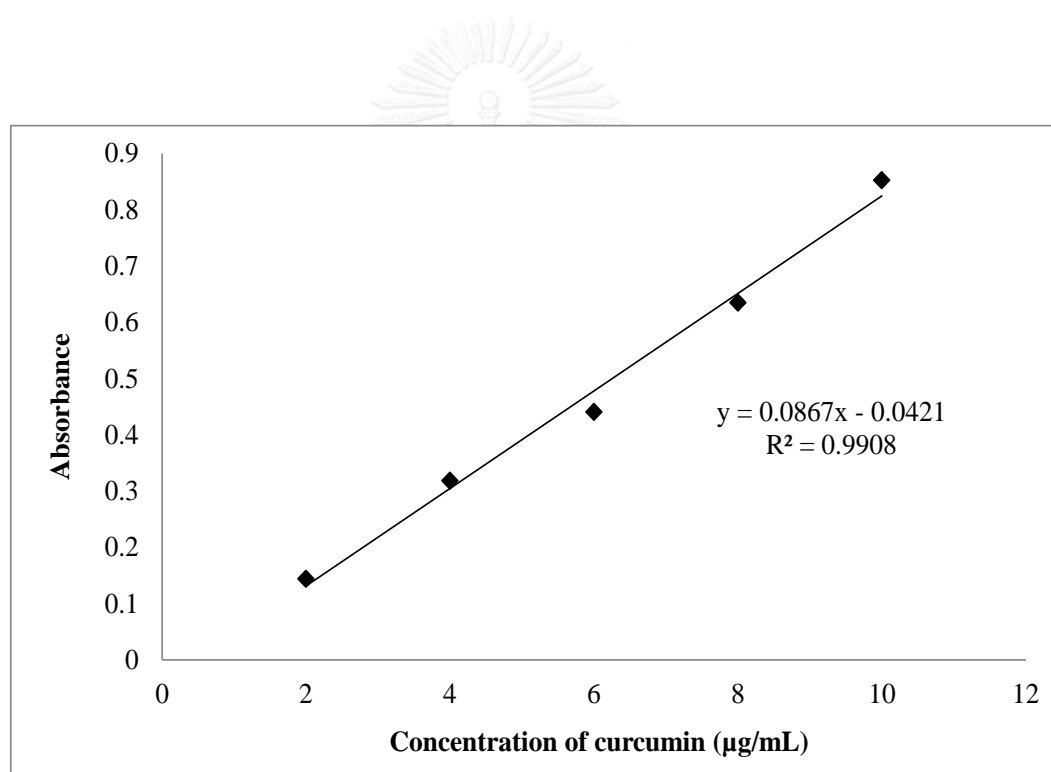
**Figure 2C** Calibration curve of curcumin in pH 1.2

Table 3C Absorbance of curcumin drug in pH 6.4 determined in 428 nm

Concentration of Cur ($\mu\text{g/mL}$)	Absorbance (Avg.)
10	0.852
8	0.635
6	0.440
4	0.318
2	0.144

**Figure 3C** Calibration curve of curcumin in pH 6.4

APPENDIX D

Drug Release

Table 1D Curcumin release from CS-Cur in pH 1.2

Time(h)	Amount of curcumin release				
	1	2	3	Average	SD
0	0	0	0	0	0
0.5	0.116	0.122	0.129	0.122	1.641
1	0.164	0.159	0.188	0.170	3.911
3	0.177	0.197	0.201	0.192	3.244
6	0.193	0.202	0.195	0.197	1.192
9	0.19	0.216	0.219	0.208	4.023
12	0.187	0.198	0.203	0.196	2.065

Table 2D Cumulative 10% curcumin release from TQCS-Cur in pH 1.2

Time(h)	Amount of curcumin release				
	1	2	3	Average	SD
0	0	0	0	0	0
0.5	0.408	0.458	0.485	0.450	5.552
1	0.471	0.519	0.493	0.494	6.825
3	0.437	0.414	0.393	0.414	9.856
6	0.385	0.361	0.415	0.387	6.062
9	0.66	0.704	0.707	0.690	3.693
12	0.589	0.638	0.622	0.616	6.303

Table 3D Cumulative 10% curcumin release from GO-Cur in pH 1.2

Time(h)	Amount of curcumin release				
	1	2	3	Average	SD
0	0	0	0	0	0
0.5	0.032	0.046	0.054	0.044	2.809
1	0.06	0.058	0.062	0.06	0.504
3	0.012	0.012	0.012	0.012	2.66
6	0.004	0.004	0.005	0.004	0.145
9	0.001	0.009	0.014	0.007	1.926
12	0	0.008	0.006	0.004	1.050

Table 4D Cumulative 10% curcumin release from G-CS-Cur in pH 1.2

Time(h)	Amount of curcumin release				
	1	2	3	Average	SD
0	0	0	0	0	0
0.5	0.112	0.126	0.14	0.126	3.532
1	0.139	0.146	0.153	0.146	1.766
3	0.178	0.196	0.19	0.188	2.312
6	0.225	0.246	0.238	0.236	2.673
9	0.241	0.262	0.256	0.253	2.728
12	0.276	0.289	0.309	0.291	4.193

Table 5D Cumulative 10% curcumin release from G-TQCS-Cur in pH 1.2

Time(h)	Amount of curcumin release				
	1	2	3	Average	SD
0	0	0	0	0	0
0.5	0.162	0.161	0.167	0.163	0.811
1	0.151	0.157	0.156	0.155	0.811
3	0.142	0.163	0.172	0.159	3.884
6	0.137	0.146	0.173	0.152	4.726
9	0.184	0.194	0.189	0.189	1.261
12	0.348	0.371	0.347	0.355	3.425

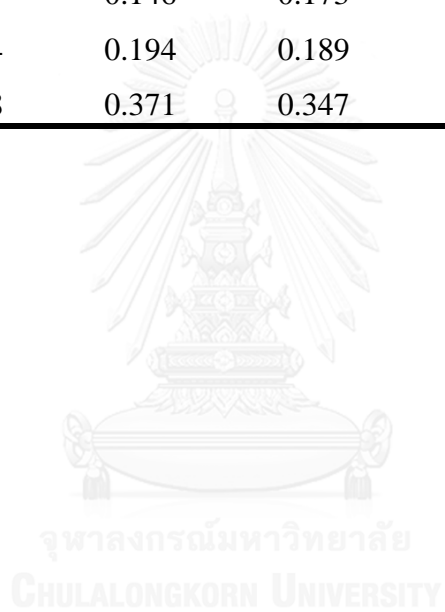


Table 6D Cumulative 10% curcumin release from CS-Cur in pH 6.4

Time(h)	Amount of curcumin release				
	1	2	3	Average	SD
0	0	0	0	0	0
0.5	0.059	0.075	0.067	0.067	1.450
1	0.037	0.086	0.071	0.064	4.550
3	0.166	0.164	0.166	0.165	0.209
6	0.186	0.195	0.194	0.191	0.894
9	0.154	0.17	0.175	0.166	1.988
12	0.155	0.153	0.161	0.156	0.754

Table 7D Cumulative 10% curcumin release from TQCS-Cur in pH 6.4

Time(h)	Amount of curcumin release				
	1	2	3	Average	SD
0	0	0	0	0	0
0.5	0.264	0.267	0.272	0.267	0.732
1	0.178	0.282	0.283	0.247	10.935
3	0.283	0.295	0.296	0.291	1.311
6	0.297	0.306	0.322	0.308	2.295
9	0.232	0.249	0.255	0.245	2.162
12	0.201	0.212	0.206	0.206	0.998

Table 8D Cumulative 10% curcumin release from GO-Cur in pH 6.4

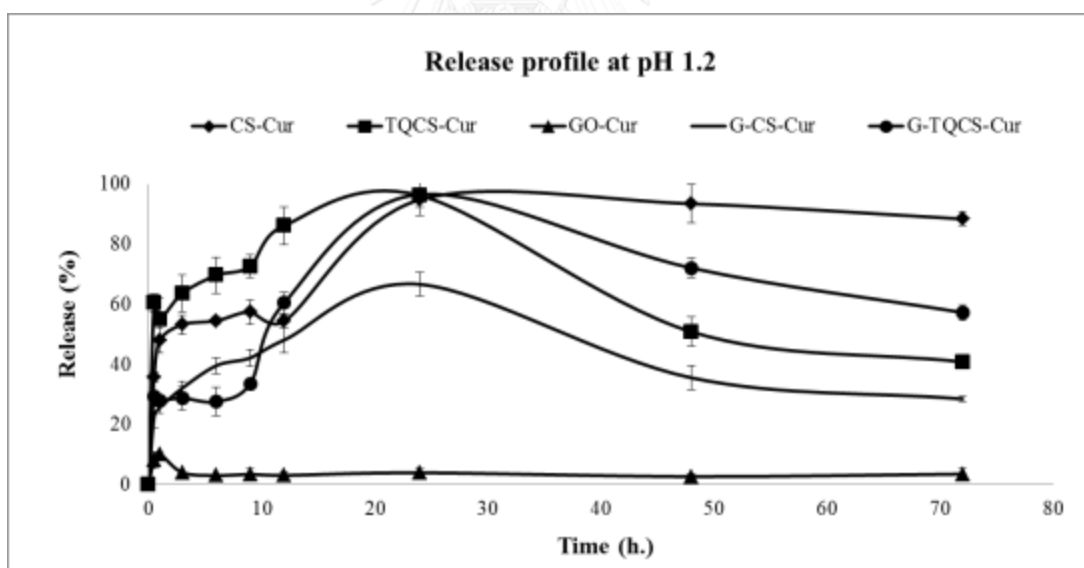
Time(h)	Amount of curcumin release				
	1	2	3	Average	SD
0	0	0	0	0	0
0.5	0.07	0.078	0.078	0.075	0.837
1	0.082	0.077	0.073	0.077	0.817
3	0.027	0.031	0.029	0.029	0.362
6	0.023	0.027	0.027	0.025	0.418
9	0.022	0.027	0.02	0.023	0.653
12	0.022	0.02	0.025	0.022	0.456

Table 9D Cumulative 10% curcumin release from G-CS-Cur in pH 6.4

Time(h)	Amount of curcumin release				
	1	2	3	Average	SD
0	0	0	0	0	0
0.5	0.067	0.073	0.067	0.069	0.627
1	0.077	0.085	0.084	0.082	0.790
3	0.102	0.103	0.103	0.102	0.104
6	0.121	0.128	0.12	0.123	0.790
9	0.099	0.115	0.108	0.107	1.453
12	0.087	0.097	0.103	0.095	1.465

Table 10D Cumulative 10% curcumin release from G-TQCS-Cur in pH 6.4

Time(h)	Amount of curcumin release				
	1	2	3	Average	SD
0	0	0	0	0	0
0.5	0.131	0.143	0.144	0.139	1.311
1	0.11	0.153	0.161	0.141	4.971
3	0.155	0.166	0.163	0.161	1.030
6	0.139	0.168	0.144	0.150	2.809
9	0.121	0.138	0.137	0.132	1.729
12	0.113	0.117	0.11	0.113	0.636

**Figure 1D** Release profiles of CS-Cur, TQCS-Cur, GO-Cur, G-CS-Cur and G-TQCS-Cur at pH 1.2 after 72 h.

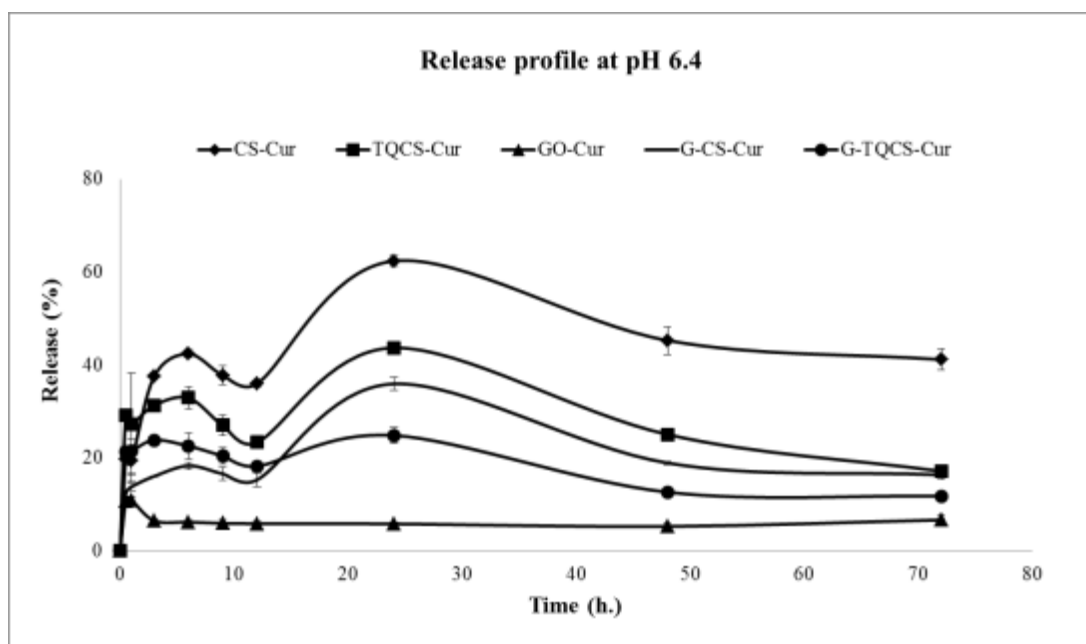


Figure 2D Release profiles of CS-Cur, TQCS-Cur, GO-Cur, G-CS-Cur and G-TQCS-Cur at pH 6.4 after 72 h.

APPENDIX E

Cytotoxicity studies (MTT assay)

The concentrations versus percentage of cell viability of curcumin-loaded polymer and composites against CHAGO (Lung cancer cell) are presented in Figure 1E-5E.

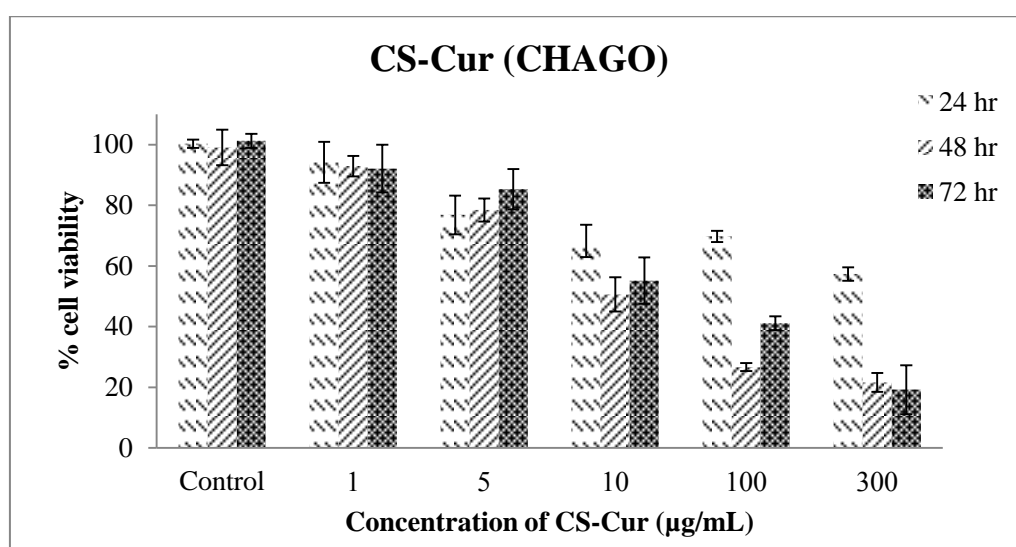


Figure 1E. Cell viability of CS-Cur against CHAGO cell lines incubated for 24, 48 and 72 h (MTT assay)

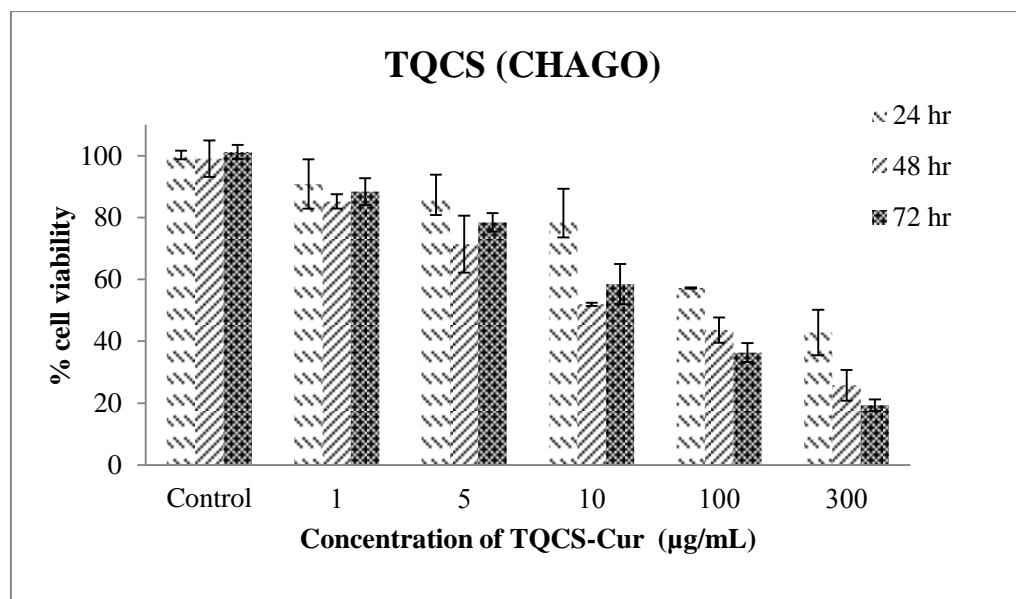


Figure 2E. Cell viability of TQCS-Cur against CHAGO cell lines incubated for 24, 48 and 72 h (MTT assay)

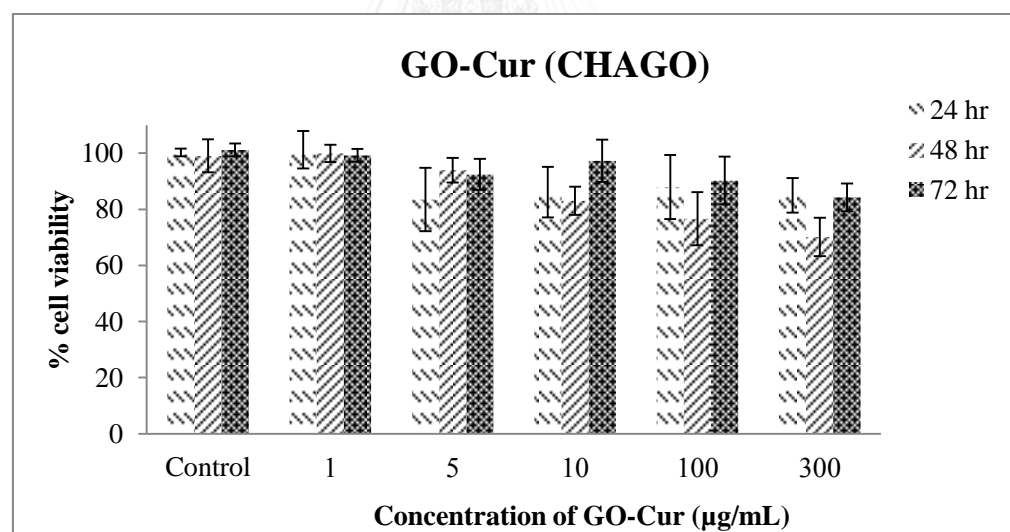


Figure 3E. Cell viability of GO-Cur against CHAGO cell lines incubated for 24, 48 and 72 h (MTT assay)

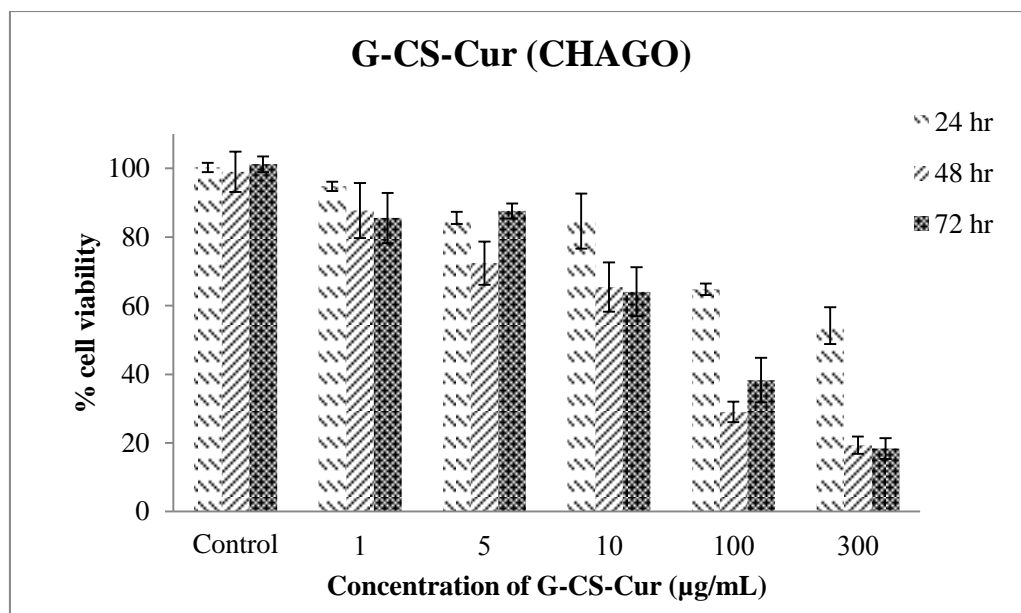


Figure 4E. Cell viability of G-CS-Cur against CHAGO cell lines incubated for 24, 48 and 72 h (MTT assay)

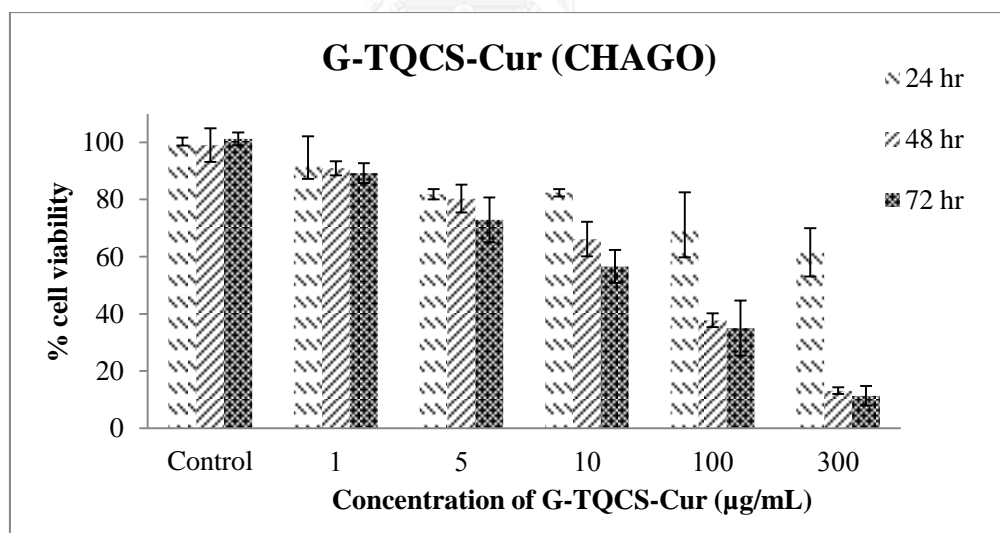


Figure 5E. Cell viability of G-CS-Cur against CHAGO cell lines incubated for 24, 48 and 72 h (MTT assay)

The concentrations versus percentage of cell viability of curcumin-loaded polymer and composites against SW620 (Colon cancer cell) are presented in Figure 6E-10E.

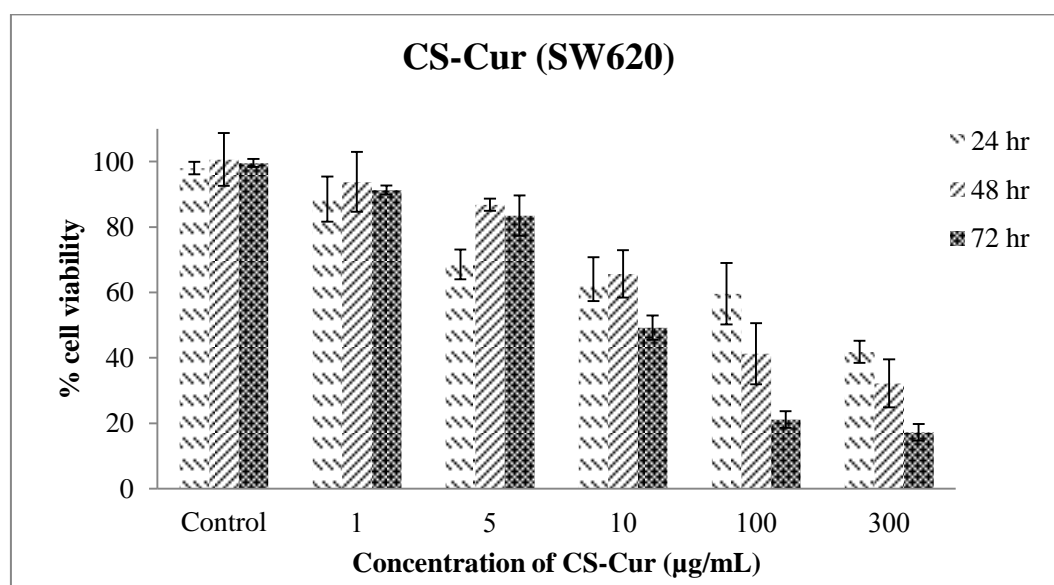


Figure 6E. Cell viability of CS-Cur against SW620 cell lines incubated for 24, 48 and 72 h (MTT assay)

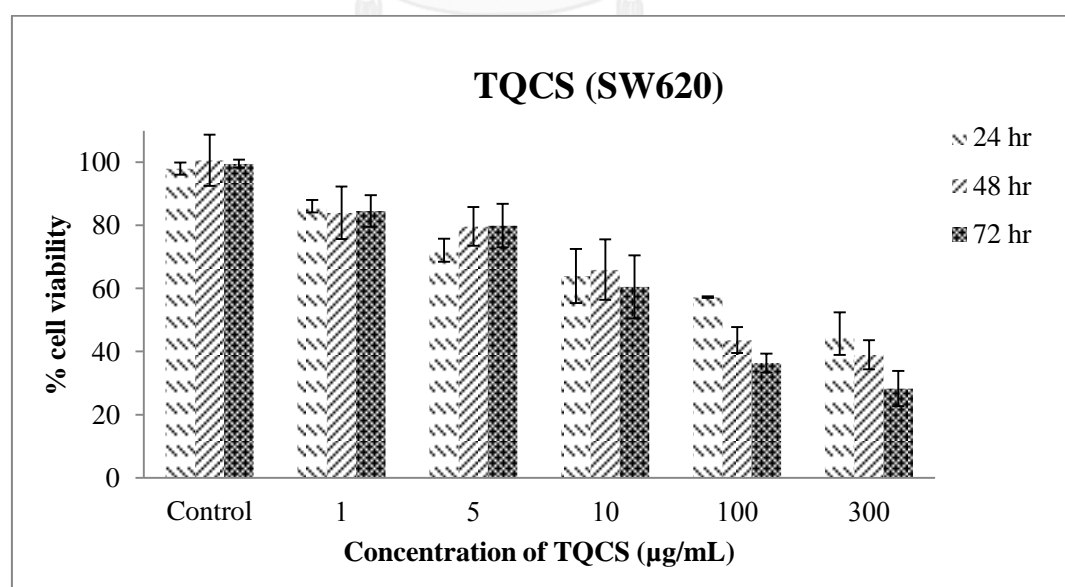


Figure 7E. Cell viability of TQCS-Cur against SW620 cell lines incubated for 24, 48 and 72 h (MTT assay)

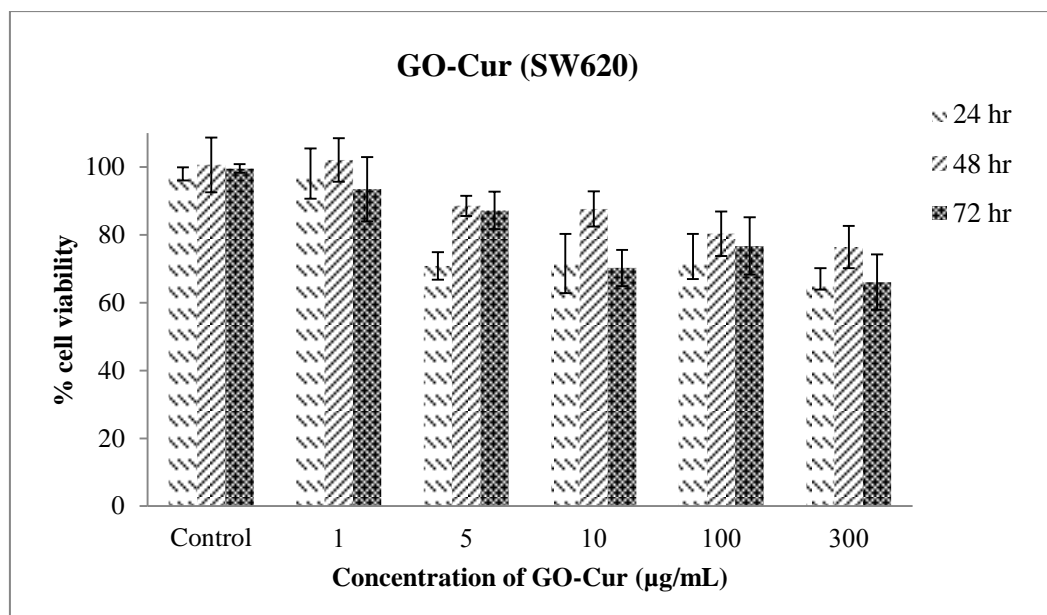


Figure 8E. Cell viability of GO-Cur against SW620 cell lines incubated for 24, 48 and 72 h (MTT assay)

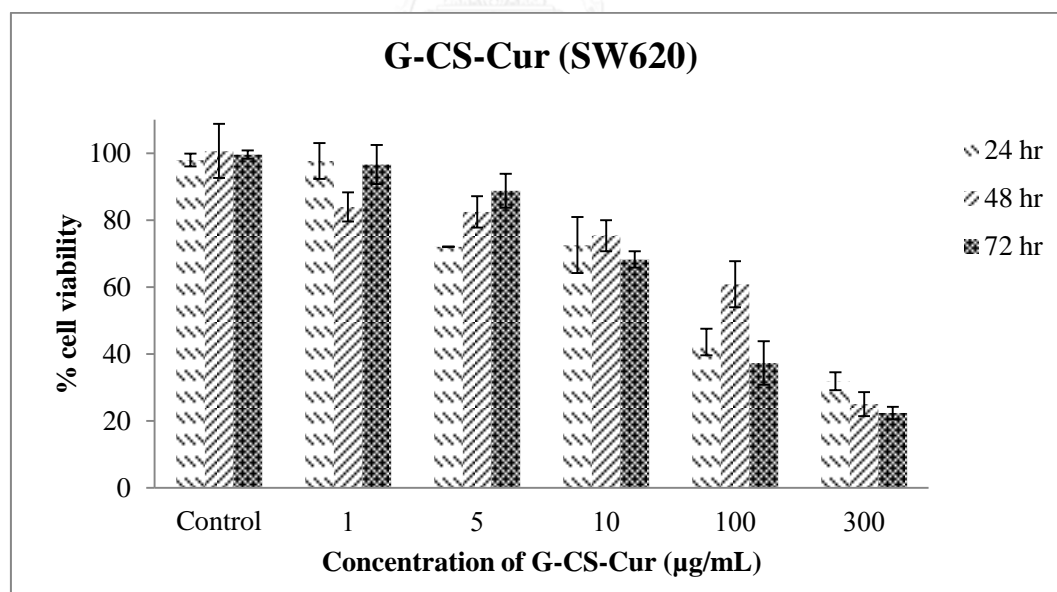


Figure 9E. Cell viability of G-CS-Cur against SW620 cell lines incubated for 24, 48 and 72 h (MTT assay)

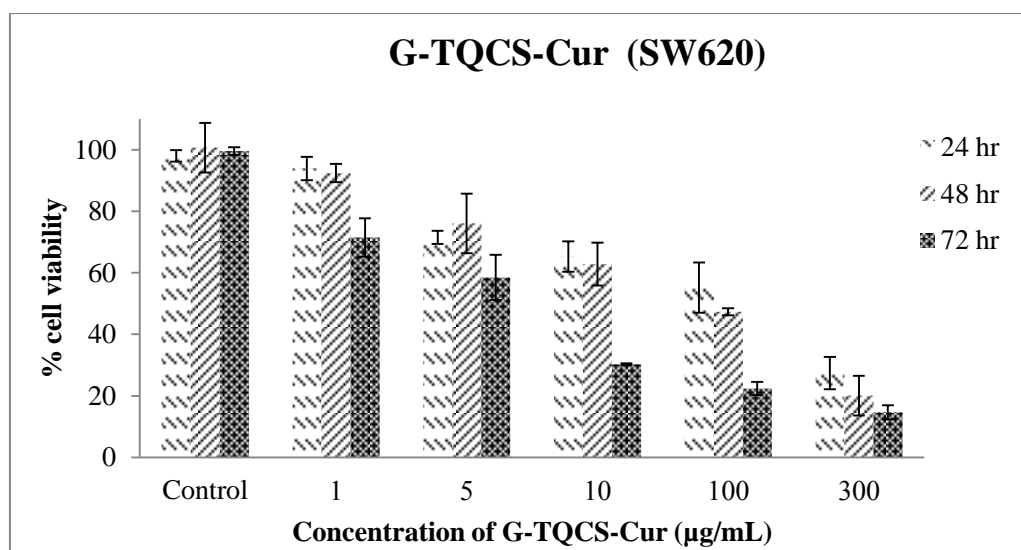
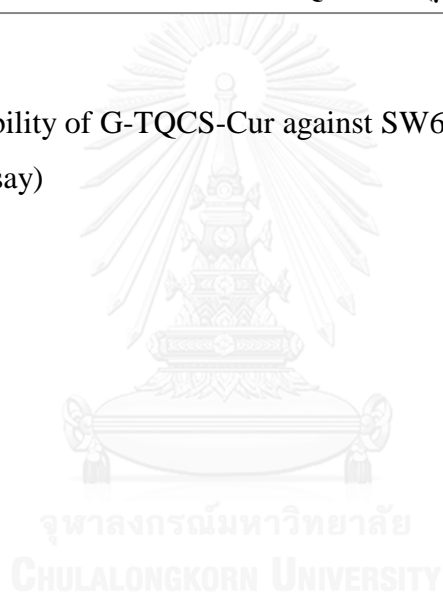


Figure 10E. Cell viability of G-TQCS-Cur against SW620 cell lines incubated for 24, 48 and 72 h (MTT assay)



VITA

Name : Miss. Pantipa Koraviyotin

Date of birth : February 14, 1989

Nationality : Thai

University Education : Bachelor's Degree from Faculty of
Science (Chemistry), Mahidol University, 2007-2010
Master's Degree from Program of
Petrochemistry and Polymer Science,
Faculty of Science, Chulalongkorn University, 2011-2014

Conference attendance : - The 10th Asia-Pacific Chitin & Chitosan Symposium and
The 27th Japanese Chitin and Chitosan Symposium,
Yonago, JAPAN (Oral presentation) October 4-8, 2013
- The 5th Research Symposium on Petrochemical and
Materials Technology and The 20th PPC Symposium
on Petroleum, Petrochemicals and Polymers Bangkok,
Thailand (Poster presentation and Proceeding)
April 22, 2014